

UNIVERSITY OF ROORKEE,
ROORKEE (U.P.)

Certified that the attached dissertation on "PROBLEM OF SINGLE PHASE INDUCTION
MOTOR WITH ASYMMETRICALLY SPACED WINDINGS"

was submitted by

.....V. K. VERMA.....

and accepted for the award of Degree of Master of Engineering in.....

.....ELECTRICAL MACHINE DESIGN.....

vide Notification No.....Ex/89/P-65(Degree).....

dated.....Sep. 7, 1965.....

Dated...Sep. 13, 1965.

PSUP (R) 291 Ch. 1964-1,000

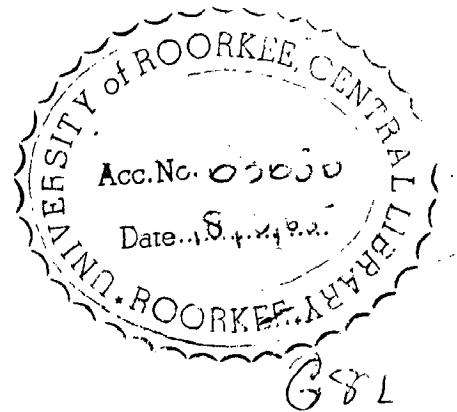
S. S. M. A.
Assistant Registrar (Exam.)

S. S. M. A.
13.9.65

**PROBLEM OF
SINGLE-PHASE INDUCTION MOTOR
WITH
ASYMMETRICALLY SPACED WINDINGS**

By
V. K. VERMA.

A Dissertation
submitted in partial fulfilment of the
requirements for the Degree of
MASTER OF ENGINEERING
in
ELECTRICAL MACHINE DESIGN



**DEPARTMENT OF ELECTRICAL ENGINEERING
UNIVERSITY OF ROORKEE
ROORKEE, U. P., (INDIA)
Sept. 1965**

ACKNOWLEDGEMENTS

The author wishes to acknowledge his deep sense of gratitude to Dr. L.M. Ray, Associate Professor in Electrical Engineering, University of Roorkee, Roorkee, for his valuable advises and suggestions at every stage of the preparation of this dissertation.

Sincere thanks are due to Professor C.S.Ghosh for the various facilities offered in the department in connection with this work.

The author also acknowledges the help of Messrs M.S.Beg, C.P.Reddy and Madanjit Singh during experimental work.

Roorkee

V.K.Verma

26 August, 1965

C E R T I F I C A T E

Certified that the dissertation entitled
" The Problem of Single-Phase Induction Motor
with Asymmetrically Spaced Windings " which is being
submitted by Shri V.K.Verma in partial fulfilment
for the award of the degree of Master of Engineering
in Electrical Machine Design of University of Roorkee
is a record of student's own work carried out by him
under my supervision and guidance. The matter embodied
in this dissertation has not been submitted for the award
of any other degree or diploma.

This is further to certify that he has worked for
a period of 8 months from 1st January, 1965 to 25th
August, 1965 for preparing dissertation for Master
of Engineering Degree of the University.

27/8/65
Dated Sept, 1965
Roorkee

L.M. Ray
(L.M.RAY)
Associate Prof. in Elect. Engg.
University of Roorkee

Roorkee

C O N T E N T S

Synopsis	1
List of Symbols	16
Introduction	v
Chapter -1 Theoretical Analysis of The Machine	
1.1 Equations and Equivalent Circuit of The Machine (Without Space-Harmonic)	1
1.2 Equations and Equivalent Circuit (With Space- Harmonic)	12
1.3 Performance Equations	17
1.4 Torque-Expression	19
1.5 Standstill Performance	20
1.6 Running Performance (A) Dips in Torque-speed Curve due to Space-Harmonics	27
(B) Determination of Running - Capacitor for Balanced Operation	30
1.7 Equivalent Quadrature Machine for A Non-Quadrature Machine.	34
Performance of Experimental Machine	
Chapter -2 Standstill Starting Performance	40
Chapter -3 Run-Up Performance	51
3.1 Run-Up Performance with Starting- Capacitor.	52
3.2 Suppression of Third Harmonic Dip	69
3.3 Reduction of Third Harmonic Dip	75
3.4 A Study of Third Harmonic Torque over whole speed Range.	81

Chapter-4	Running Performance	89
Chapter-5	Plugging	95
Chapter-6	Some Applications of Non-Quadrature 1-phase, Induction Motor (Capacitor run).	107
Chapter-7	Conclusions	110
Appendix - A	Fundamental Torque Expression	114
Appendix- B	Developments of Standstill-Equations	118
	References.	121

S Y N O P S I S

The dissertation deals with the performance-prediction of the single-phase induction motor with two asymmetrical stator-windings not in space quadrature, taking into account the effect of space-harmonics. Cross-field theory in a generalised form has been applied as dealt in reference ² with a modification. A transformer analogue analyser type equivalent circuit is also developed. The machine is shown to be equivalent to a machine with two stator-windings in space quadrature for full-load running (i.e. near synchronous speeds) and a simpler and handy equivalent circuit is determined, neglecting the space-harmonics without appreciable error.

The performance of a single phase induction motor having non-quadrature stator-windings has been analysed, with stress on starting torque, ~~starting torque~~, starting-capacitor requirement, suppression or reduction of asynchronous dips in the torque-speed characteristic, running and plugging operations.

LIST OF SYMBOLS

a	Ratio of Starting-winding turns to main winding turns.
b	Any odd integer
e_m	Main winding voltage (= v_s)
e_s	Starting winding voltage (= $v_s - i_s Z_c$)
i_m	Main winding current
i_s	St Starting Winding Current
i_{dr}	d-axis rotor current
i_{qr}	q- axis rotor current
n	Suffix or multiple factor for nth order space harmonic.
r_m	Resistance of main winding
r_s	Resistance of starting winding.
r_r	Resistance of rotor winding referred to main winding as in 2 phase motors.
T_{α}	Torque with α electrical degrees space separation between stator windings
T_{90°	T_{α} with $\alpha = 90^\circ$
T_b	Torque for balanced 2-phase machine
v	Rotor speed as a fraction of the fundamental synchronous speed.
v_s	Supply Voltage
x_m	Leakage reactance of the main winding due to its pure leakage flux.
x_s	Leakage reactance of the starting winding due to its pure leakage flux.

x_{sm} Leakage reactance of the main winding due to the Leakage flux which does not cross the air-gap but links the main and the starting windings.

x_r Leakage reactance of rotor referred to the main winding as in 2 phase motors.

X_M Air-gap magnetising reactance, referred to the main winding.

$$X_r = X_M + x_r$$

$$X_{sm} = X_M + x_{sm}$$

X_c Reactance of the phase converting capacitor.

$$x = \left| \frac{z(Z_n \cos n \alpha)}{Z_0} \right|$$

$$y = \left| \frac{z}{Z_0} \right|$$

$$Z = \frac{r_s + j x_s + Z_c}{a^2} - (r_m + j x_m)$$

Z_c = Phase convertor impedance.

Z_0 Main winding stand-still impedance,

$$= R_0 + jX_0 = r_m + jx_m + \sum_n \left(jX_{Mn} + \frac{X_{Mn}^2}{r_{rn} + jX_{rn}} \right)$$

$$Z_n = \sum \left(jX_{Mn} + \frac{X_{Mn}^2}{r_{rn} + jX_{rn}} \right) = R_n + jX_n$$

$$Z_{rn} = \frac{r_{rn}}{1-n^2v^2} + jX_{rn}$$

$$Z_M = (r_m + jx_m + jx_{sm} + jX_M)$$

$$Z_s = (r_s + jx_s + jx_{sm}a^2 \cos^2 \alpha + j X_M a^2)$$

Z_{MM} Total impedance of main winding

Z_{SS} Total impedance of starting winding

$Z_{ms},$
 Z_{sm} Total Mutual impedance between main and starting windings.

Z_{ds} Equivalent impedance of main winding ~~alone~~ alone in equivalent 90° machine (equation 59)

Z_{qs} Equivalent impedance of starting winding alone in equivalent 90° machine

Z'_m Equivalent Mutual impedance between main and starting winding in equivalent 90° machine (equation 59)

α Space angle between main and starting windings, in electrical degrees.

α_1 Phase angle of i^M

α_2 Phase angle of i^S

γ Argument of x

δ Argument of y

$$\sigma = \frac{r_r}{r_r + r_m}$$

$\phi = (\alpha_1 - \alpha_2)$ time phase difference between main and starting winding currents.

INTRODUCTION

Though the single-phase induction motors are easy to design, their performance prediction is difficult. In such machines the space harmonic play a very prominent part and this makes the analysis more complicated.

The problem of single-phase induction machine with asymmetrical non-quadrature stator windings is rather old¹². Almost up to the last decade this problem was dealt by all the existing theories of electrical machine analysis, but all of them have neglected the space harmonic effects. There is a recent paper by G.S.Jha³ dealing with this problem, in which he has taken into account the space harmonic effects. His approach is by revolving-field in a generalised form. In the present work, based on a paper by G.Kron² the cross-field theory is used in a generalised form to take into account the asynchronous effects of the space-harmonics.

In the present article harmonic effects have been more thoroughly investigated, effects of capacitor on harmonic dip suppression and thus run-up performance have been noted and advantage of plugging with non-quadrature windings has been pointed out.

There is very little to choose between the two theories, cross-field and revolving field, in explaining the behaviour of a single-phase motor. However, cross-field approach has been applied as an exercise and in doing so, an equivalent circuit has been developed which takes into account the harmonic effects.

CHAPTER - 1

THEORETICAL ANALYSIS OF THE MACHINE

1.1 Equations and Equivalent Circuit for the Machine
(without space Harmonics)^{1,2}

The machine has two stator windings with 'a' turns-ratio at a space separation of 'α' electrical degrees between them.

For theoretical analysis the space harmonics are neglected first. Two exactly similar stator coils, main and starting, of unity turns are assumed to lie along the main winding axis, called the 'd' axis.

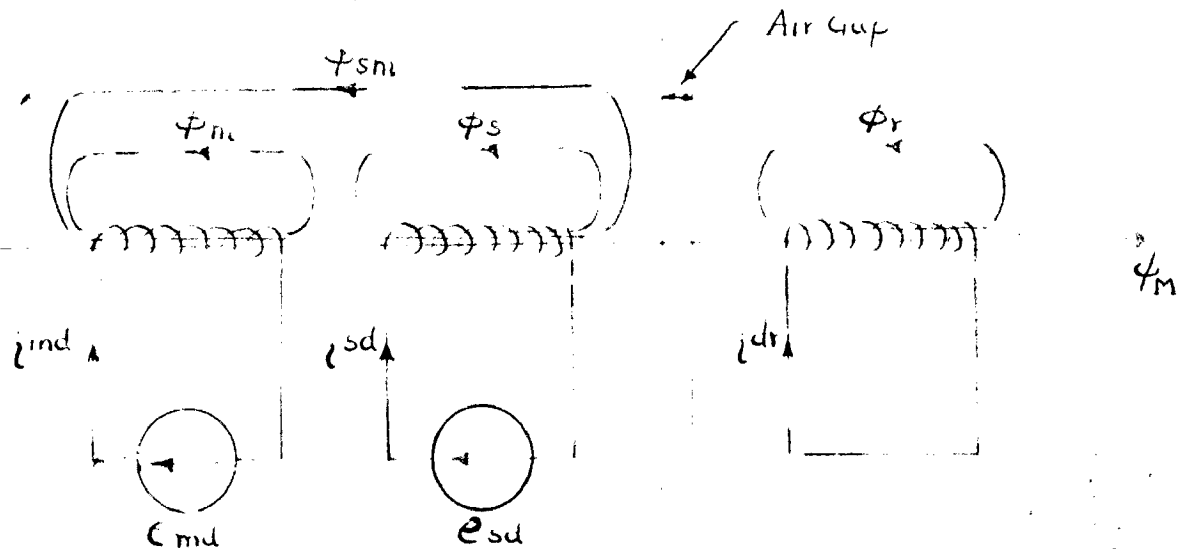


Fig 1(A) d-axis arrangement of coils

Along the d-axis the rotor is thought to have a similar coil of unity turns.

In Fig. 1 is shown the various fluxes linking the coils.

ϕ_M = Mutual flux, linking all the three coils

It gives rise to X_M , the air gap reactance

ϕ_{sm} = Mutual flux linking only the stator coils but not crossing the air gap. It gives rise to X_{dsm} reactance.

ϕ_m = A leakage flux linking the main winding only and giving rise to a leakage reactance x_{md}

ϕ_s = A leakage flux linking the starting winding only and giving rise to a leakage reactance x_{sd}

ϕ_r = A leakage flux linking the rotor coil only and giving rise to a leakage reactance x_r .

Writing down the equations for these three ~~statistic~~ circuits, with the reactances so defined we get

$$\phi_{md} = (r_{md} + j x_{md} + j X_M) i_{md} + (j X_M + j x_{dsm}) i_{sd} + j X_M i_{dr}$$

$$\phi_{sd} = (j X_M + j x_{dsm}) i_{md} + (r_{sd} + j x_{sd} + j x_{dsm} + j X_M) i_{sd} + j X_M i_{dr}$$

$$0 = j X_M i_{md} + j X_M i_{sd} + (R_r + j x_r + j X_M) i_{dr}$$

The following Figure 1(B) satisfies these equations.

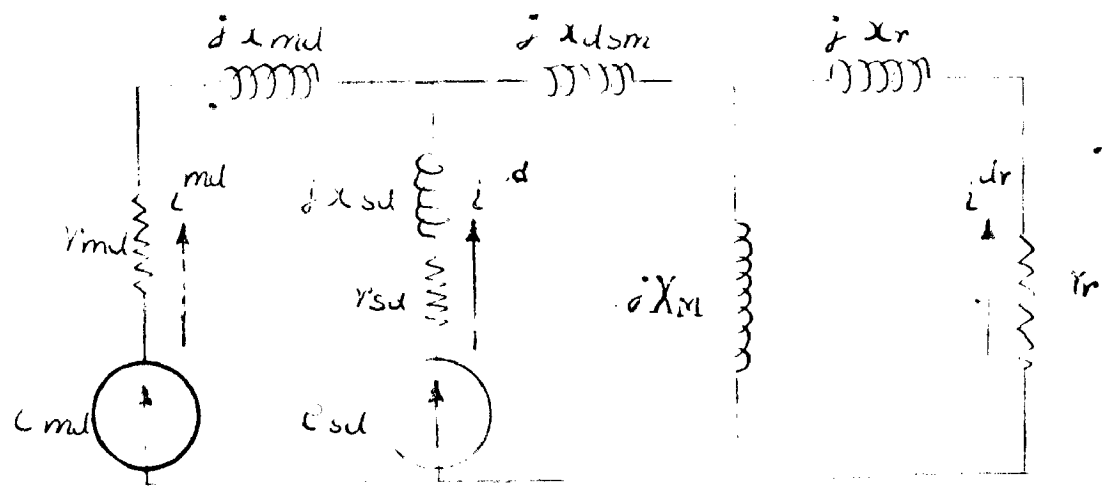


Fig. 1 (B)

The starting winding, displaced by α degrees is actually having 'a' times the turns of main-winding. It may be substituted by two coils, having a $\cos \alpha$ turns along d-axis and $a \sin \alpha$ turns along q axis.

Hence the circuit of Fig. 1 (B) may be modified to take into account a $\cos \alpha$ turns of the start winding instead of unity.

Fig. 2 shows such a modification. r_{sd} and x_{sd} are now thought to be the resistance and leakage reactance of this new d-axis starting winding.

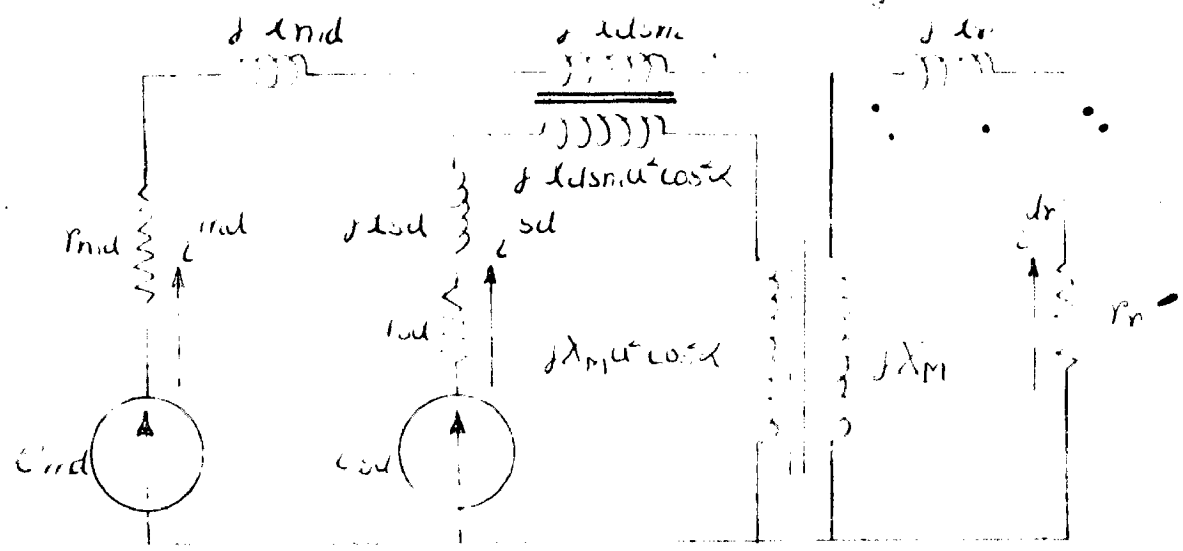


Fig. 2

Along the q-axis we have the starting winding alone with a $\sin\alpha$ turns. Along the same lines q axis equivalent circuit can also be developed (Fig. 3)

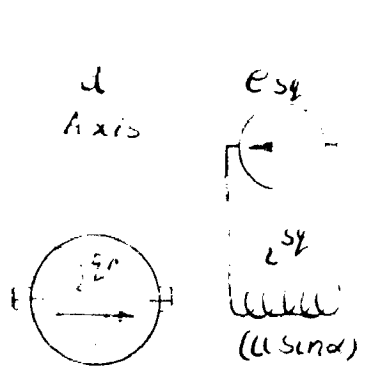


FIG 3 [A]

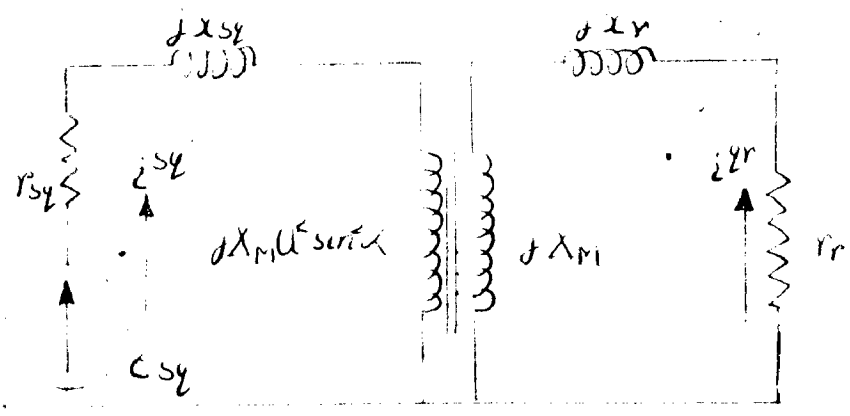


FIG 3 [B]

Figures 2 and 3(B) may be combined together into Fig.5 which will be the equivalent circuit for the actual machine, of Fig. 4, at rest

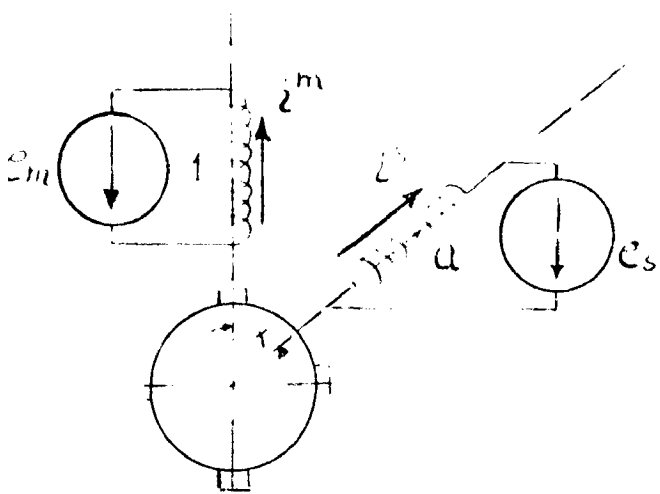


FIG. 4(A)

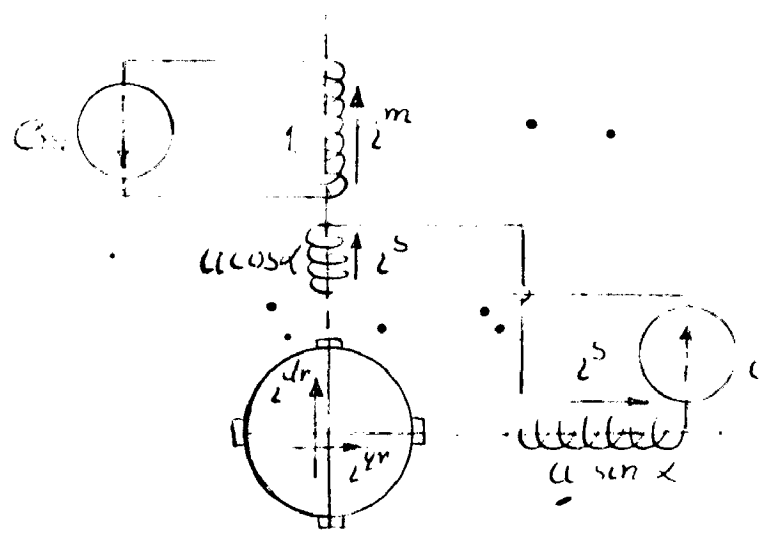


FIG. 4(B)

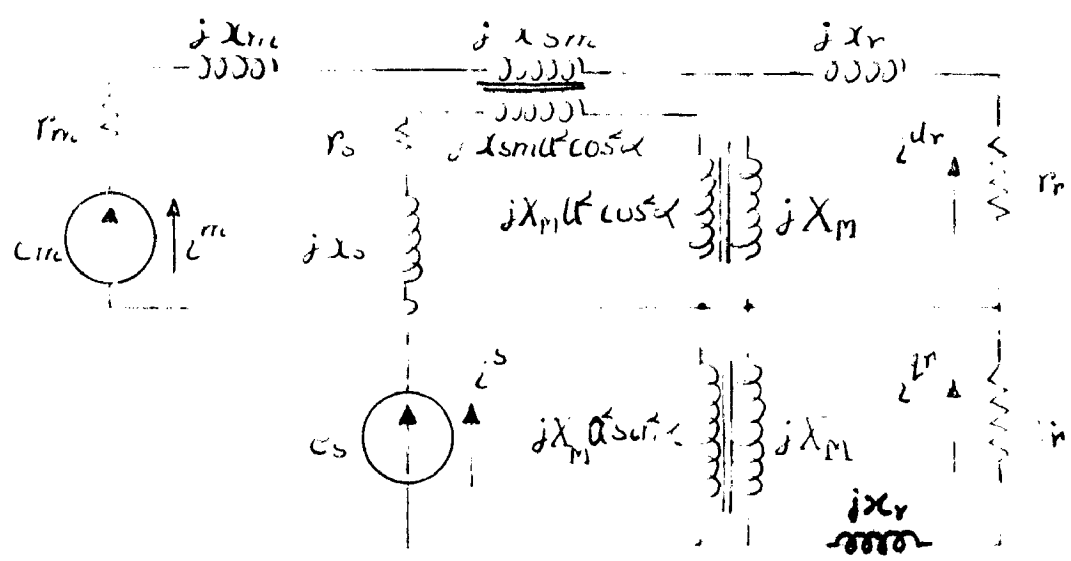


FIG. 5 Equivalent Circuit At Standstill.

At any speed v , expressed as a fraction of the fundamental synchronous speed the impedance matrix of the machine may be written as follows :

	m	s	dr	qr
m	$r_m + j x_m + j x_{sm}$ $+ j X_M$ $= Z_M$	$j(x_{sm} + X_M) a \cos \alpha$ $= j X_{SM} a \cos \alpha$	$j X_M$.
s	$j X_{SM} a \cos \alpha$	$r_s + j x_s + j X_M a^2$ $+ j x_{sm} a^2 \cos^2 \alpha$ $= Z_s$.	.
dr	$j X_M$	$j X_M a \cos \alpha$ $+ X_M a \sin \alpha \cdot V$	$r_r + j X_r$	$X_r V$
qr	$-X_M V$	$j X_M a \sin \alpha$ $- X_M a \cos \alpha \cdot V$	$- X_r V$	$r_r + j X_r$

....(1)

As such from equation (1) it is difficult to modify Fig. 5 to take into account the speed.

Hence the impedance-matrix of equation (1) is converted into the impedance matrix Z_2 using the transformation matrix of eq. (2)

$$C_1 = \frac{1}{\sqrt{2}}$$

	fs'	bs	fr	br
m	1	1		
s	-j	j		
dr			1	1
qr			-j	j

..... (2)

$$Z_2 = C_1^* Z_1 C_1$$

	f_s	b_s	f_r	b_r
f_s	$\frac{Z_M + Z_s}{2}$	$\frac{Z_M - Z_s}{2} X_{SM} \cos \alpha$	$\frac{X_M(j - a \cos \alpha + ja \sin \alpha)}{2}$	$\frac{X_M(j - a \cos \alpha - ja \sin \alpha)}{2}$
b_s	$\frac{Z_M - Z_s}{2} X_{SM} \cos \alpha$	$\frac{Z_M + Z_s}{2}$	$\frac{X_M(j + a \cos \alpha - ja \sin \alpha)}{2}$	$\frac{X_M(j + a \cos \alpha + ja \sin \alpha)}{2}$
f_r	$\frac{(1-v)}{2} \{ jX_M + X_M a \cos \alpha + jX_M a \sin \alpha \}$	$\frac{(1-v)}{2} \{ jX_M - X_M a \cos \alpha - jX_M a \sin \alpha \}$	$r_r + jX_r(1-v)$	
b_r	$\frac{(1+v)}{2} \{ jX_M + X_M a \cos \alpha - jX_M a \sin \alpha \}$	$\frac{(1+v)}{2} \{ jX_M - X_M a \cos \alpha + jX_M a \sin \alpha \}$		$r_r + jX_r(1+v)$

-- (3)

Now multiplying the impedance matrix Z_2 by the inverse of the 'absolute frequency matrix'

	f_s	b_s	f_r	b_r
f_s	1			
b_s		1		
f_r			$\frac{1}{(1-v)}$	
b_r				$\frac{1}{(1+v)}$

..... (4)

We obtain the new impedance matrix

$$Z_3 = n^{-1} Z_2$$

	$f's$	b_s	f_r	b_r
$f's$	$\frac{Z_M + Z_s}{2}$	$\frac{Z_M - Z_s - X_{SM} \cos d}{2}$	$X_M(j - a \cos d + ja \sin d)$	$\frac{X_M(j - a \cos d - ja \sin d)}{2}$
b_s	$\frac{Z_M - Z_s}{2} + X_{SM} \cos d$	$\frac{Z_M + Z_s}{2}$	$X_M(j + a \cos d - ja \sin d)$	$\frac{X_M(j + a \cos d + ja \sin d)}{2}$
$Z_3 =$				
f_r	$\frac{X_M(j + a \cos d + ja \sin d)}{2}$	$\frac{X_M(j - a \cos d - ja \sin d)}{2}$	$\frac{R_r}{1-v} + j X_r$	
b_r	$\frac{X_M(j + a \cos d - ja \sin d)}{2}$	$\frac{X_M(j - a \cos d + ja \sin d)}{2}$		$\frac{R_r}{1+v} + j X_r$

.... (5)

Now returning back to the cross field axes by using the transformation matrix.

$C_2 = \frac{1}{\sqrt{2}}$

	m	s	dr	qr
$f's$	1	j		
b_s	1	$-j$		
f_r			1	j
b_r			1	$-j$

.....(6)

$$Z_4 = C_{2t}^* Z_3 C_2$$

			dr	qr
m	Z_M	$jX_{SM} \cos \delta$	jX_M	
s	$jX_{SM} \cos \delta$	Z_S	$jX_M \cos \delta$	$jX_M \sin \delta$
$Z_d =$ dr	jX_M	$jX_M \sin \delta$	$\frac{r_r}{1-v^2} + jX_r$	$\frac{v r_r}{1-v^2}$
qr		$jX_M \sin \delta$	$\frac{-jv r_r}{1-v^2}$	$\frac{r_r}{1-v^2} + jX_r$

.....(7)

Hence now from fig. 5 we obtain the equivalent circuit taking speed into consideration.

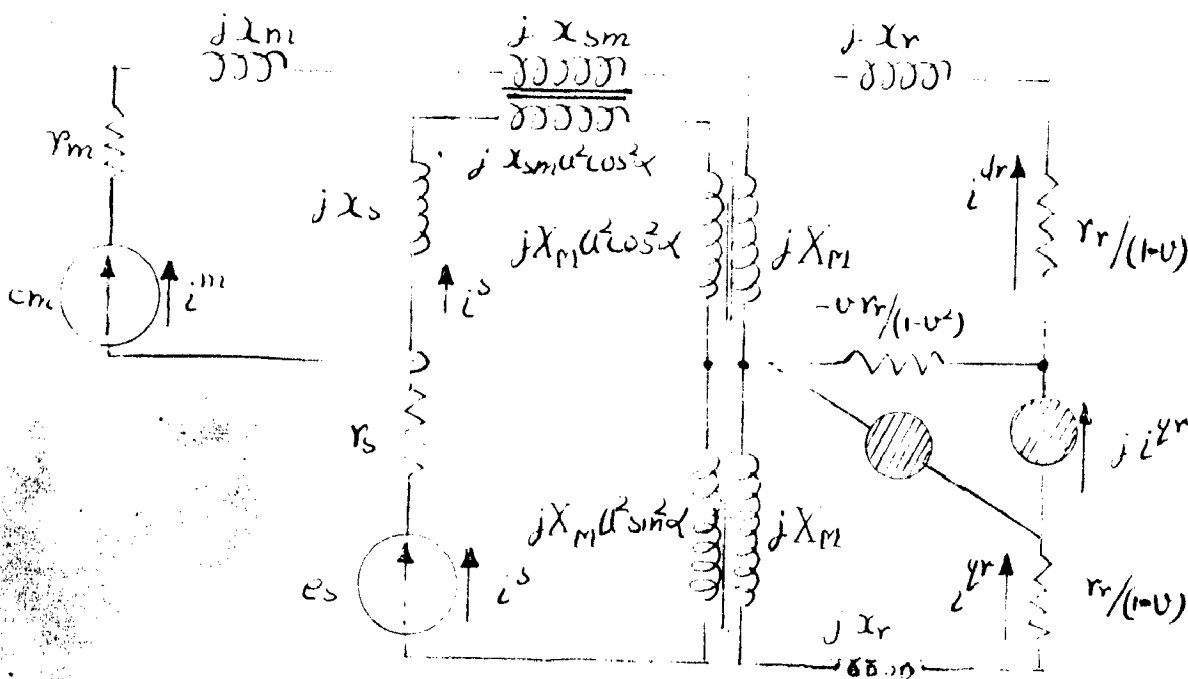


FIG. 6. Equivalent Circuit At Any Speed v .

The Phase-Shifter²

It should be noted that the expression in Z_4 impedance matrix representing the mutual term between the rotor d- and q- axes does not occur in a symmetrical manner. While analytically only a change in sign occurs, physically in the equivalent circuit a phase shifter must be placed. Its role is to rotate the current and the voltage by 90° in the same direction.

Hence the voltage equations for the rotor d- and q-axes from the equivalent circuit of Fig. 6 are :

$$i^M (j X_M) + i^S (j X_M a \cos \alpha) + i^{dR} \left(\frac{R_R}{1-v} - \frac{v R_R}{1-v^2} + j X_R \right) - j i^{qR} \left(-\frac{v R_R}{1-v^2} \right) = 0$$

$$\text{i.e. } i^M (j X_M) + i^S (j X_M a \cos \alpha) + i^{dR} \left(\frac{R_R}{1-v^2} + j X_R \right) + i^{qR} \cdot \frac{j v R_R}{1-v^2} = 0$$

and

$$i^S (j X_M a \sin \alpha) + i^{dR} \left(\frac{R_R}{1-v} + j X_R \right) + \frac{1}{j} \left[j i^{qR} \left(-\frac{v R_R}{1-v^2} \right) - i^{dR} \left(-\frac{v R_R}{1-v^2} \right) \right] = 0$$

$$\text{i.e. } i^S (j X_M a \sin \alpha) - j \frac{v R_R}{1-v^2} i^{dR} + i^{qR} \left(\frac{R_R}{1-v^2} + j X_R \right) = 0$$

which are the same as obtained from equation (7)

Shifting Phase-shifter to the Stator

The rotor meshes of the equivalent circuit may be brought to more familiar form if $j i^s$ and $j i^{qr}$ are introduced as new variables in place of i^s and i^{qr} by the matrix.

$$C_3 = \begin{array}{c} \begin{array}{c} m \\ s \\ dr \\ qr \end{array} \\ \begin{array}{c|c|c|c} m & s & dr & qr \\ \hline 1 & & & \\ \hline & -j & & \\ \hline & & 1 & \\ \hline & & & -j \end{array} \end{array}$$

....(8)

$$\text{Then } Z_5 = C_{3t}^* Z_4 C_3$$

$$Z_5 = \begin{array}{c} \begin{array}{c} m \\ s \\ dr \\ qr \end{array} \\ \begin{array}{c|c|c|c} m & s & dr & qr \\ \hline X_M & X_M a \cos \alpha & j X_M & \\ \hline -X_M a \cos \alpha & Z_0 & -X_M a \cos \alpha & j X_M a \sin \alpha \\ \hline j X_M & X_M a \cos \alpha & \frac{R_r}{1-v^2} + j X_r & v \frac{R_r}{1-v^2} \\ \hline & j X_M a \sin \alpha & v \frac{R_r}{1-v^2} & \frac{R_r}{1-v^2} + j X_r \end{array} \end{array}$$

..... (9)

$$\begin{matrix}
 15 & = & \begin{matrix} m & s & dr & qr \\ \hline i^m & j i^s & i^{dr} & j i^{qr} \end{matrix} & \begin{matrix} \\ \\ \\ 10 \end{matrix} \\
 5 & = & \begin{matrix} m & s & dr & qr \\ \hline e_m & j e_s & - & - \end{matrix} & \dots (11)
 \end{matrix}$$

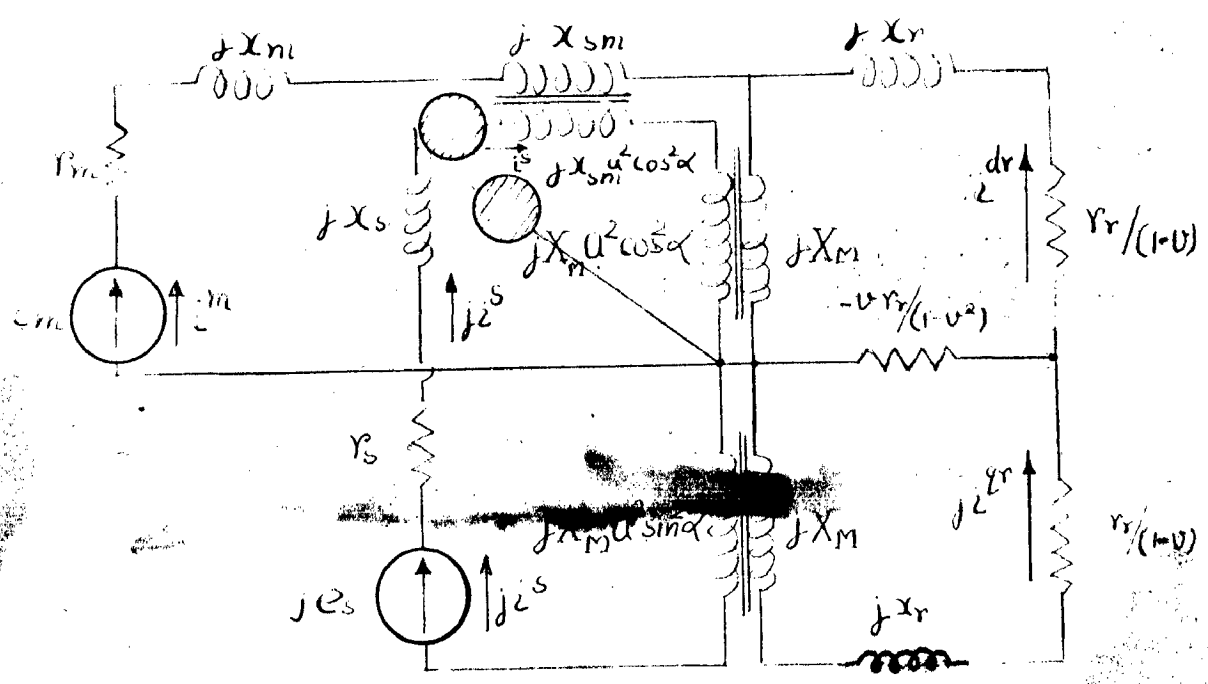


FIG. 7. Equivalent Circuit At Any Speed U With Phase Shifter In Stator

1.2 Equation and Equivalent -Circuit with Space-Harmonics

Each stator current (i^m and i^s) produces a series of fluxes with P, 3P, 5P etc. pairs of poles. Each of these fluxes cut the rotor producing in it a current density and flux density wave having the same number of pairs of poles as the stator flux producing them. Hence so far as the asynchronous phenomenon in the machine is concerned each such machine may be looked upon as consisting of several motors with different number of pairs of poles whose stator windings are connected in series (Fig. 8)

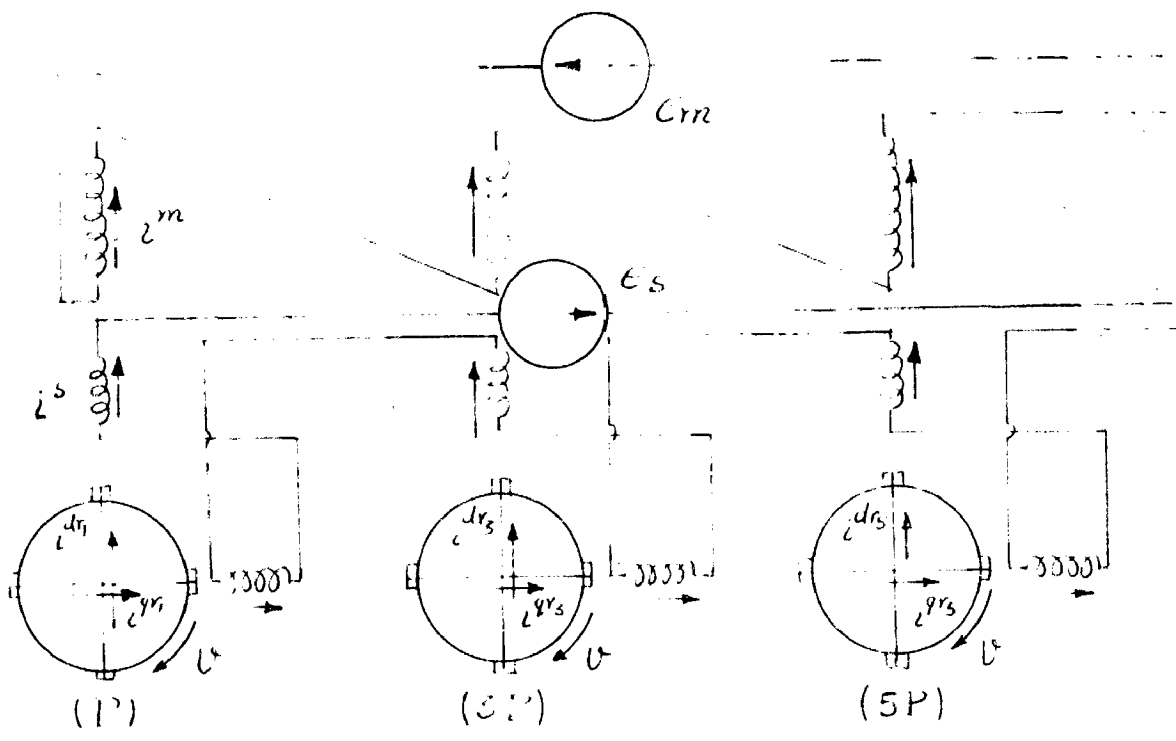


FIG. 8. Interconnection of Harmonic Motors With P, 3P, 5P, etc. Pairs of Poles

Various harmonics motor-s are interconnected, all running at the same speed v .

Fundamental slip of rotor

$$(1 - v) = \frac{N_{s1} - N_r}{N_{s1}}$$

where N_{s1} = Fundamental synchronous speed

N_r = Actual rotor speed.

Third space-harmonic slip of rotor

$$\begin{aligned} &= \frac{N_{s1|3} - N_r}{N_{s1|3}} \\ &= (1 - 3v) \end{aligned}$$

Where $N_{s1|3}$ is the third ^{space} ~~speed~~ harmonic syn. speed.

Similarly Fifth ^{space} ~~speed~~ harmonic slip

$$= (1 - 5v) \quad \text{and so on.}$$

For each harmonic machine an equivalent circuit may be developed. The changes to be put in equation (9) will be $n.v$ instead of v , suffix n for each of the machine constants, $n.c$ for c and $n.a$ for a , the effective turns ratio.

It may be pointed out here that the author's approach to this problem is almost on the same lines as that of a Kron's paper². In his paper Kron has shown that the machine with two asymmetrical stator windings not in quadrature may be shown to be equivalent to a machine with two stator windings in quadrature, for any space harmonic. But while interconnecting the equivalent circuits of various harmonic machines it was overlooked that the currents and voltages quantities in the equivalent stator windings in quadrature are function of ' α ', the space-angle between the

stator-windings of the actual machine. In fact for harmonic machine 'd' should have been replaced by nd in all the expressions, n being the order of the space harmonic. Hence the inter-connection of the various equivalent harmonic machines, as dealt in his paper, resulting in the same stator current for all the equivalent machines, is not justified. That is why in the present work no attempt is made to replace the actual machine with two stator windings in nonquadrature by an equivalent machine with the stator windings in quadrature.

A complete impedance matrix of the machine with space-harmonics may be written as follows : -

	m	s	dr_1	qr_1	dr_3	qr_3
m	$Z(Z_{Mn})$	$Z(X_{SMn} \sin n\alpha \cos n\alpha)$	jX_{M1}		jX_{M3}	
s	$Z(X_{SMn} \sin n\alpha \cos n\alpha)$	$Z(Z_{Sn})$	$-X_{M1} a_1 \cos \alpha$	$jX_{M1} a_1 \sin \alpha$	$-X_{M3} a_3 \cos 3\alpha$	$jX_{M3} a_3 \sin 3\alpha$
dr_1	jX_{M1}	$X_{M1} a_1 \cos \alpha$	$\frac{r_{r1}}{1-v^2} + jX_{r1}$	$j \frac{v r_{r1}}{1-v^2}$		
qr_1		$jX_{M1} a_1 \sin \alpha$	$j \frac{v r_{r1}}{1-v^2}$	$\frac{r_{r1}}{1-v^2} + jX_{r1}$		
dr_3	jX_{M3}	$X_{M3} a_3 \cos 3\alpha$			$\frac{r_{r3}}{1-9v^2} + jX_{r3}$	$j \frac{3v r_{r3}}{1-9v^2}$
qr_3		$jX_{M3} a_3 \sin 3\alpha$			$j \frac{3v r_{r3}}{1-9v^2}$	$\frac{r_{r3}}{1-9v^2} + jX_{r3}$

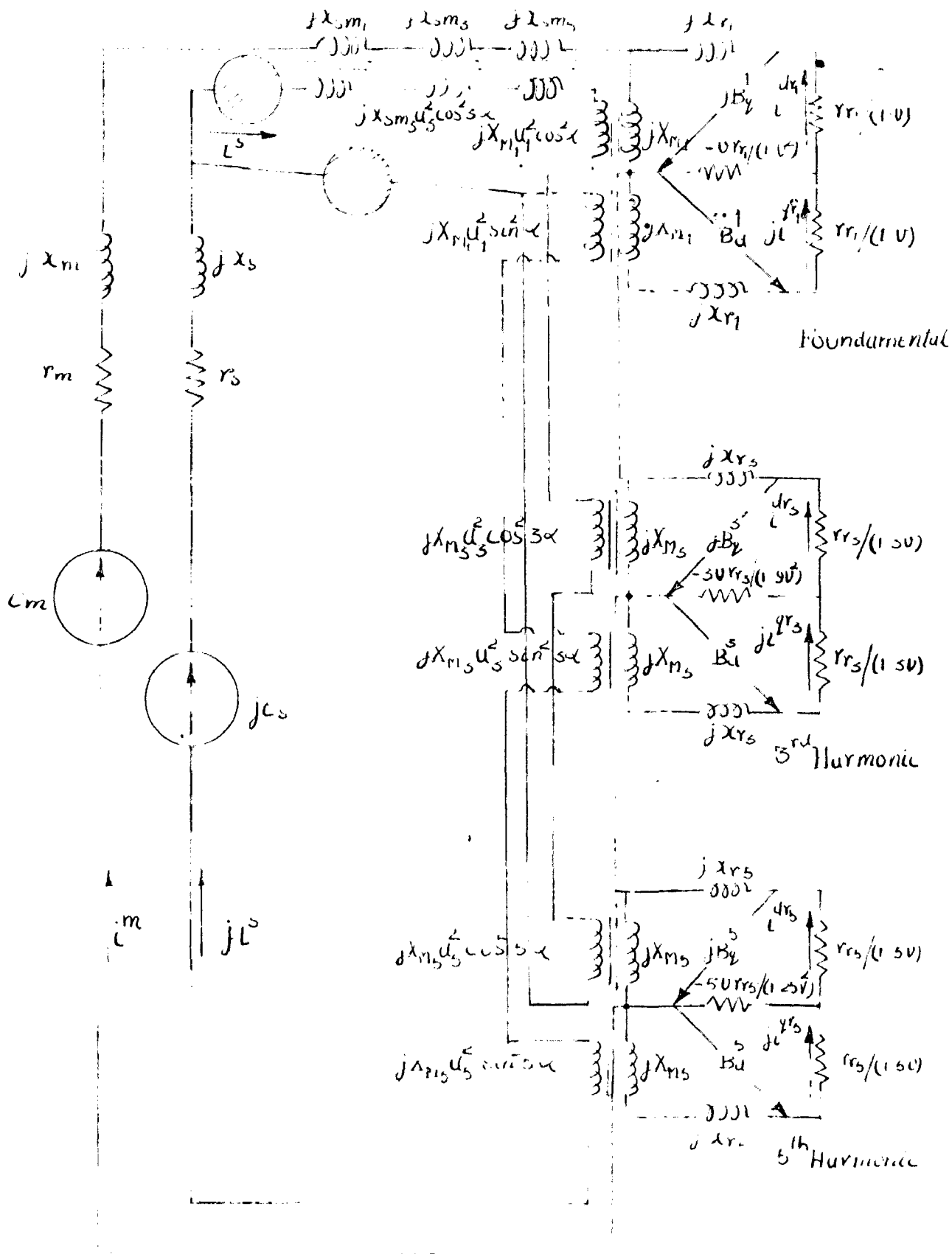


Fig 9 Equivalent Circuit With Space Harmonics

$$i = \begin{array}{|c|c|c|c|c|c|} \hline n & s & d_{r_1} & q_{r_1} & d_{r_2} & q_{r_2} \\ \hline j^n & j^s & j^{d_{r_1}} & j^{q_{r_1}} & j^{d_{r_2}} & j^{q_{r_2}} \\ \hline \end{array} \dots (13)$$

$$e = \begin{array}{|c|c|c|c|c|c|} \hline n & s & d_{r_1} & q_{r_1} & d_{r_2} & q_{r_2} \\ \hline e_n & j^s & - & - & - & - \\ \hline \end{array} \dots (14)$$

1.3 Performance -Equations

From impedance matrix Z of equation (12) the rotor mesh equations are

$$j X_{M,1^m} + j X_{M,a} \cos d i^s + \left(\frac{r_{r1}}{1-v^2} + jX_{r1} \right) i^{dr1} + jv \frac{r_{r1}}{1-v^2} i^{dr1} = 0$$

$$jX_{M,a} \sin d j i^s + v \frac{r_{r1}}{1-v^2} i^{dr1} + \left(\frac{r_{r1}}{1-v^2} + jX_{r1} \right) j i^{dr1} = 0$$

Solving for i^{dr1} and i^{dr2} we obtain

$$i^{dr1} = \left[\frac{jX_{M,1^m} Z_{r1} i^m + \left\{ j X_{M,a} \cos d Z_{r1} + v r_{r1} X_{M,a} \sin d \right\} i^s}{Z_{r1}^2 - v^2 R_{r1}^2} \right] \dots (15)$$

$$j i^{dr2} = \left[\frac{jX_{M,2^m} v R_{r1} i^m + \left\{ X_{M,a} \sin d Z_{r1} + jX_{M,a} \cos d v R_{r1} \right\} i^s}{Z_{r1}^2 - v^2 R_{r1}^2} \right] \dots (16)$$

Where $Z_{r1} = R_{r1} + j X_{r1}$
 $= \frac{r_{r1}}{1-v^2} + jX_{r1}$

Other rotor currents may be found simply by changing the suffix and putting nv for v .

Hence

$$e_m = \left[r_m + jx_m + \sum_1^n \left\{ (jX_{Mn} + j x_{sm}) + \frac{X_{rn}^2 Z_{rn}}{Z_{rn}^2 - n^2 v^2 R_{rn}^2} \right\} \right] i^m$$

$$+ \left[\sum \left\{ j(X_{Mn} + x_{sm}) a_n \cos nd + \frac{an X_{rn}^2 M_n (Z_{rn} \cos nd - jnv R_{rn} \sin nd)}{Z_{rn}^2 - n^2 v^2 R_{rn}^2} \right\} \right] i^s \dots (17)$$

$$e_s = \left[\sum_n \left\{ j(X_{Mn} + x_{smn}) \frac{a_n}{n} \cos nd + \frac{(Z_{fn} \cos nd + jnvR_{fn} \sin nd) a_n X_{Mn}^2}{Z_{fn}^2 - n^2 v^2 R_{fn}^2} \right\} \right] e^{j\omega t}$$

$$+ \left[(r_s + jx_s) + \sum_n \left\{ j(X_{Mn} + x_{smn}) \frac{a_n}{n} \cos^2 nd + \frac{a_n^2 X_{Mn}^2 Z_{bn}}{Z_{fn}^2 - n^2 v^2 R_{fn}^2} \right\} \right] e^{j\omega t}$$

....(18)

If the two windings on stator have same winding-factors for any order of space-harmonic, a_n may be replaced by a . Assuming rotation from q-axis to d-axis i.e with v negative, the above two equations may be put in other forms easily:-

$$e_m = \left[r_m + jx_m + \sum jx_{smn} + \sum z_{fn} + \sum z_{bn} \right] i^m$$

$$+ \left[\sum jx_{smn} \cos nd + \sum \epsilon^{-jnd} z_{fn} + \sum \epsilon^{jnd} z_{bn} \right] a i^s$$

... (19)

$$e_s = \left[\sum jx_{smn} \cos nd + \sum \epsilon^{jnd} z_{fn} + \sum \epsilon^{-jnd} z_{bn} \right] a i^m$$

$$+ \left[r_s + jx_s + ja^2 \sum x_{smn} \cos^2 nd + a^2 \sum z_{fn} + a^2 \sum z_{bn} \right] i^s$$

....(20)

Where $z_{fn} = j \frac{X_{Mn}}{2} \left(\frac{R_{fn}/2}{1-nv} + j \frac{X_{fn}}{2} \right)$

$$\frac{\frac{R_{fn}}{2(1-nv)} + j \frac{X_{fn}}{2}}$$

..... (21)

and $z_{bn} = j \frac{X_{Mn}}{2} \left(\frac{R_{fn}/2}{1+nv} + j \frac{X_{fn}}{2} \right)$

$$\frac{\frac{R_{fn}}{2(1+nv)} + j \frac{X_{fn}}{2}}$$

..... (22)

1.4 Torque- Expressions

Fundamental torque in synchronous watts

$$T_1 = \text{Real} \left[i^{dr_1} \cdot B_d^{1*} + i^{qr_1} \cdot B_q^{1*} \right] \dots\dots (23)$$

where B_d^1 and B_q^1 as shown in Fig. 9 are given by

$$B_d^1 = \frac{r_{r_1}}{(1-v^2)} (v i^{dr_1} + j i^{qr_1}) \dots\dots (24)$$

$$j B_q^1 = \frac{r_{r_1}}{1-v^2} (i^{dr_1} + j v i^{qr_1}) \dots\dots (25)$$

Substituting for i^{dr_1} and i^{qr_1} from equations (15) and (16)

the torque expression in final form is given by

$$T_1 = \frac{r_{r_1}}{1-v^2} \frac{1}{\frac{r_{r_1}^2}{(1-v^2)^2} + X_{r_1}^2 + \frac{2r_{r_1}^2 X_{r_1}^2 (1+v^2)}{(1-v^2)^2}} \left[v X_{M_1}^2 \left(X_{r_1}^2 - \frac{r_{r_1}^2}{1-v^2} \right) \cdot \right. \\ \left. \cdot \left(I^{m^2} + 2a_1 \cos \phi \cos \phi I^m \cdot I^s + a_1^2 \frac{I^m I^s}{I^2} \right) + 2X_{M_1}^2 a_1 \cdot \right. \\ \left. \cdot \left(\frac{X_{r_1}^2}{1-v^2} + \frac{r_{r_1}^2}{1-v^2} \right) I^m \cdot I^s \sin \delta \sin \phi \right] \dots\dots (26)$$

$$\text{where } i^m = I^m \quad / \alpha_1$$

$$i^s = I^s \quad / \alpha_2$$

$$\phi = (\alpha_1 - \alpha_2)$$

For any other harmonic torque, say T_n put suffix n in place of suffix 1 , nv for v and $n\alpha$ for α . Also multiply the whole expression by n to convert the torque expressed in syn. watts to a common base speed, i.e. the fundamental space harmonic syn. speed.

1.5. Standstill Performance³

Putting $v=0$ and neglecting x_{sm} , the mutual reactance between the main and starting winding due to the flux which do not cross the air gap (more over as d is not much different from 90°) we obtain from equations (17), and (18).

$$e_m = \left[r_m + j x_m + \sum \left(j X_{Mn} + \frac{X_{Mn}^2}{r_{rn} + j X_{rn}} \right) \right] i_m$$

$$+ \left[\sum \left(j X_{Mn} \cos n\alpha + \frac{X_{Mn}^2 \cos n\alpha}{r_{rn} + j X_{rn}} \right) \right] a i_s \dots (27)$$

$$e_s = \left[\sum \left(j X_{Mn} \cos n\alpha + \frac{X_{Mn}^2 \cos n\alpha}{r_{rn} + j X_{rn}} \right) \right] a i_m$$

$$+ \left[\frac{r_s + j x_s}{a^2} + \sum \left(j X_{Mn} + \frac{X_{Mn}^2}{r_{rn} + j X_{rn}} \right) \right] a^2 i_s \dots (28)$$

The two stator windings are assumed to have identical layout, thus making the effective turns ratio 'a' independent of the harmonic winding factors.

In the starting winding circuit a phase converter is put, having Z_0 impedance. With v_s supply voltage,

$$e_m = \sqrt{v_s} \dots (29)$$

$$e_s = v_s - i_s Z_0 \dots (30)$$

$$\text{Let } \frac{r_s + j x_s + Z_0}{a^2} = (r_m + j x_m + Z) \dots (31)$$

Solving for i^m and i^s

$$i^m = \frac{v_s}{a} \cdot \frac{a(Z + Z_0) - \sum (Z_n \cos n \alpha)}{(Z + Z_0)Z_0 - [\sum Z_n \cos n \alpha]^2} \dots (32)$$

$$i^s = \frac{v_s}{a^2} \cdot \frac{Z_0 - a \sum (Z_n \cos n \alpha)}{(Z + Z_0)Z_0 - [\sum Z_n \cos n \alpha]^2} \dots (33)$$

$$\begin{aligned} \text{Where } Z_0 &= r_m + j x_m + \sum \left(j X_{Mn} + \frac{X_{Mn}^2}{r_{rn} + j x_{rn}} \right) \\ &= (R_0 + j X_0) \text{ say} \end{aligned}$$

$$\begin{aligned} \text{and } Z_n &= \sum \left(j X_{Mn} + \frac{X_{Mn}^2}{r_{rn} + j x_{rn}} \right) \\ &= (R_n + j X_n) \text{ say} \end{aligned}$$

From the torque expression of equation (26) the standstill torque, when the fundamental space angle between the two stator winding is α , may be found as

$$T_\alpha = 2 a I^m I^s \sin \phi \sum n R_n \sin n \alpha \dots (34)$$

$$\text{Say } Z_0 = |Z_0| \angle -\phi_0$$

$$\text{and } Z = |Z| \angle -\beta$$

$$y \angle -\delta = \frac{Z}{Z_0} \angle -\beta + \phi_0$$

$$\text{and } x \angle -\gamma = \left| \frac{\sum Z_n \cos n \alpha}{Z_0} \right| \angle -\phi_x + \phi_0$$

$$-\phi_x \text{ being the argument of } \sum (Z_n \cos n \alpha)$$

Hence after simplification,

$$I^M \cdot I^S \cdot \sin \phi = \frac{-v_s^2}{a^2 Z_0^2} \left[\frac{a^2 x \sin \gamma + ay \sin \delta - x \sin \gamma + a^2 y x \sin(\gamma - \delta)}{1 + y^2 + x^2 + 2yx \cos(\delta - 2\gamma) - 2x^2 \cos 2\gamma + 2y \cos \delta} \right] \dots\dots(35)$$

Under 2-phase balance operation with two identical windings in space-quadrature

$$I_b^M = \frac{v_s}{Z_0} \mid \phi_0$$

$$I_b^S = \frac{v_s}{Z_0} \mid 90^\circ + \phi_0$$

$$\text{and } \sin \phi_b = -1$$

Hence from (34)

$$\left[\frac{T_d}{T_b} \right]_n = \frac{\sin n\alpha}{\sin \frac{n\pi}{2}} \left[\frac{(a^2 - 1)x \sin \gamma + ay \sin \delta + a^2 y x \sin(\gamma - \delta)}{1 + y^2 + x^2 + 2y \cos \delta - 2yx \cos(\delta - 2\gamma) - 2x^2 \cos 2\gamma} \right]$$

$$\approx \frac{\sin n\alpha}{\sin \frac{n\pi}{2}} \left[\frac{ay \sin \delta + a^2 y x \sin(\gamma - \delta)}{a^2 [1 + y^2 + 2y \cos \delta]} \right] \dots\dots(36)$$

Neglecting x^2 and $(a^2 - 1)x \sin \gamma$

$$\text{Also } \left[\frac{T_{90^\circ}}{T_b} \right]_n = \frac{y \sin \delta}{a(1 + y^2 + 2y \cos \delta)} \dots\dots(37)$$

For the maximum $\left(\frac{T_d}{T_b} \right)$ ratio, the first differentiation

of equation (36) is equated to zero which gives

$$y = 1$$

$$\text{i.e. } |Z| = |Z_0| \dots\dots(38)$$

From (36) and (37)

$$\left[\frac{T_d}{T_{90^\circ}} \right]_n = \frac{\sin n\alpha}{\sin \frac{n\pi}{2}} \left[1 + ax \sin(\gamma - \delta) \cos \alpha \cos \delta \right] \dots\dots(39)$$

For resistance start

$$Z \approx R, \quad \beta \approx 0^\circ$$

$$\therefore \left[\frac{T_\alpha}{T_{90^\circ}} \right]_n = \frac{\sin n \alpha}{\sin n \frac{\pi}{2}} \left[1 - \frac{a}{X_0} \sum_{n=2}^{\infty} X_n \cos n \alpha \right] \quad \dots (40)$$

For pure capacitor start,

$$Z \approx \frac{-j}{c\omega}, \quad \beta = \frac{\pi}{2}$$

$$\therefore \left[\frac{T_\alpha}{T_{90^\circ}} \right]_n = \frac{\sin n \alpha}{\sin n \frac{\pi}{2}} \left[1 - \frac{a}{R_0} \sum R_n \cos n \alpha \right] \quad \dots (41)$$

The above two expressions are true when the deviation of the angle between the stator windings from 90° is small.

In wound rotor machines, the higher harmonics of stator m.m.f produce negligible reaction in the rotor. Hence the torque of such machines is entirely due to the fundamental m.m.f, and

$$\sum R_n \cos n \alpha \approx R_1 \cos \alpha$$

$$\text{Hence } \left[\frac{T_\alpha}{T_{90^\circ}} \right] = \sin \alpha (1 - a \sigma \cos \alpha) \quad \dots (42)$$

$$\text{Where } \sigma = \frac{R_1}{R_0}$$

Since R_1 is approximately equal to R_r , the rotor resistance per phase referred to the stator main-winding as in balanced 2-phase machines

$$\sigma = \frac{R_r}{R_r + r_m}$$

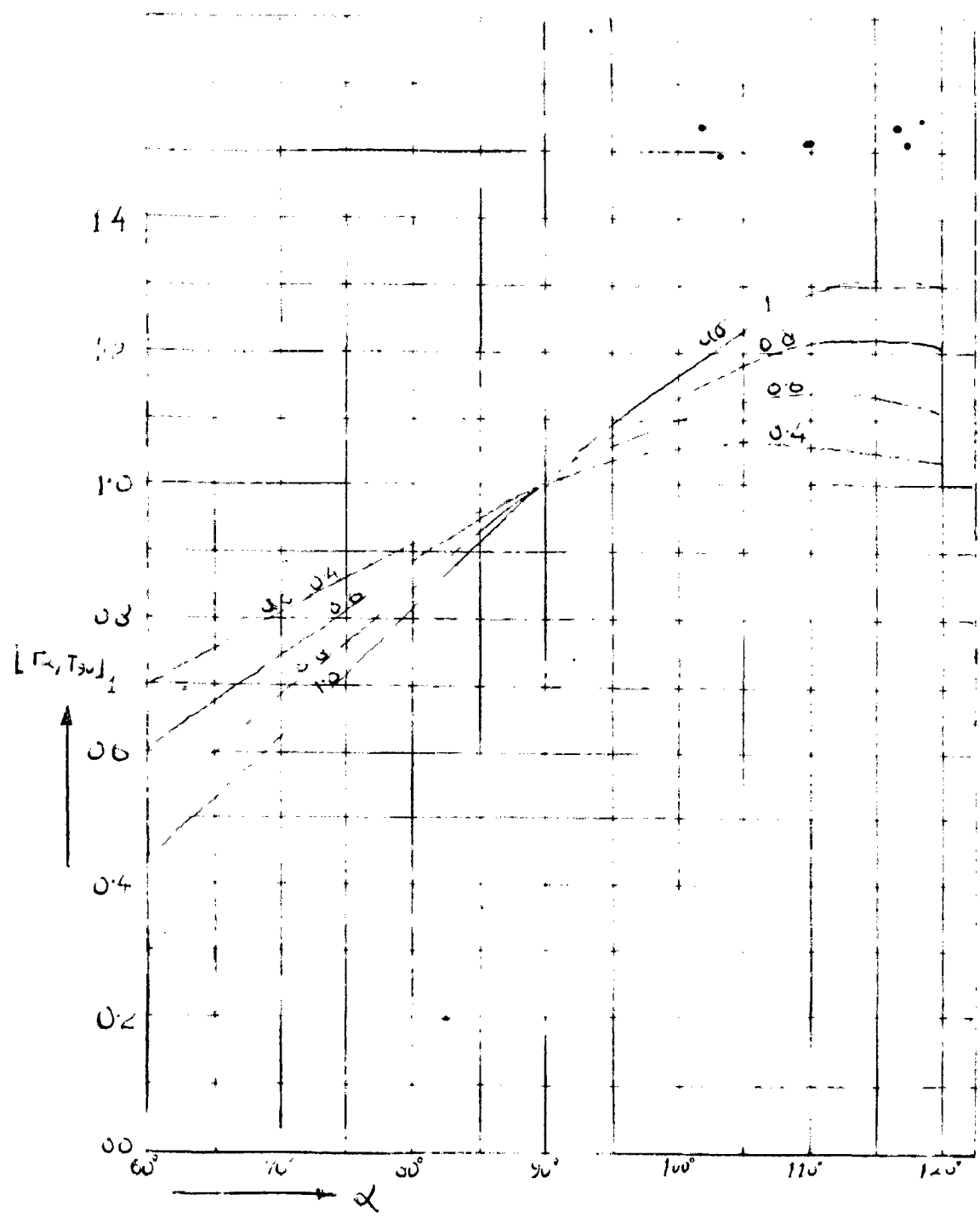


FIG 10 $[\Gamma_1 / T_{30}]_1$ vs α

For maximum $\frac{T_{\alpha}}{T_{90^{\circ}}}$ ratio

$$\alpha = \cos^{-1} \left[\frac{(1 - \sqrt{1 + 2a^2 \sigma^2})}{2a\sigma} \right] \quad \dots (43)$$

Since most induction machines have squirrel cage type rotors which react strongly to the harmonics of the air-gap field, equation (41) gives these torque variations with angle. The term $\left(\frac{\sum R_n \cos n\alpha}{R_0} \right)$ is usually not much different from $\frac{R_1}{R_0} \cos \alpha$ i.e. $\sigma \cos \alpha$ even in presence of harmonics.

Hence $\left[\frac{T_{\alpha}}{T_{90^{\circ}}} \right]_n \approx \frac{\sin n\alpha}{\sin n \frac{\pi}{2}} \left[1 - a\sigma \cos \alpha \right] \quad \dots (44)$

From equation (31) and (38) it is seen that the optimum capacitor for maximum starting torque is inversely proportional to a^2 where as from equation (37) the maximum starting torque is inversely proportional to 'a'. To satisfy this twin criteria of ^{large} starting torque and a small starting capacitor the value of 'a' in capacitor start motors is usually limited to a maximum of about 2. The value of ' σ ' is fairly low, between 0.2 to 0.4, because of the use of low resistance rotors in order to ensure sufficient pull-out torque and to minimise the backward field losses. The maximum $a\sigma$ is thus 0.8, with the result that about 21% more starting torque is possible by use of α greater than 90° .

Starting Currents

From equations (32),

$$I_d^m = \frac{V_s}{aZ_0} \left[\frac{a^2 + x^2 + a^2y^2 + 2a^2y \cos \delta - 2ax \cos \gamma - 2axy \cos (\gamma - \delta)}{1 - y^2 + x^2 + 2y \cos \delta - 2yx^2 \cos (\delta - 2\gamma) - 2x^2 \cos 2\delta} \right]^{1/2}$$

Hence ,

$$I_{90^\circ}^m = \frac{V_s}{aZ_0} \left[\frac{a^2 (1 + y^2 + 2y \cos \delta)}{1 + y^2 + 2y \cos \delta} \right]^{1/2}$$

$$= \frac{V_s \cdot a}{Z_0}$$

$$\therefore \left[\frac{I_d^m}{I_{90^\circ}^m} \right] \approx \left[1 - \frac{2x}{a} \left\{ \cos \gamma + y \cos (\gamma - \delta) \right\} \right]^{1/2} \dots (45)$$

Neglecting x^2 terms for $60^\circ < \alpha < 120^\circ$

From equation (33),

$$I_d^s = \frac{V_s}{aZ_0} \left[\frac{1 + a^2x^2 - 2ax \cos \gamma}{1 + y^2 + x^2 + 2y \cos \delta - 2yx^2 \cos (\delta - 2\gamma) - 2x^2 \cos 2\gamma} \right]^{1/2}$$

$$I_{90^\circ}^s = \frac{V_s}{aZ_0} \left[1 + y^2 + 2y \cos \delta \right]^{-1/2}$$

$$\therefore \left[\frac{I_d^s}{I_{90^\circ}^s} \right] \approx (1 - 2ax \cos \gamma)^{1/2} \dots (46)$$

1.6 Running Performance^{3,4,6}

1.6 A. Dips in Torque-speed Curve due to Space-Harmonics^{3,6}

The air-gap field of the nonquadrature winding single phase induction motor contains a large number of space harmonic flux waves of appreciable proportions. In case of the wound type machine the rotor responds mainly to the fundamental space-harmonic flux but in the case of cage type machines the rotor reacts strongly to these space harmonics, as a result the torque-speed curve is very much affected. The principle effect of these harmonics is to produce harmonic dips in the torque-speed curve and hence they increase the possibility of the motor to crawl at low speeds. Hence reduction in this harmonic effect is highly desirable.

This dip is due to the forward component of the harmonic m.m.f. It is possible to eliminate it at its own synchronous speed by proper selection of the starting capacitor for any angle between the stator windings.

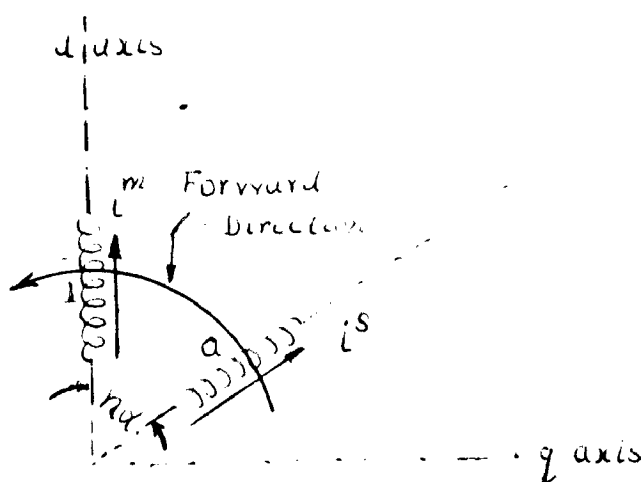


FIG. 11. Two Stator Windings, Displaced By An Angle α For The n^{th} Space Harmonic

Resolving the nth space harmonic mmf along the d- and q- axes

$$H_{dn} = C_n \left[i^m + a i^s \cos nd \right]$$

$$H_{qn} = C_n \left[+ a i^s \sin nd \right]$$

Where C_n is a constant.

To cancel the forward component of the nth harmonic field

$$\frac{H_{dn}}{H_{qn}} = 1 \quad | \pi | 2$$

$$\text{Hence, } i^m = a i^s \quad | \pi - nd | \quad \dots \dots (47)$$

Where b is any odd-integer.

From equations (17) and (18),

$$e_m = Z_{mm} i^m + Z_{ms} i^s \quad \dots \dots (17)$$

$$e_s = Z_{sm} i^m + Z_{ss} i^s \quad \dots \dots (18)$$

$$\text{Where } Z_{mm} = \left[r_m + j x_m + \sum_1^n \left\{ (j X_{Mn} + j x_{smn}) + \frac{X_{Mn}^2 Z_{rn}}{Z_r^2 n - n^2 v^2 R_r^2} \right\} \right]$$

$$Z_{ss} = \left[r_s + j x_s + \sum_1^n \left\{ j (X_{Mn} + x_{smn}) a^2 + \frac{a^2 X_{Mn}^2 Z_{rn}}{Z_r^2 n - n^2 v^2 R_r^2} \right\} \right]$$

$$Z_{ms} = \left[Z \left\{ j (X_{Mn} + x_{smn}) a \cos nd + \frac{a X_{Mn}^2 (Z_{rn} \cos nd + j n v R_{rn} \sin nd)}{Z_r^2 n - n^2 v^2 R_r^2} \right\} \right]$$

$$Z_{sm} = \left[Z \left\{ j (X_{Mn} + x_{smn}) a \cos nd + \frac{a X_{Mn}^2 (Z_{rn} \cos nd + j n v R_{rn} \sin nd)}{Z_r^2 n - n^2 v^2 R_r^2} \right\} \right]$$

'a' has been assumed to be independent of the winding-factor.

But $e_m = v_s$

$$e_s = v_s - Z_c i^s$$

By putting $\frac{r_s + j x_s + Z_c}{a^2} = r_m + j x_m + Z$

$$\frac{i^m}{i^s} = \frac{a^2 (Z_{mm} + Z) - Z_{ms}}{Z_{mm} - Z_{ms}} \dots\dots (48)$$

Hence from equation (47) and (48) we get

$$Z_c = \left[- Z_{mm} (a^2 + a \cos n\alpha) + Z_{ms} + a Z_{sm} \cos n\alpha \right] \dots\dots (49)$$

Here the parameters are at ^{the} synchronous speed of the nth space harmonic. Generally the mutual impedance terms are quite small compared to the ^{self} term even up to the 3rd harmonic synchronous speed that these may be neglected safely. Then the capacitor reactance is

$$X_c = (a^2 + a \cos n\alpha) X_{mm} - (a \sin n\alpha) R_{mm} \dots(50)$$

Where $Z_{mm} = R_{mm} + j X_{mm}$

From Equation (47) $\phi = (b\omega - n\alpha)$

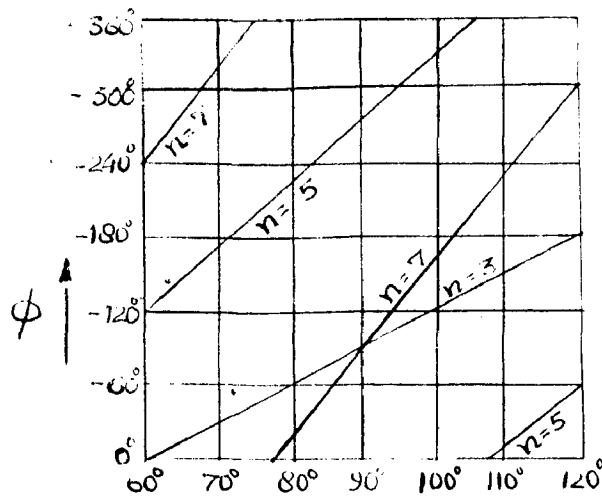


FIG. 12

Fig. 12 shows the values of ϕ required to suppress the ~~forward~~^{forward} component of the 3rd, 5th and 7th harmonic field for values of α between 60° and 120° .

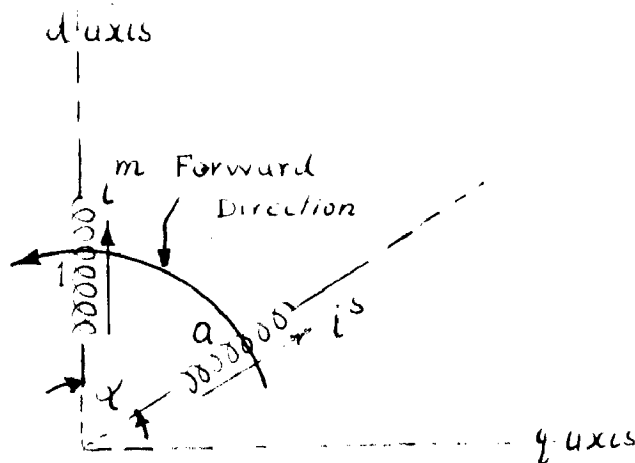
From equation (34) it is clear that with I^m , I^s and α fixed, the starting torque is maximum when $\phi = 90^\circ$. It may be proved as in 5(b) that for pure fundamental forward field ϕ should be equal to $(-\pi + \alpha)$. Hence ϕ will vary from -60° to -120° for the above limits of α , then only we will get sufficient found. forward torque.

Now it may be noted from Fig. 12 that the forward component of the 5th space- space harmonic can not be suppressed by this method, while those of 3rd and 7th can be suppressed only if α is between 80° and 100° for 3rd space harmonic and between 85° to 95° for the 7th space harmonic.

A proper selection of α and the capacitor can thus help to suppress the forward 3rd or 7th harmonic field if either of these is present in the mmf wave of the individual winding.

1.6(B) Determination of the Running Capacitor for Balanced Operation ^{3,4,6}

This is done almost on the same lines as for dip-reduction.



To obtain a perfect balance operation at any speed, so far as the fundamental field is concerned, a critical running capacitor may be found for any angle between the stator windings.

Again, resolving the fundamental mmf along the d - and q -axis

$$\begin{aligned} H_d &= C_1 \left[i^m + a i^s \cos \alpha \right] \\ H_q &= C_1 \left[a i^s \sin \alpha \right] \end{aligned}$$

For balanced operation

$$\frac{H_d}{H_q} = 1 \quad \left| \frac{-\pi/2}{} \right.$$

Hence

$$i^m = a i^s \left| \frac{-b\pi + \alpha}{} \right. \quad \dots\dots (51)$$

Where b is any odd integer.

Hence

$$Z_c = - Z_{mm} (a^2 + a \left| \frac{\alpha}{} \right.) + Z_{ms} \frac{-\pi + \alpha}{} + a Z_{sm} \left| \frac{\alpha}{} \right. \quad \dots\dots(52)$$

The parameters are calculated or measured at the desired speed. At high speeds the mutual impedance terms have quite large values and so these cannot be neglected.

Whereas in a capacitance-start motor the starting winding is designed on starting-torque considerations, in a capacitance-start and-run motor it is designed to simulate, with the assistance of an appropriate capacitor, a nearby balanced 2-phase operation of the machine under load. This makes 'a', the turns-ratio a function of the power-factor.

From equation (51), for $b = 1$

$$i^s = - \frac{1}{a} i^m e^{-j\alpha}$$

$$\text{Hence } \phi_m = \left(Z_{ms} + Z_{ms} \cdot \frac{-1}{a|d|} \right)$$

$$\text{Let } Z_{ms} + Z_{ms} \frac{-1}{a|d|} = Z_1 | \underline{\phi}_1$$

Where ϕ_1 is the p.f. angle of main-winding
Equation (52) may be put in the form

$$Z_c = -a^2 \left[Z_{ms} - \frac{Z_{ms}}{a} |d| \right] = a|d| \left[Z_{ms} - \frac{Z_{ms}}{a} |d| \right]$$

Only for a particular case of $\alpha = 90^\circ$,

$$Z_1 | \underline{\phi}_1 = Z_{ms} + j \frac{Z_{ms}}{a} ; Z_{ms} = -Z_{ms}$$

$$\text{and } Z_c = -(a^2 + ja) (Z_1 | \underline{\phi}_1)$$

$$\text{Say } Z_c = Z_c | \underline{-\beta}$$

$$\text{Hence } \left| \frac{Z_c}{Z_1} \right| | \underline{-(\beta + \phi_1)} = -a(a + j)$$

On solving for a and $\left| \frac{Z_c}{Z_1} \right|$ we get

$$A = -\cot \epsilon (\beta + \phi_1) \dots \dots \dots (53)$$

$$\text{and } \left| \frac{Z_c}{Z_1} \right| = a \sqrt{1 + a^2} \dots \dots \dots (54)$$

In capacitor start and run motors i^s usually has a lead angle of approximately 30° with reference to supply voltage and i^m lags the supply voltage by a p.f. of 0.6 to 0.85 β is nearly 90° for a capacitor phase convertor.

Hence 'a' will have values between 0.6 to 1.35

For space angles slightly different from 90° , say 80° and 100° to a good approximation 'a' may be said to have the same range.

It may be pointed out here that with maximum 'a' of about 1.35 and ' σ ' of 0.4, a maximum of 0.54 a σ is obtained and hence about 11% more starting torque is possible in capacitance start and run motors through the use of a space angle α greater than 90° .

1.7 Equivalent Quadrature Machine for A Non-Quadrature Machine

When the nonquadrature machine comes up to speed, it is the fundamental which is mainly responsible for the torque production. In this near synchronous speed region the harmonic effect may be neglected without much error.

With this simplification the machine performance equation may be put into a more compact form and a simpler equivalent circuit results. It is thus possible to find out a machine with the stator windings in quadrature which is equivalent to the machine with nonquadrature stator windings.

Let us replace the mmf of individual stator windings of a machine with nonquadrature stator windings by resultant mmf along two quadrature axes, main winding axis being the direct axis.

i^M , and i^S , the currents of the main and starting windings are replaced by two new currents i^{ds} and i^{qs} such that

$$i^{ds} = i^M + a i^S \cos \alpha \quad \dots (55)$$

$$\text{and } i^{qs} = a i^S \sin \alpha \quad \dots (56)$$

In the impedance matrix i^S and i^{qs} are appearing as $j i^S$ and $j i^{qs}$

Hence

$$i^{ds} = i^M - j a (j i^S) \cos \alpha$$

$$j i^{qs} = a (j i^S) \sin \alpha$$

$$i^{dr} = i^{dr}$$

$$j i^{qr} = j i^{qr}$$

Then the matrix connecting these variables is

$$C_1 = \begin{array}{c|cccc} & m & s & dr & qr \\ \hline ds & 1 & -j a \cos \alpha & & \\ \hline qs & & a \sin \alpha & & \\ \hline dr & & & 1 & \\ \hline qr & & & & 1 \\ \hline \end{array} \dots (57)$$

and $i^m = i^{ds} + j (j i^{qs}) \cos \alpha$

$$j i^s = j i^{qs} / a \sin \alpha$$

$$C_2 = \begin{array}{c|cccc} & ds & qs & dr & qr \\ \hline m & 1 & j \cot \alpha & & \\ \hline s & & \frac{1}{a \sin \alpha} & & \\ \hline dr & & & 1 & \\ \hline qr & & & & 1 \\ \hline \end{array} \dots (58)$$

Hence the new impedance matrix will be

$$Z = C_{2t}^* Z_0 C_2, \quad Z_0 \text{ from equation (9)}$$

	ds	qs	dr	qr
ds	$Z_{ds} + Z'_m$	jZ'_m	jX_M	.
qs	$-jZ'_m$	$Z_{qs} + Z'_m$		jX_M
dr	jX_M		$\frac{r_r}{1-v^2} + jX_r$	$v \frac{r_r}{1-v^2}$
qr		jX_M	$v \frac{r_r}{1-v^2}$	$\frac{r_r}{1-v^2} + jX_r$

... (59)

Where

$$Z_{ds} = r_m (1 - \cot \alpha) + j x_m (1 - \cot \alpha) + j x_{sm} + j X_M$$

$$= r_{ds} + j x_{ds} + j X_M \quad (\text{say})$$

$$Z_{qs} = \frac{r_s}{a^2 \sin^2 \alpha} + r_m \cot \alpha (\cot \alpha - 1)$$

$$+ j \left[\frac{x_s}{a^2 \sin^2 \alpha} + x_m (\cot \alpha - 1) \right] + j X_M$$

$$= r_{qs} + j x_{qs} + j X_M \quad (\text{say})$$

$$Z'_m = (r_m + j x_m) \cot \alpha$$

The new voltage matrix

$$e = C_{2t}^* e_5$$

	ds	qs	dr	qr
e	e_m	$j(e_s / a \sin \alpha - e_m \cot \alpha)$		

In order to introduce the phase converter impedance Z_c

$$j \phi_{qs} = j (\phi_s / a \sin \alpha - \phi_m \cot \alpha)$$

$$\text{But } \phi_m = \phi_s + i_s Z_c$$

$$\text{Hence } j \phi_{qs} = j \phi_m \left(\frac{1}{a \sin \alpha} - \cot \alpha \right) - j i_s \frac{Z_c}{a \sin \alpha}$$

Substituting i_{qs} for i_s

$$j \phi_{qs} = j \phi_m \left(\frac{1}{a \sin \alpha} - \cot \alpha \right) - j i_{qs} \frac{Z_c}{a^2 \sin^2 \alpha} \dots (60)$$

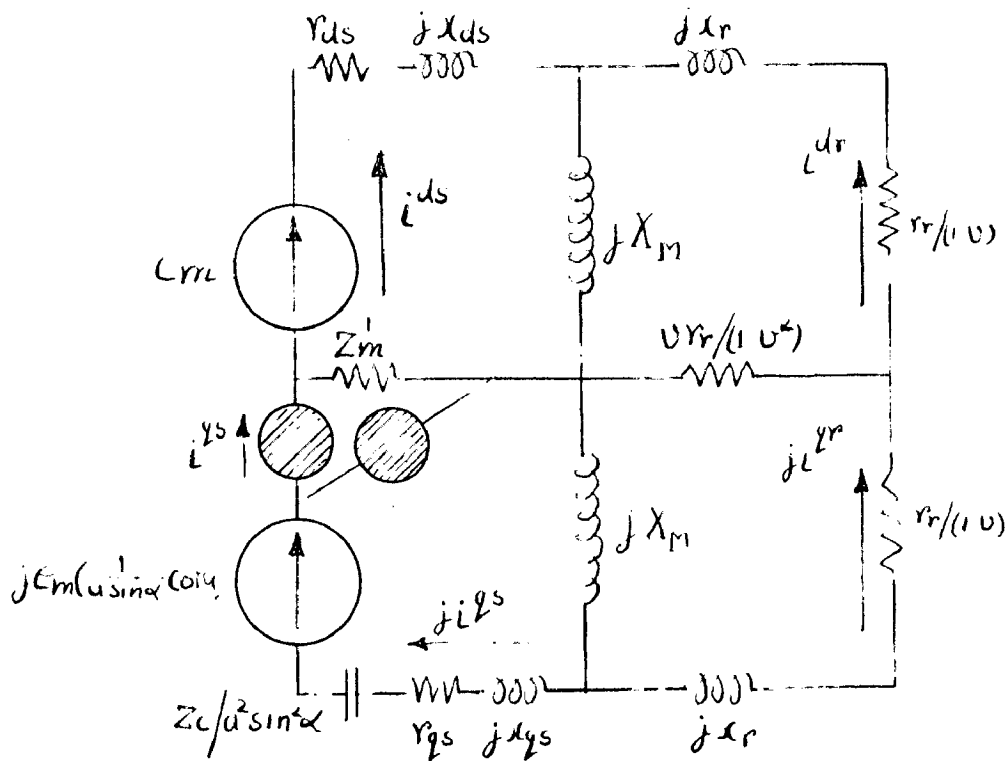


FIG. 14. Equivalent Circuit

PERFORMANCE OF EXPERIMENTAL MACHINE

SPECIFICATION OF EXPERIMENTAL MACHINE

3 phase, 440 volt, Delta connection, 2 horse power motor
Squirrel cage type rotor.

The machine has double layer winding, number of stator slots being 36. All the 36 coil ends are brought out to a circular terminal board. This makes it possible to connect the machine for various modes of operation. As a single phase machine, it was possible to have two stator-windings of equal number of turns with 60°, 80°, 100° and 120° space angle between them. But 90° space angle between the windings or turns-ratio other than unity was not possible.

The constants of the machine were determined by conventional tests. They are as follows :-

Leakage impedance of main winding

$$R_m + j X_m = (9.24 + j 7.37) \text{ ohms}$$

Rotor leakage impedance for fundamental (referred to the main-winding on stator)

$$R_r + j X_r = (4.21 + j 7.37) \text{ ohms}$$

Magnetising reactance for fundamental flux

$$j X_M = j 240 \text{ ohms}$$

Rotor leakage impedance for third-space harmonic (referred to Main-winding on stator)

$$R_{r_3} + j X_{r_3} = (0.572 + j 1.0) \text{ ohms}$$

Third harmonic magnetising reactance

$$j X_{M_3} = j 3.62 \text{ ohms}$$

Fifth and above space-harmonic constants are neglected as they are sufficiently small.

Chapter - 8

Standstill Starting Performance

In the following it is attempted to find a capacitor suitable for starting.

From equations (31) and (33), the optimum starting capacitor from starting torque consideration is given by the following relation.

$$|Z_0| = a^2 |Z_0|$$

Thus the optimum starting capacitor is a function of the standstill impedance of main-winding and the turn-ratio, being independent of the space angle between the stator-windings

The standstill impedance of the main winding Z_0 , by direct measurement -

$$Z_0 = 10.2 \text{ ohms}$$

Hence

$$Z_0 = 40.2a^2 \text{ ohms}$$

Table 2.1 Optimum Starting Capacitor

Turns-ratio a	1.0	1.2	1.4
Converter Impedance Z_0 ohms	10.2	23.4	33.7
Converter Capacity C μ F.	370	120	80

For unity turns-ratio machine two more values of starting capacitor are taken arbitrarily for comparison, one value above 175 microfarad i.e. 200 MF and the other below 175 MF i.e. 150 MF.

To determine the starting torques for different space angles between the ^{stator} starting windings, the machine was coupled to a well calibrated d.c. machine. The induction motor was run by the d.c. motor and braked by applying reduced single phase voltage to it. The resultant steady speed of the set under this situation was controlled by varying the voltage to the armature of this separately excited d.c. motor. A number of observations were taken at crawling negative speeds. The induction motor torque was calculated from the input to the d.c. machine and then referred to 300 volts, using a square proportionality of the induction motor voltage. Then by graphical extrapolation the starting torque was obtained.

Figure 2.1 to 2.4

All readings are converted to those for 300 volts because it is found during run-up tests that with lesser voltage the machine does not come up to speed while greater voltage will give rise to prohibitively large current.

Table 2.2 shows the starting torque for different space-angles between the stator-windings, and the starting capacitors for unity turns ratio.

80° SP. 13 . . . 0112

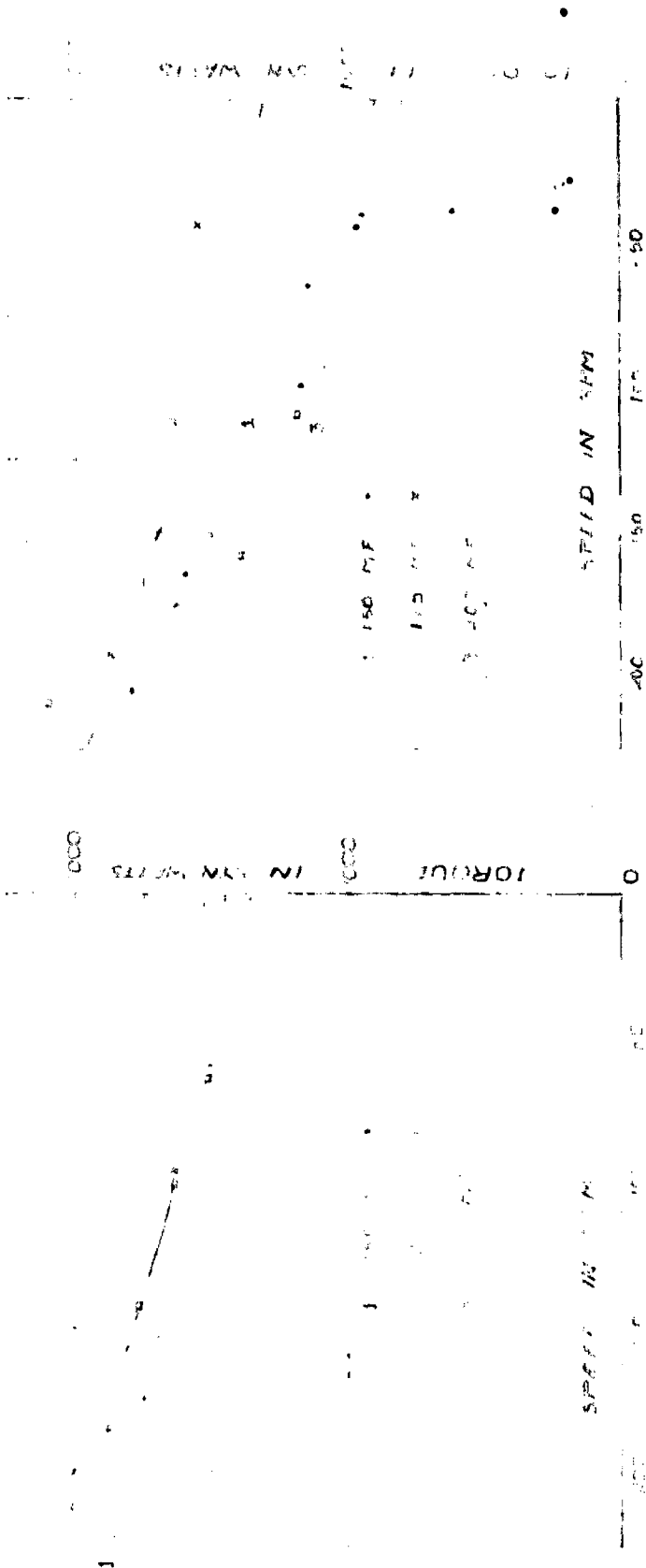


Table 2.2

Starting Torque in Dyn. Watts For Different Capacitors			
Winding Angle	100 MF Starting Capacitor	178 MF Starting Capacitor	200 MF Starting Capacitor
60°	1450	1525	1350
80°	850	1300	850
100°	1500	1600	1250
120°	1550	1700	1575

It is seen that a critical capacitor used in the starting winding circuit results in more starting torque than any other capacitor for any winding angle.

It is noted that the starting torques determined experimentally are quite different from the calculated values.

Following are the possible reasons for it : -

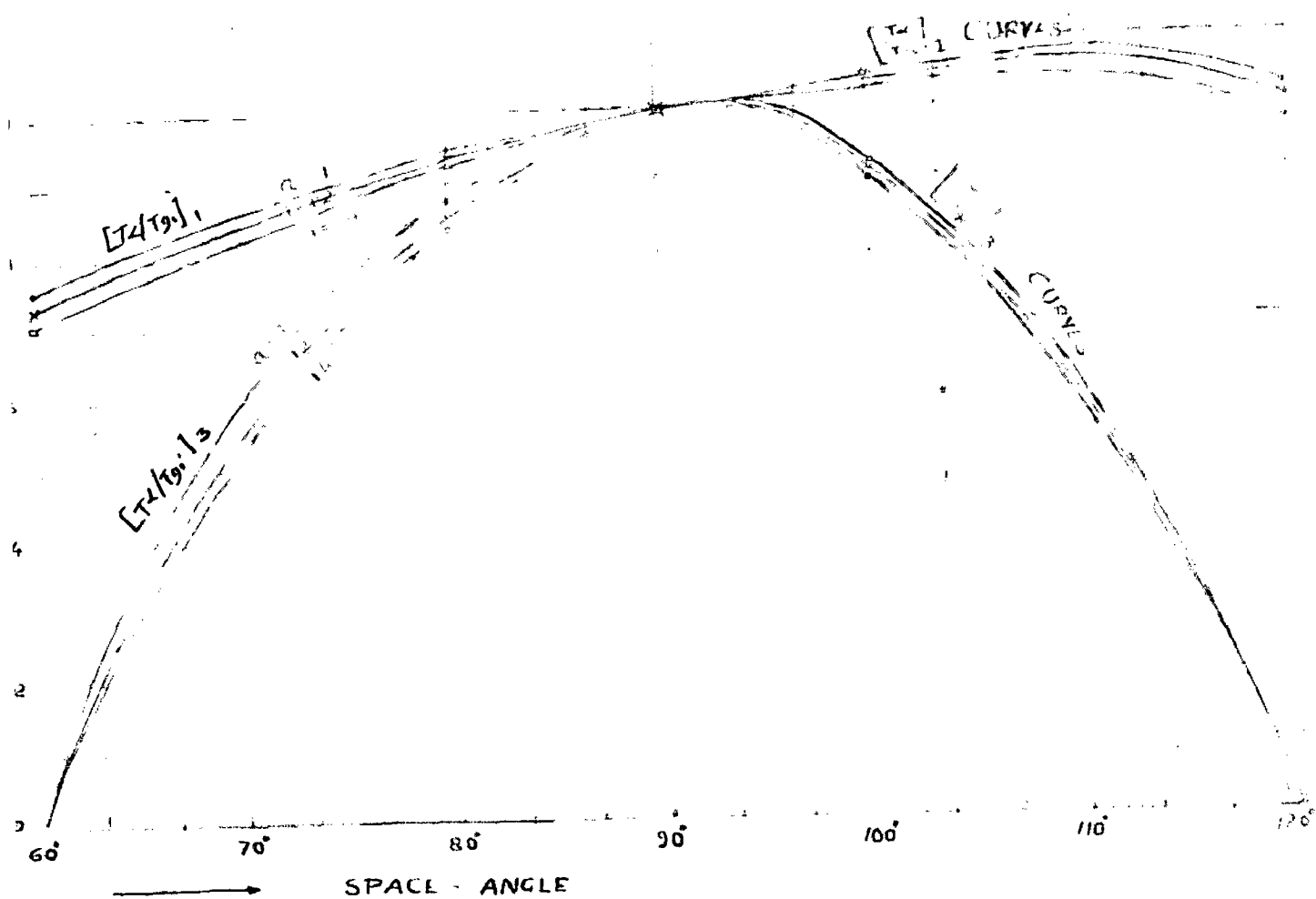
1. Low voltage (80 volts) was applied to the machine during the brake test because of current limitations. Hence developed torque and the friction windage torque were found to be of the same order. This leads to high errors when the friction-windage loss was subtracted from the input to the d.c. motor to obtain the useful power developed.

Further it was not possible, due to same reasons as above, to drive the machine steadily at forward crawling speeds. This leads to error while extrapolating the results for zero speed.

2. Rotor cross-current phenomenon⁹ - The calculations were made by assuming insulated bar rotor while it is not so. The cross-current phenomenon in the rotor produces detrimental effect, especially at lower and negative speeds. In case of small motors this effect is expected to be more pronounced. Hence the calculated values should be some what higher than the experimental values.

It will be interesting at this point to compare the fundamental and third space-harmonic standstill torque components for any space angle to the corresponding values for 90° space-angle between the windings. In the Figure 2.5 are drawn the $(T_d / T_{90^\circ})_1$ and $(T_d / T_{90^\circ})_3$ curves as a function of the space angle for different turns-ratios.

FIG. 2-5

 $\left[\frac{T_x}{T_{90^\circ}} \right]_1$ AND $\left[\frac{T_x}{T_{90^\circ}} \right]$ CURVES


It is seen that $(T_d/T_{90^\circ})_1$ reaches a maximum value for the space angle α above 90° . This space angle is approximately for turns-ratio equal to unity. For higher turns-ratio it increases very slightly. For space angles less than 90° $(T_d/T_{90^\circ})_1$ decreases very rapidly.

Maximum value of $(T_d/T_{90^\circ})_1$ increases with the turns-ratio. For $a = 1$ it is 1.04 and for $a = 1.4$ it is 1.06.

$(T_d/T_{90^\circ})_3$ reaches a maximum value^{1.02} for nearly 92° space angle between the windings and neither the maximum value nor the angle at which it occurs changes materially with the turns-ratio. For angles on either side of the maxima $(T_d/T_{90^\circ})_3$ decreases very rapidly, reaching zero value for both 60° and 120° space angle between windings.

Hence more fundamental torque can be obtained at starting by making the space-angle between the stator-windings greater than 90° . The net torque developed will, however, depend on the harmonic content of the air-gap field.

Total starting-torque per ampere line current is also calculated for all the cases. It is found from Table 2.3, 2.4 and 2.5 that its value with (say) optimum starting capacitor is always lower for the 90° space-angle, it increases on either side of 90° space-separation.

For 90° case T/I^2 does not change appreciably with the turns-ratio whereas for lesser angles it goes on decreasing with increase in turns-ratio but for angles higher than 90° it increases with turns-ratio. Hence this shows an advantage of using a space-angle between windings greater than 90° .

Table 2.3
Starting Performance As Calculated For Unity Turns-Ratio

Space Angle α	Capacitor (MF)	Starting Torque in Syn. Watts			Starting Current Amps.			%3rd Harmonic Dip	T/IL	T/Im ² +a ² Is ²
		T ₁	T ₂	T	Im	Is	IL			
60°	150	1890	0	1890	15.2	18.1	24.2	37.6	78.2	3.37
	175	1905	0	1905	14.6	19.7	27	34.0	70.5	3.19
	200	1815	0	1815	14.1	20.5	29.2	15.5	62.2	2.93
80°	150	2350	-560	1790	15.2	20.4	27.5	-	65	2.8
	175	2390	-560	1820	14.9	22	30.9	-	59	2.67
	200	2200	-520	1690	14.7	22.7	33	-	51	2.3
90°	150	2450	-645	1785	15.3	21.4	29.2	-	61.2	2.53
	175	2520	-670	1850	15.3	23.3	33	-	56.1	2.39
	200	2310	-620	1690	15.3	23.8	35.5	-	47.7	2.12
100°	150	2550	-610	1940	15.4	22.7	31	12	62.6	2.58
	175	2590	-605	1975	15.6	24.4	35	17.4	56.4	2.35
	200	2400	-560	1940	15.9	25	37.1	31	49.5	2.09
120°	150	2430	0	2430	15.8	24.9	34.7	132	70.2	2.8
	175	2490	0	2490	16.8	27.2	39.7	133	62.7	2.43
	200	2335	0	2335	17.6	29.1	42.6	133	54.8	2.12

Table 2.4

Starting Performance As Calculated for Turns-Ratio 1.32
(For Critical Starting Capacitor only)

Phase Angle α	Critical Capacitor (MF)	Starting Torque Syn. Watts			Starting Current (Amps)			%3rd Harmonic Dip.	$\frac{T}{I_L}$	$\frac{T}{I_M^2 + I_S^2}$
		T_1	T_2	T	I_M	I_S	I_L			
0°	120	1515	0	1515	14.6	13.1	22.2	30.2	68.2	3.29
5°	120	1940	-455	1485	14.9	15.1	25	-	59.5	2.7
10°	120	2100	-560	1540	15.3	16.2	26.7	-	57.7	2.53
15°	120	2170	-510	1660	15.5	17.1	28.2	19.6	59	2.51
20°	120	2150	0	2150	16.5	19.3	30.3	127	71	2.65

Table 2.5

Starting Performance As Calculated for Turns Ratio 1.4
(For Critical Starting Capacitor only)

Phase Angle α	Critical Capacitor (MF)	Starting Torque (Syn. Watts)			Starting Current (Amps)			% 3rd Harmonic Dip	$\frac{T}{I_L}$	$\frac{T}{I_M^2 + I_S^2}$
		T_1	T_2	T	I_M	I_S	I_L			
0°	90	1270	0	1270	14.9	9.4	20	26.4	63.7	3.23
5°	90	1650	-390	1260	15	11	21.8	-	58	2.75
10°	90	1800	-490	1320	15.3	11.8	23.1	-	57.3	2.6
15°	90	1900	-445	1455	15.5	12.7	24.3	27.5	60.1	2.61
20°	90	1880	0	1880	16.3	14.6	27.3	121	69.3	2.78

Also developed torque per watt power loss in the stator copper is calculated or actually $T/I^2 + a^2 I_s^2$ value was calculated. Again 90° case gives poor values. 100° space-angle is very much similar to 90° case but for angles beyond 100° and less than 90° there is much increase in torque per watt power loss in stator copper. For higher turns-ratio the nature of variation still holds, except that there values go on improving for all space-angles.

Chapter - 3

Run Up Performance

The main point of interest here is to study the torque-speed characteristics of the machine during run-up with different space angles between the stator-windings and different starting capacitors.

The torque-speed characteristics were mathematically obtained from the machine performance equations as well as experimentally determined for unity turns-ratio case.

Description of the Experimental Set-up for the Determination of Torque-speed Curves

As seen in Fig. 3.1 a small d.c. machine was coupled to the induction motor and separately excited. The voltage of the d.c. machine thus gives the speed signal and is applied to the X-plates of an oscilloscope. A capacitor of 200 microfarad was connected across the armature of d.c. machine, in series with a resistor of about 100 ohms. The capacitor-resistor acts as a differentiating circuit and thus the voltage across the resistor is proportional to acceleration and hence torque. This torque signal was applied to the Y-plates of the oscilloscope. To amplify the torque-signal d.c. amplification inherent to the oscilloscope was used.

Hence as the induction motor speeds up from rest to full-speed a trace of torque versus speed is obtained on the screen of the oscilloscope. The display of the spot was filmed by

an ordinary camera. Except for the starting-torque the system has worked exceedingly well.

This particular method of recording the torque-speed curve was employed because the machine used to draw quite large current, much greater than its rated current, or otherwise at lower voltages it never came to speed. Thus steady-state test for finding torque speed relation over whole speed range was not possible.

The torque-speed curves are quite comparable with those obtained from the machine performance equations.

3.1 Run-up performance with Starting-Capacitors

(A) 60° Space Angle :-

The third space harmonic dip is found to decrease with increase in the starting capacitor, dip becomes quite large with 150 MF capacitor.

Experimentally there is also found the fifth space-harmonic dip appearing at just above 300 rpm though of smaller magnitude the dip is found to increase with starting capacitor.

The calculated torque-speed curves (Fig. 3.2) compares well with the experimental curves (Fig.3.2 a,b and c) Fifth space harmonic was neglected in calculations.

From calculations it is also seen that the third harmonic dip calculated as a percentage of the fundamental torque at 500 rpm (the Syn. speed for third space harmonic), decreases slowly with increase in turns-ratio with corresponding critical capacitors. Refer to Tables 2.3,2.4 and 2.5 as well as the Fig. 3.3

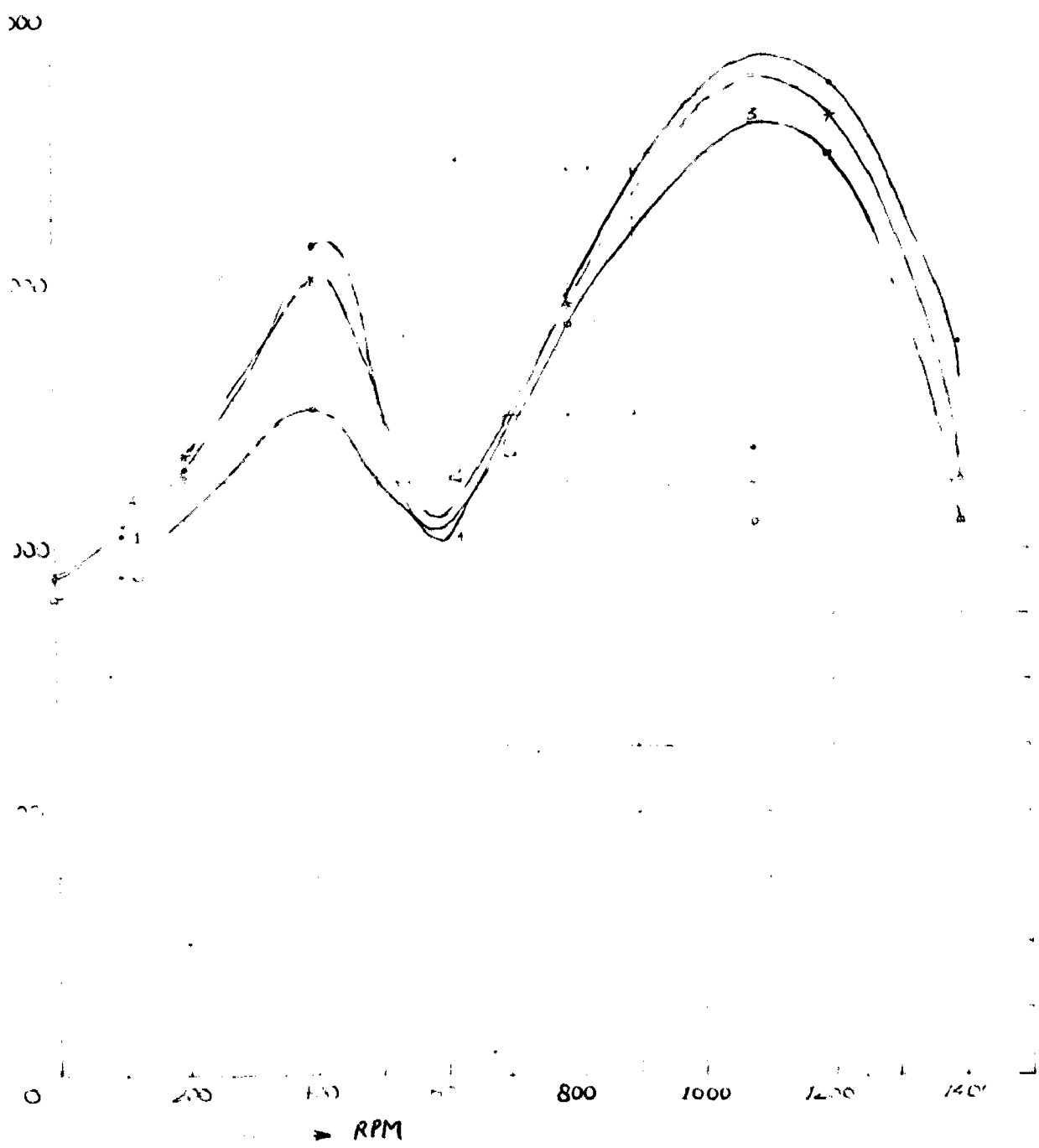


FIG. 3.2 (a)
P.O. (G.M.)

$\alpha = 60^\circ$, 240 MP

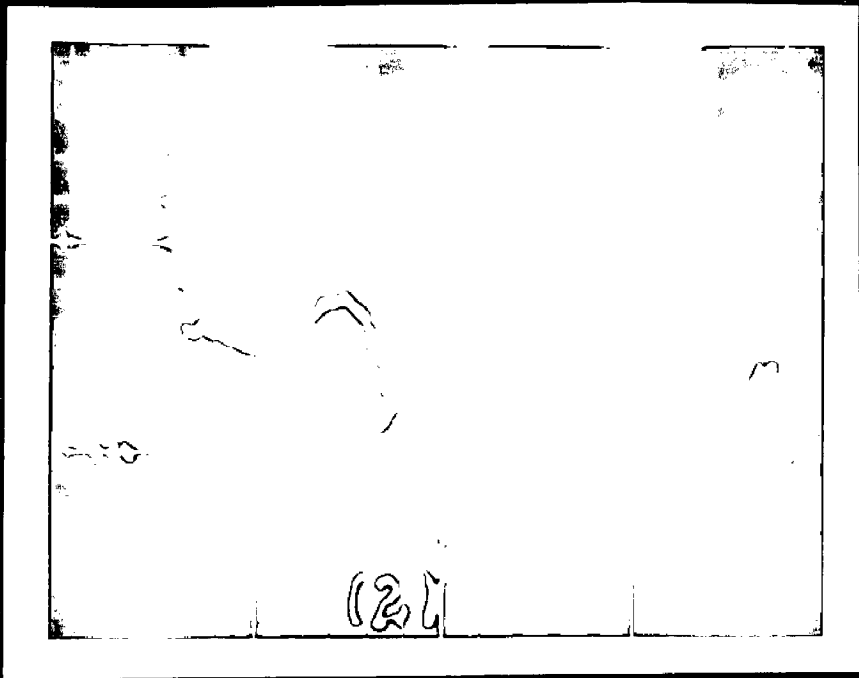
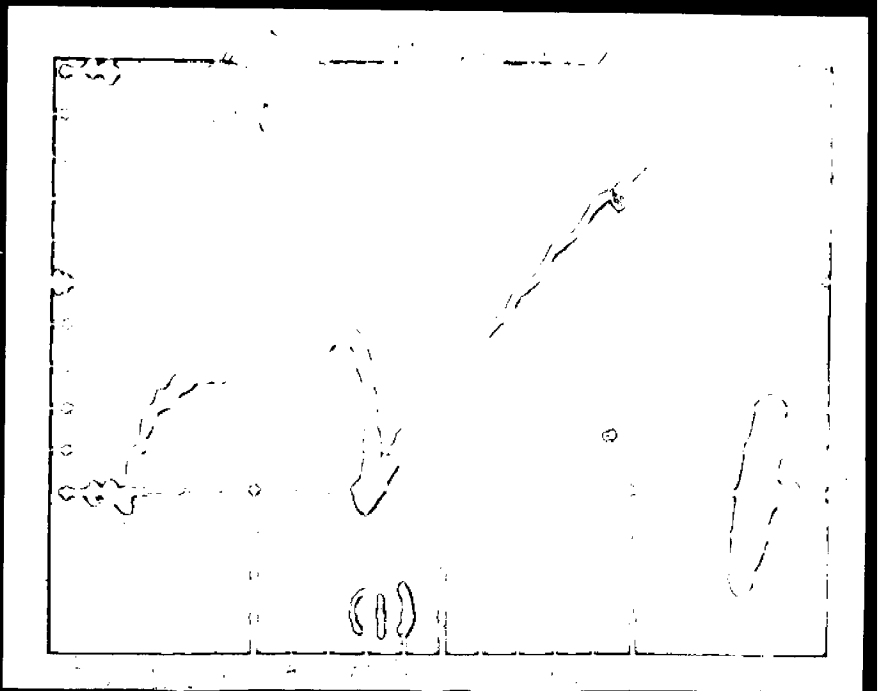
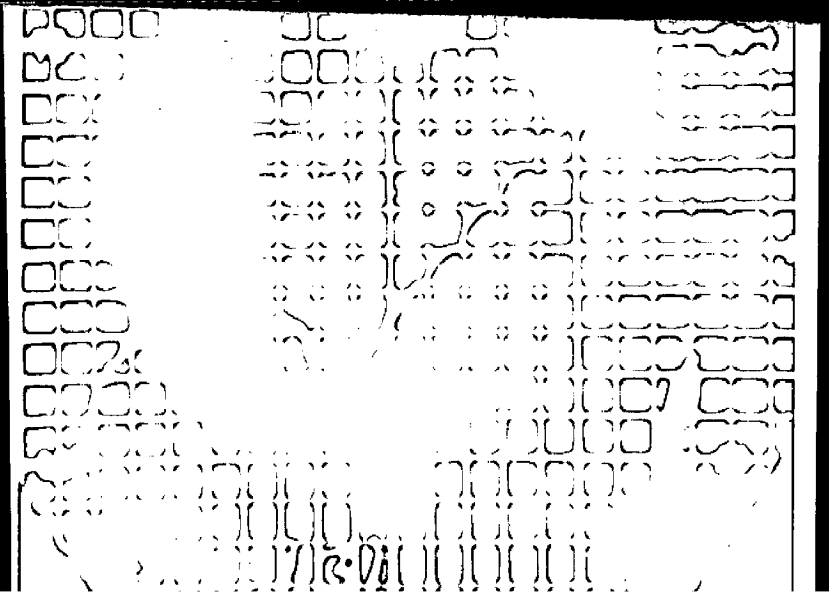


FIG. 3.2 (b)
P.O. (G.M.)

$\alpha = 60^\circ$, 170 MP

FIG. 3.2 (c)
P.O. (G.M.)



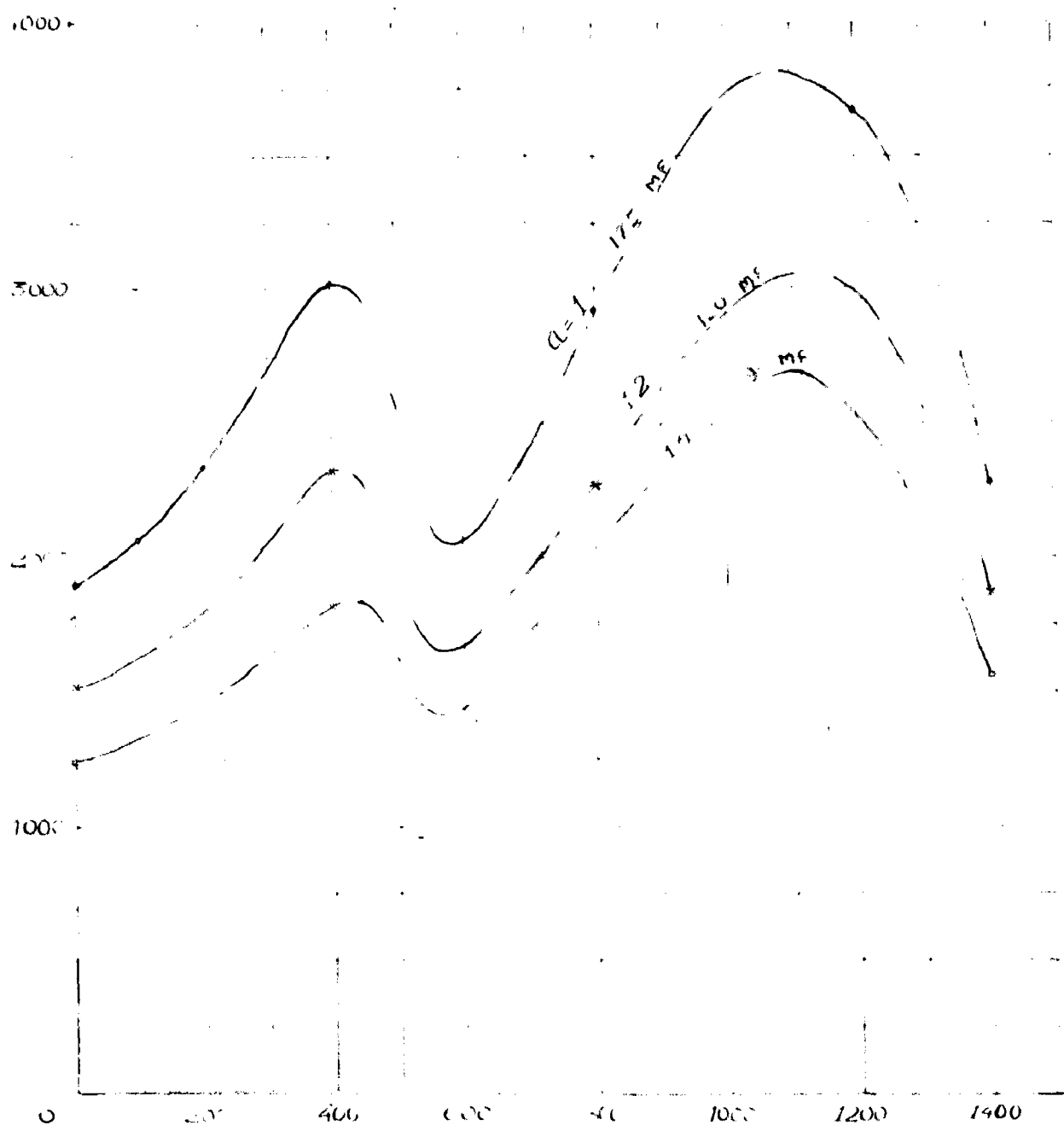


FIG 3.4 (a)
T.-S CURVE
 $\alpha = 80^\circ, 150 \text{ MF}$

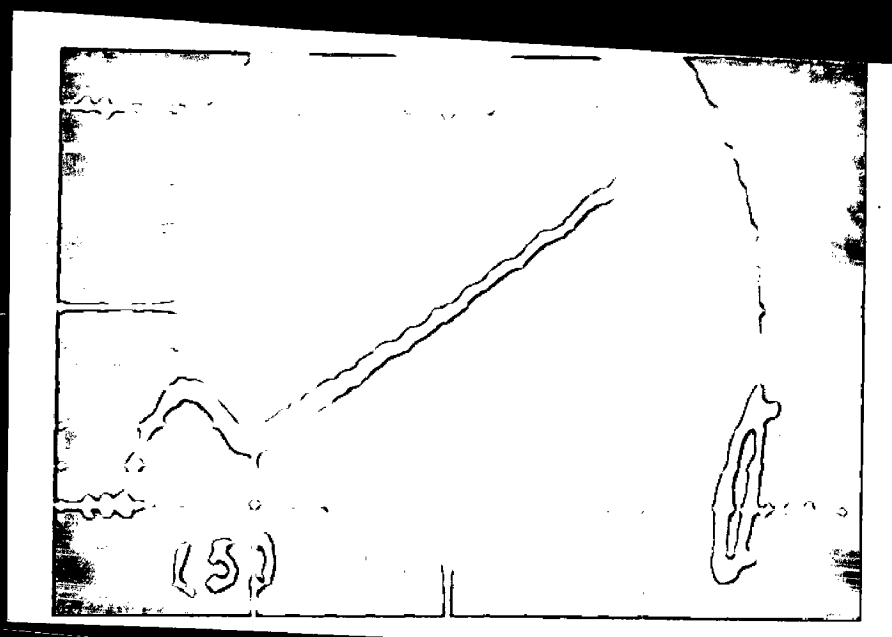
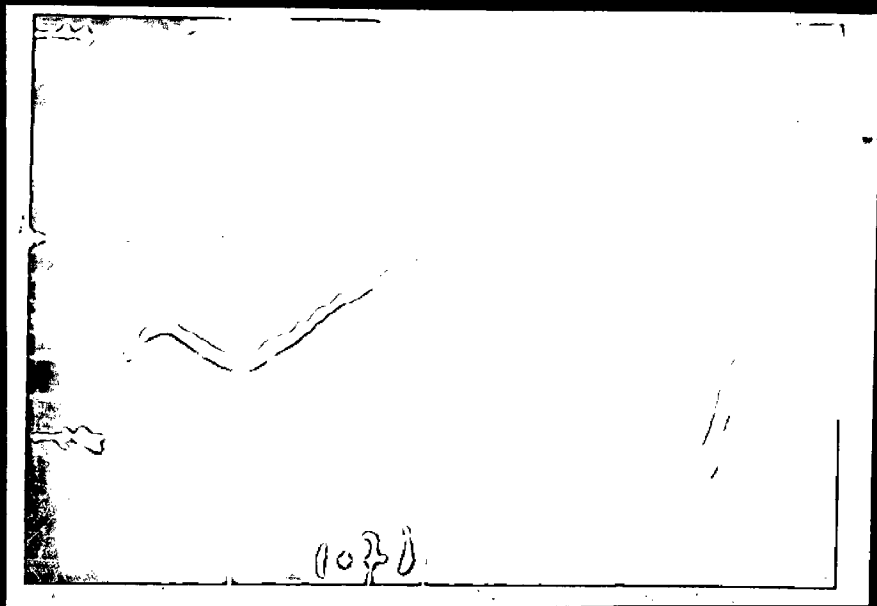


FIG 3.4 (b)
T.-S. CURVE
 $\alpha = 80^\circ, 175 \text{ MF}$

FIG 3.4 (c)
T.-S. CURVE
 $\alpha = 80^\circ, 200 \text{ MF}$

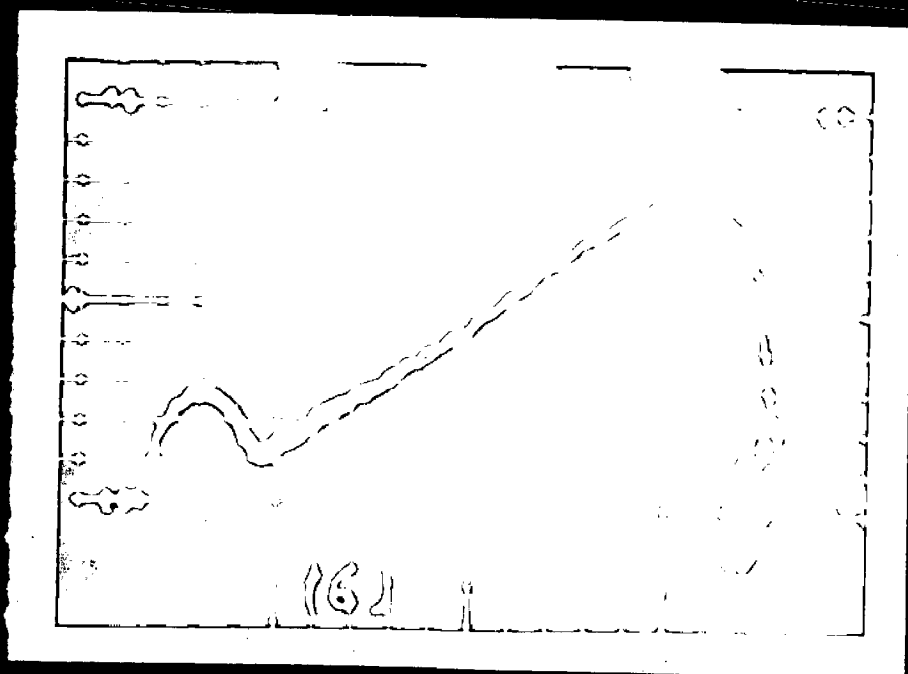


FIG. 8.15 SPEED-TIME OF CURVES

90 DEGREE ANGLES

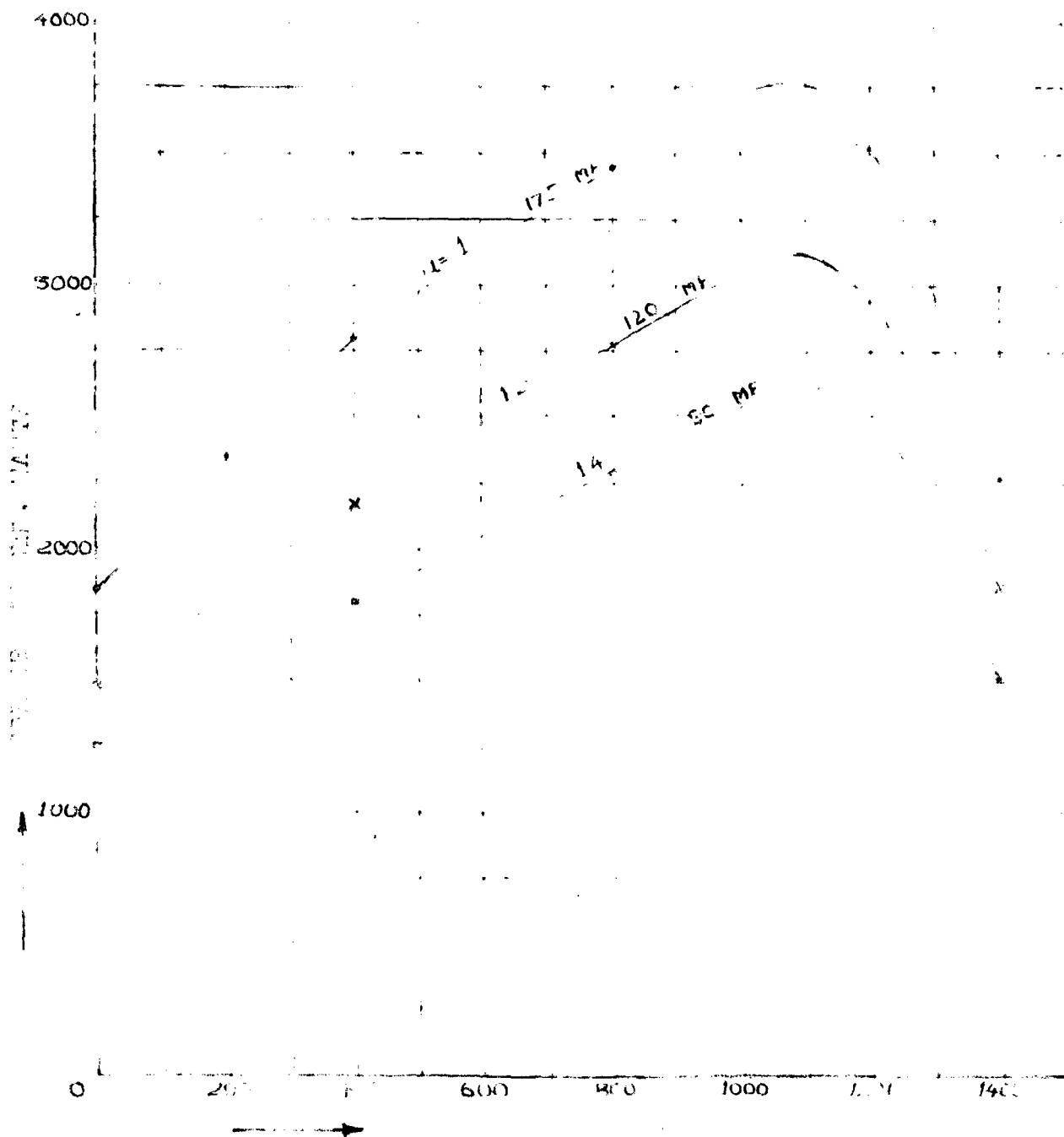


FIG. 3.6 REQUIRED SPEED CURVE

90° SPACE-ANGLE

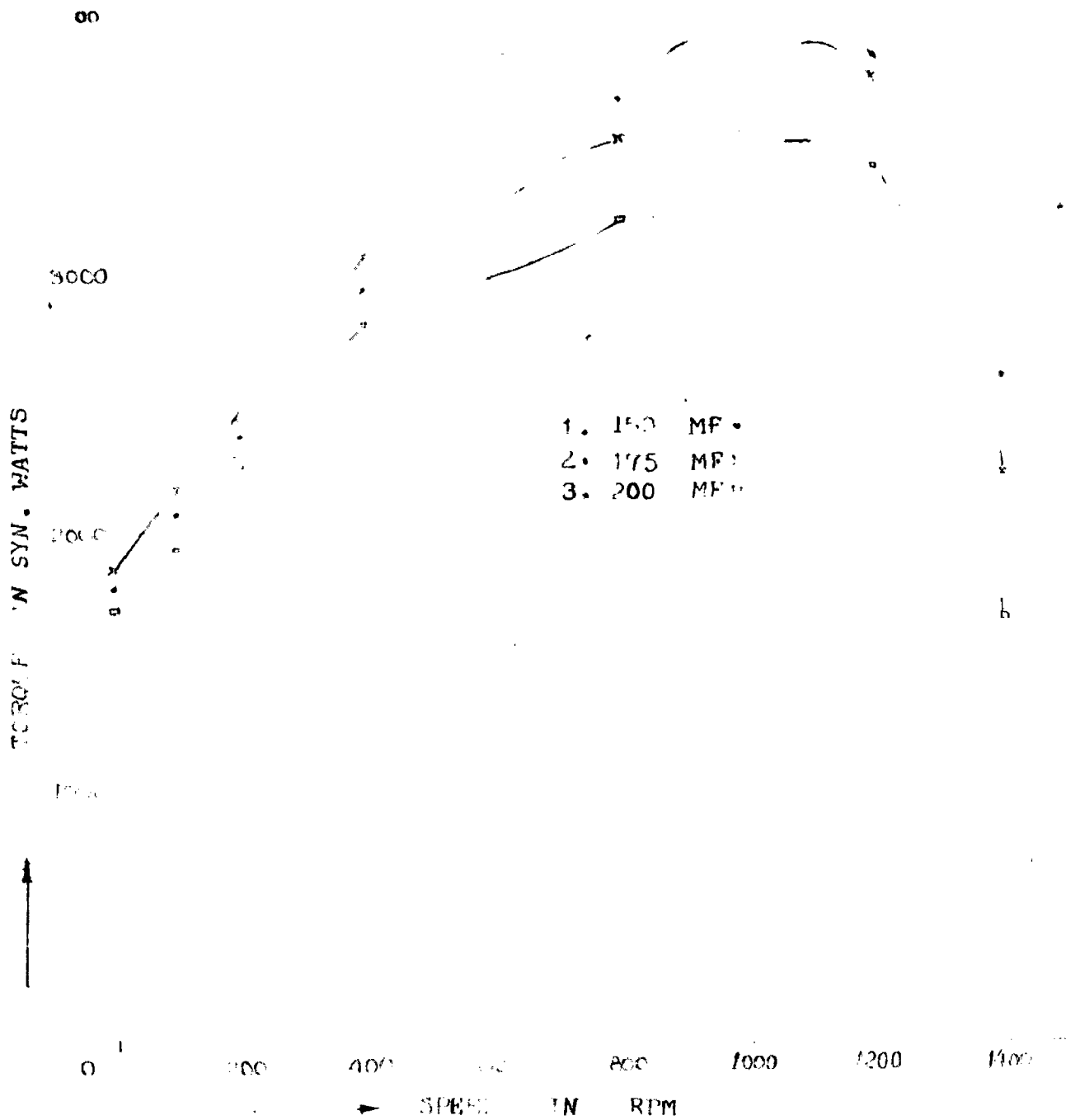
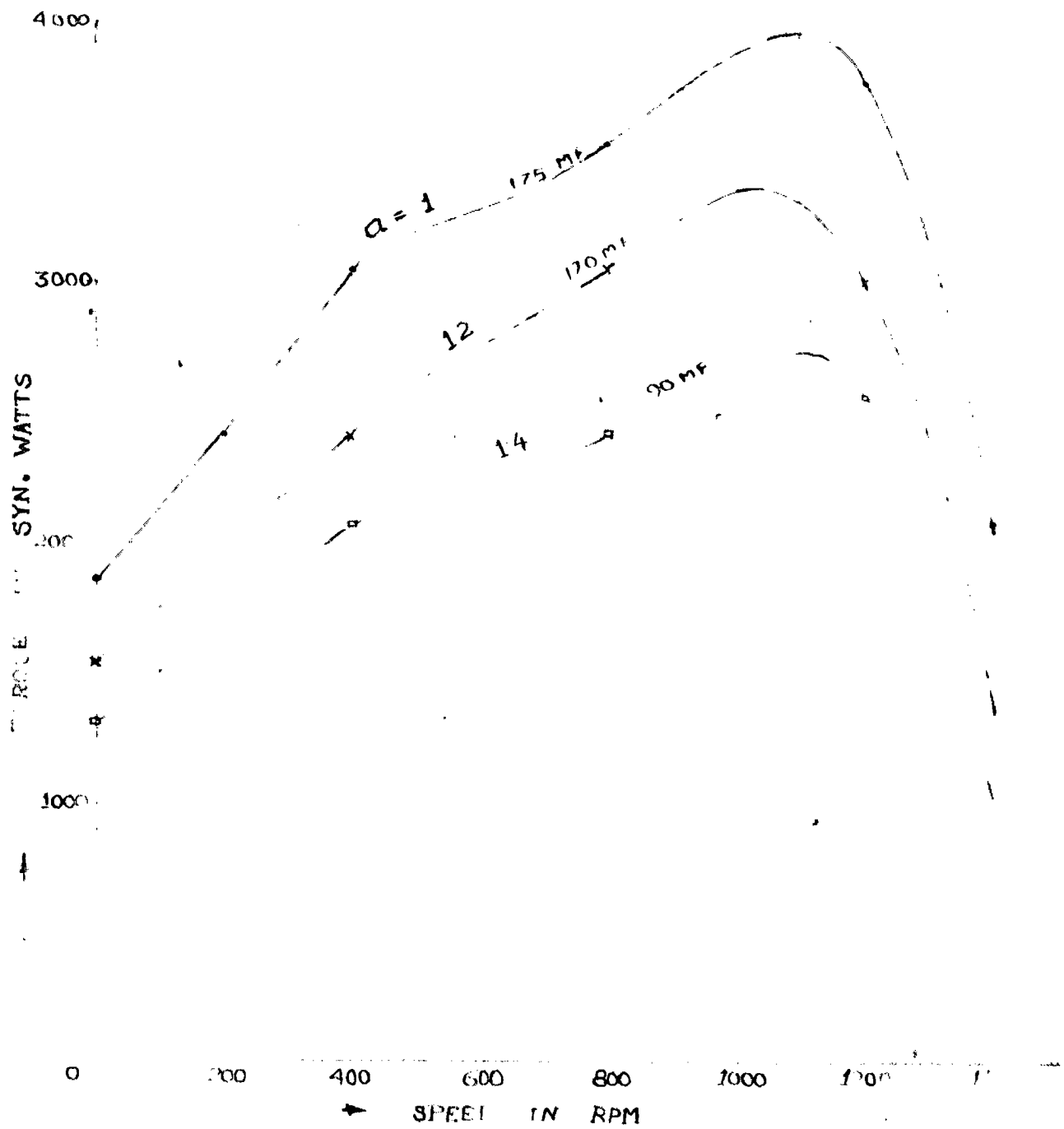
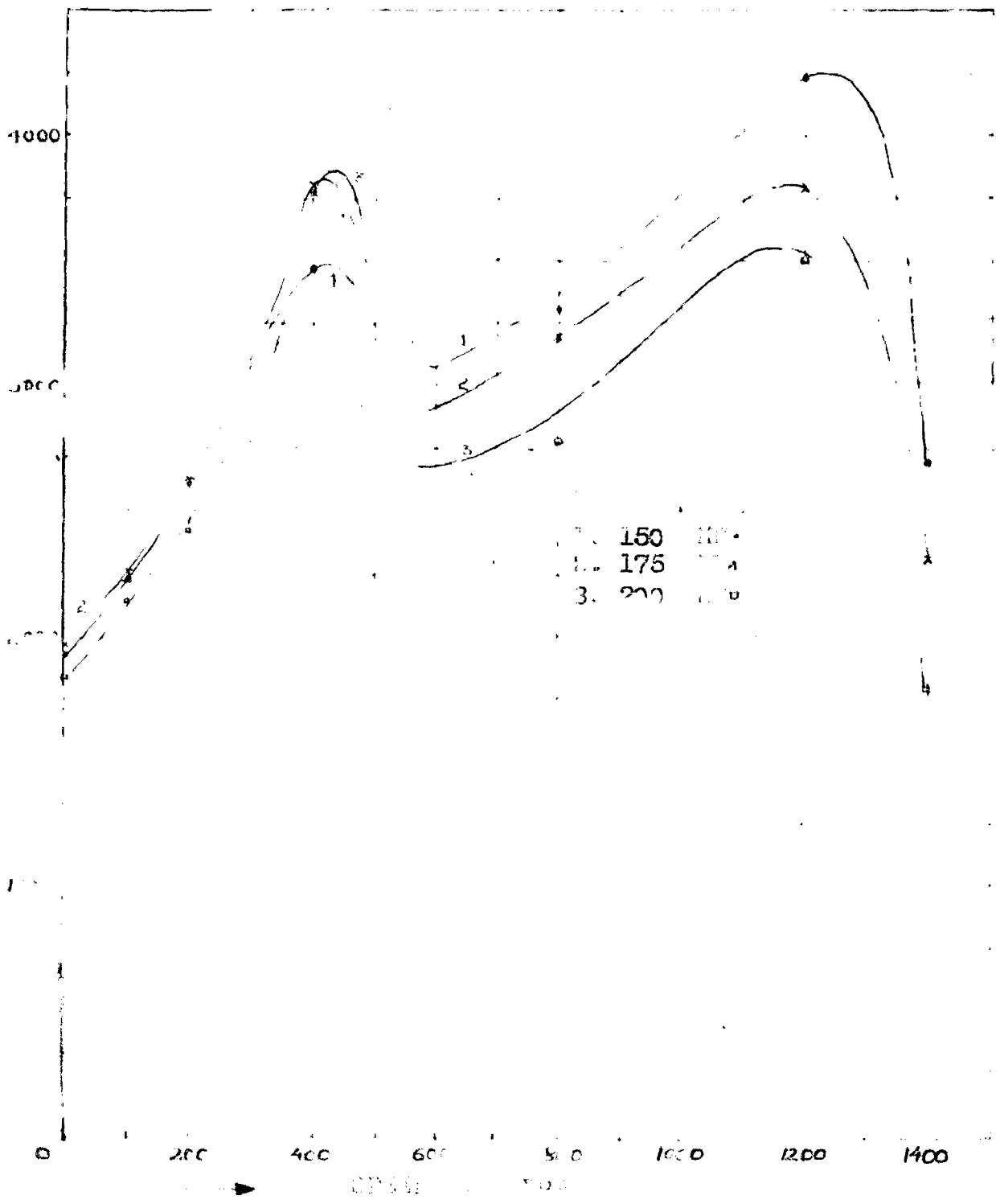


FIG. 3.7 TORQUE - SPEED CURVE
90° SPACE ANGLE





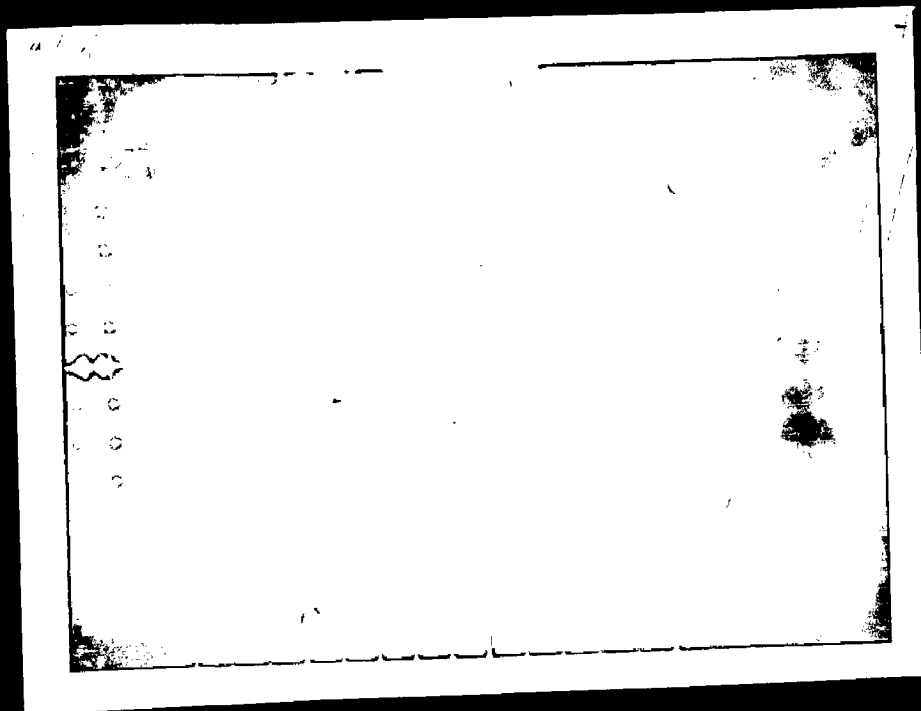
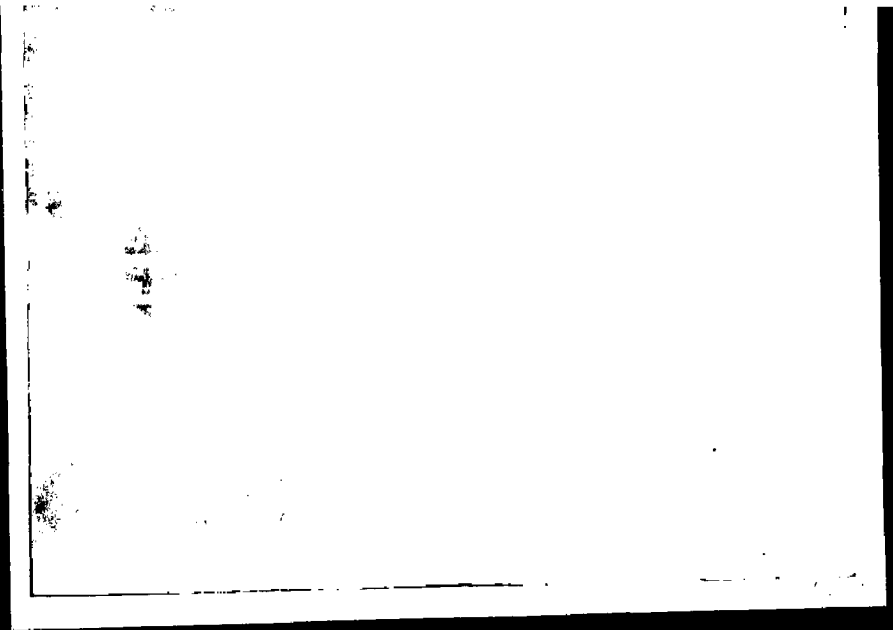


FIG. 33(B)
T.-S. CURVE
 $d = 100^\circ, 175 \text{ MP}$

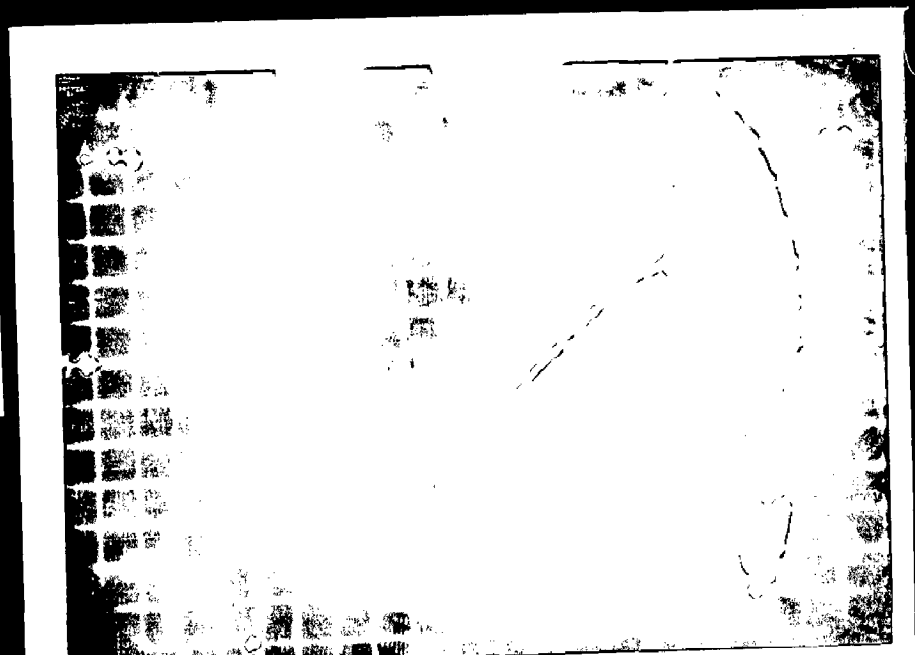


FIG. 3.3 (c)
T.-S. CURVE
 $d = 100^\circ, 300 \text{ MP}$

FIG. 2.9. 100% ...
100% ...

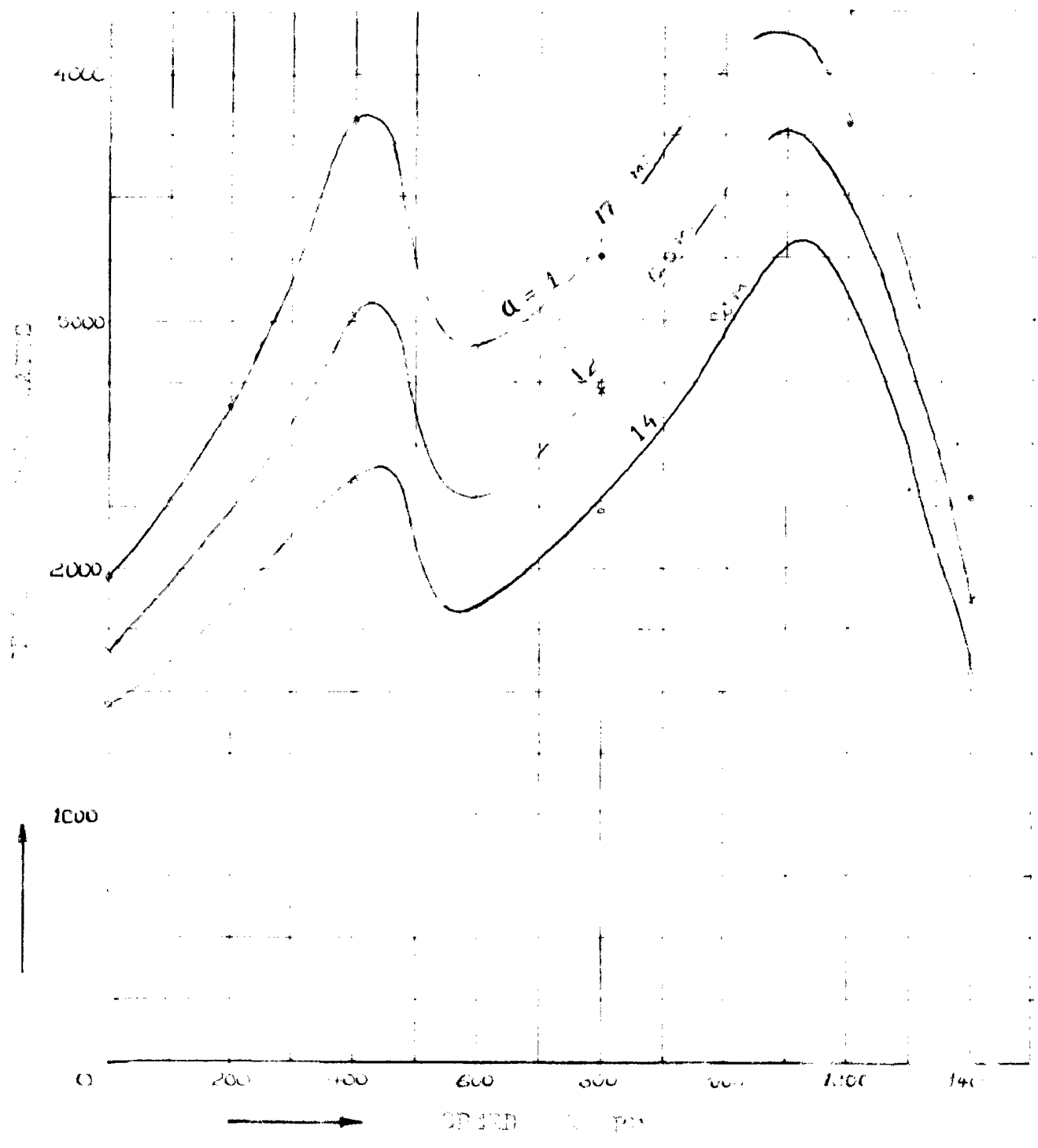


Fig. 3.10 TORQUE-SPEED CURVE
120° SPACE-ANGLE

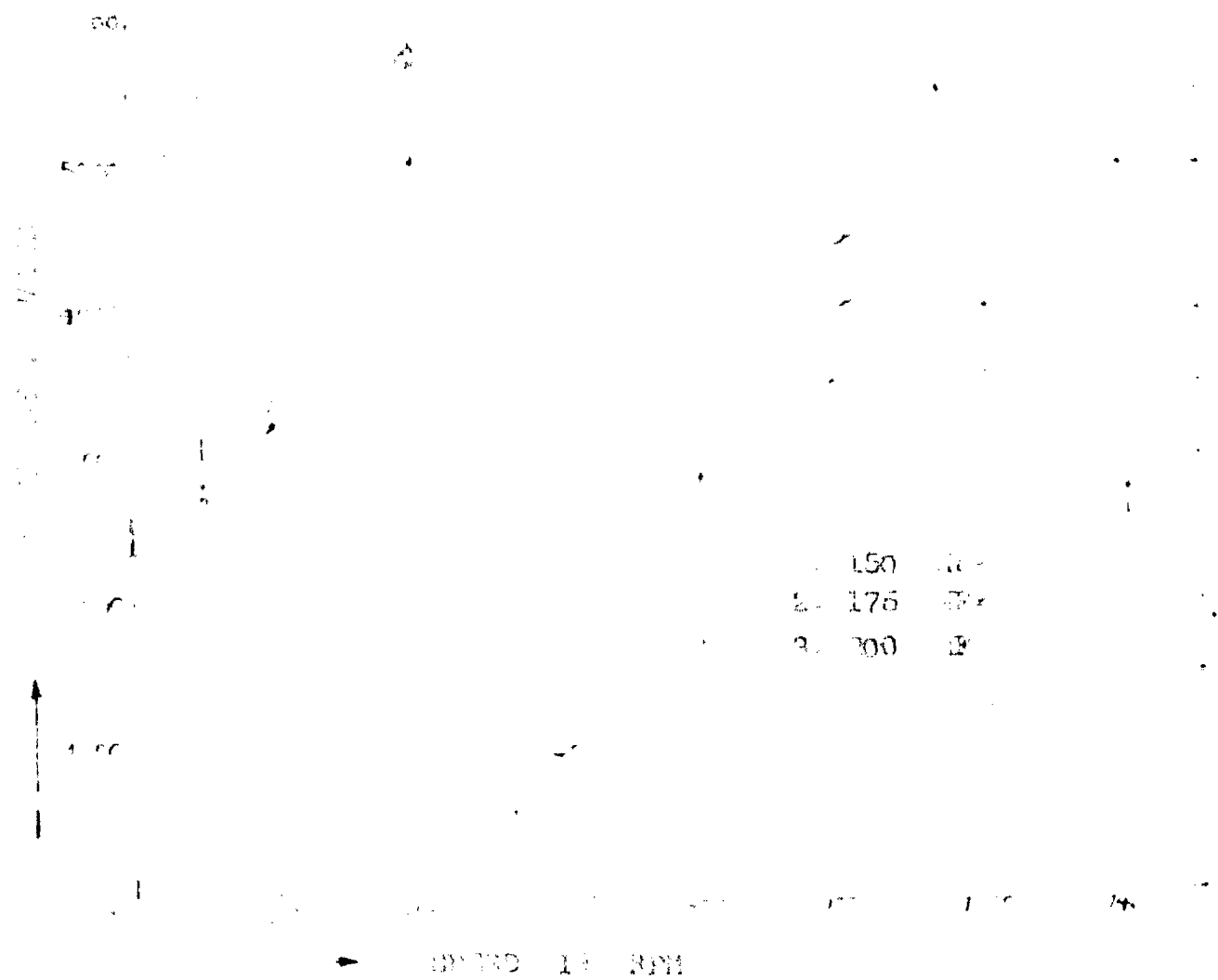


FIG. 3.10 (a)
T.-S. CURVE
 $\alpha = 120^\circ, 160 \text{ MF}$

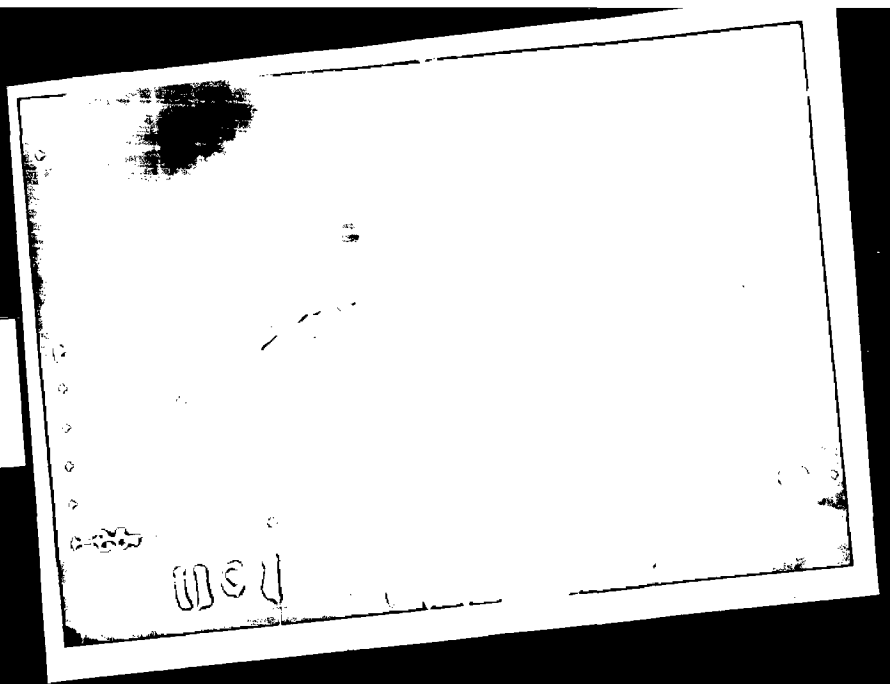


FIG.3.10 (b)
T.S. CURVE
 $\alpha = 120^\circ:175 \text{ MF}$

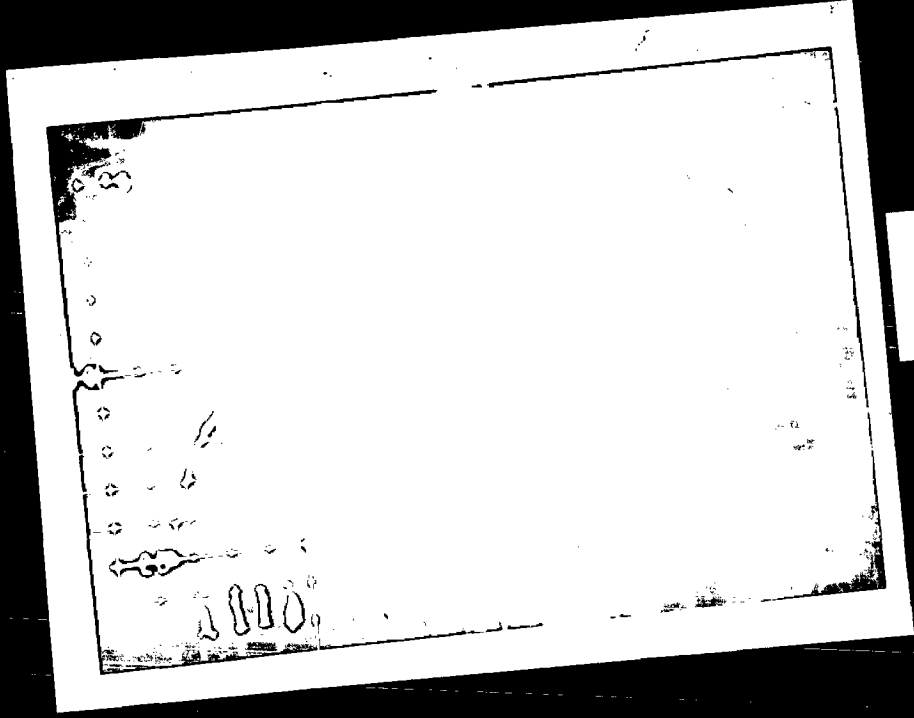
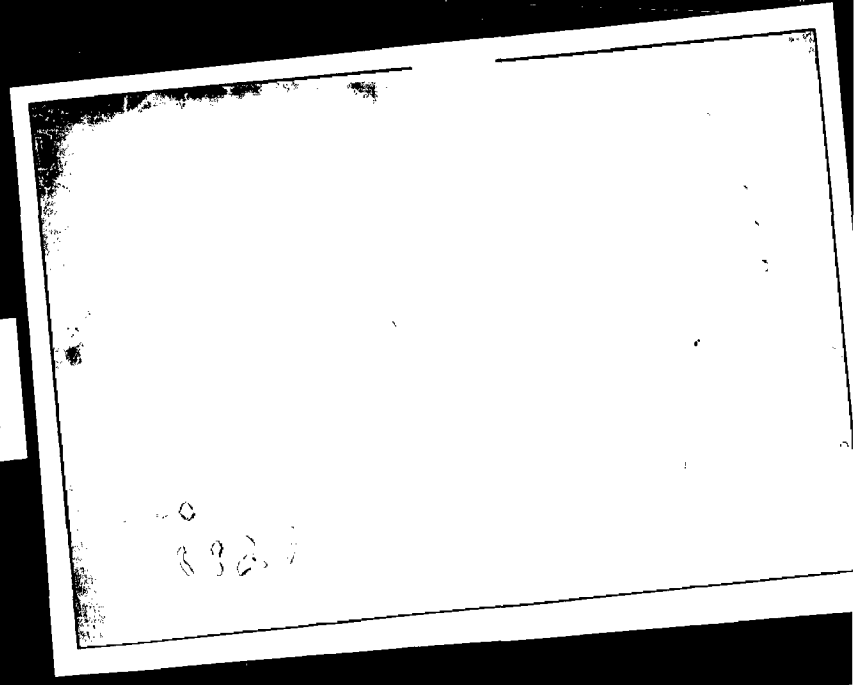


FIG 3.10 (c)
T.-S. CURVE
 $\alpha = 120^\circ, 200 \text{ MF}$



The large third harmonic dip in the torque-speed curve for 60° space-angle between the stator-windings is an objectionable feature.

B. 90° Space Angle:-

For this space-angle between the stator-windings no third space-harmonic dip is found for all the three capacitor values used. Refer to Tables 2.3, 2.4 and 2.5 Fig. 3.4 and Figures 3.4 a, b, and c.

The fifth harmonic dip is quite appreciable in this case which is found to increase with the starting-capacitor. If unchecked, it may produce crawling at just above 300 rpm.

In calculations third harmonic is found to produce a negative torque for all forward speeds, thus producing no dip in the torque speed curves. 5th harmonic was neglected in calculations. As seen in fig 3.5 for all turns-ratios there is no third-harmonic dip in the run-up performance.

(C) 90° Space-Angle

Unfortunately for 90° space-angle case no experimental data is available. Only the calculated performance is available. Figures 3.6 and 3.7.

The third harmonic torque has quite small values compared to the fundamental. The steep rise in fundamental torque overshadows the third harmonic effect except for some minor undulations in the total torque speed curves.

Even with higher turns ratio third space harmonic does not show any dip in curves.

(D) 100° Space Angle :-

Figures 3.8 , 3.8 a, b and c show the torque-speed curves for 100° space angle case.

The torque-speed curves give clear indication of third-

harmonic dip which is found to increase with the starting capacitor. The 200 MF value produces quite large dip.

In fig. 3.8 a,b and c The fifth harmonic dip is noted to be almost vanished

Figure 3.9 shows sufficiently large third harmonic dips with different turns-ratio but they are not of objectionable proportions. Lowest point on the dip is still quite higher than the standstill torque point for any curve. As seen from Tables 2.3, 2.4 and 2.5 with increase in turns ratio the dip is slightly increased.

(E) 120° Space Angle

Fig. 3.10 shows that for 120° space angle third harmonic effect is most predominant. The third-harmonic dip is so large that it make the machine to crawl at just above 500 rpm, the synchronous-speed of the third space harmonic wave- Fig 3.10 a,b and C.

Table 2.3 shows that the dip increases much with the starting capacitor.

No fifth harmonic dip is visible in the experimental curves.

Fig. 3.11 shows large third harmonic dips with different turns ratio cases.

Thus it is seen that third harmonic dips in torque-speed curves of 60° and 120° max space angles are objectionable.

For 80° space angle torque-speed curves do not show any third harmonic dip but they show appreciable fifth space harmonic dip and this may produce objectionable crawling at synchronous speed of the 5th harmonic.

100° seems to be a quite encouraging space-angle. Except for the 200 MF case, both 175 MF (optimum starting capacitor)

and 150 MF show very promising experimental run-up performance. Even the 5th harmonic dip is almost invisible at this angle.

Hence 100° space angle with greater starting-torque seems to be a very appropriate space angle from the point of view of run-up performance.

3.2 Suppression of Third Harmonic Dip

The asynchronous dips in the torque-speed curves due to the space-harmonics are often quite objectionable which may result in low speed crawling of the induction-motor. Hence an attempt can be made to suppress the detrimental third harmonic dip.

The capacitors to suppress the third harmonic dip for different space-angle cases for unity turns-ratio only are calculated from the equation (49) and are given in the table below-

Table 3.1 Critical Capacitors to Suppress 3rd Harmonic Dip Unity Turns-Ratio

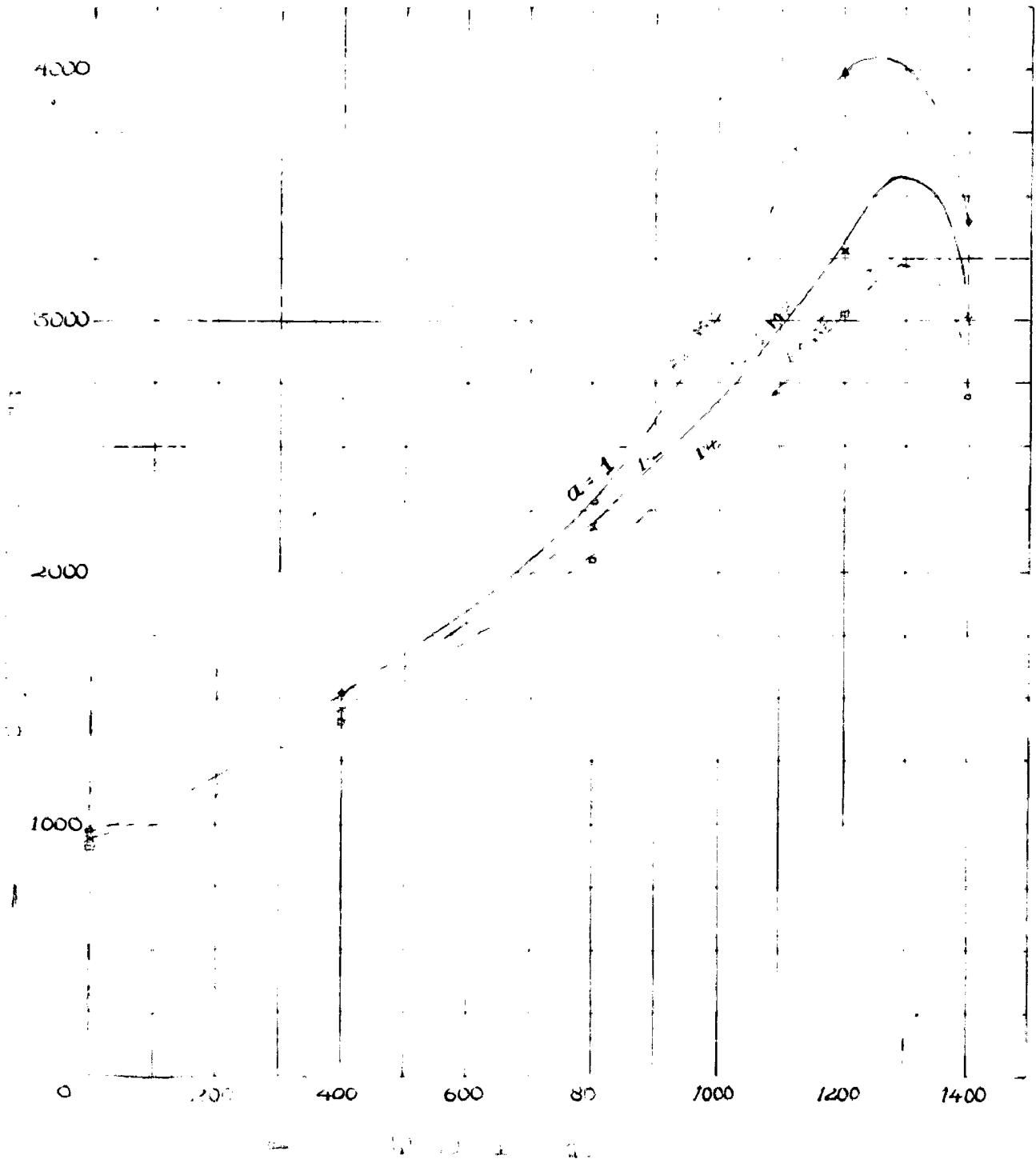
Space Angle	60°	80°	100°	120°
Capacitor, MF	Theoretically Infinite	166	82	96

No attempt is made to see performance of 60° space-angle machine with this critical capacitor for dip suppression which is large, resulting in almost zero starting torque.

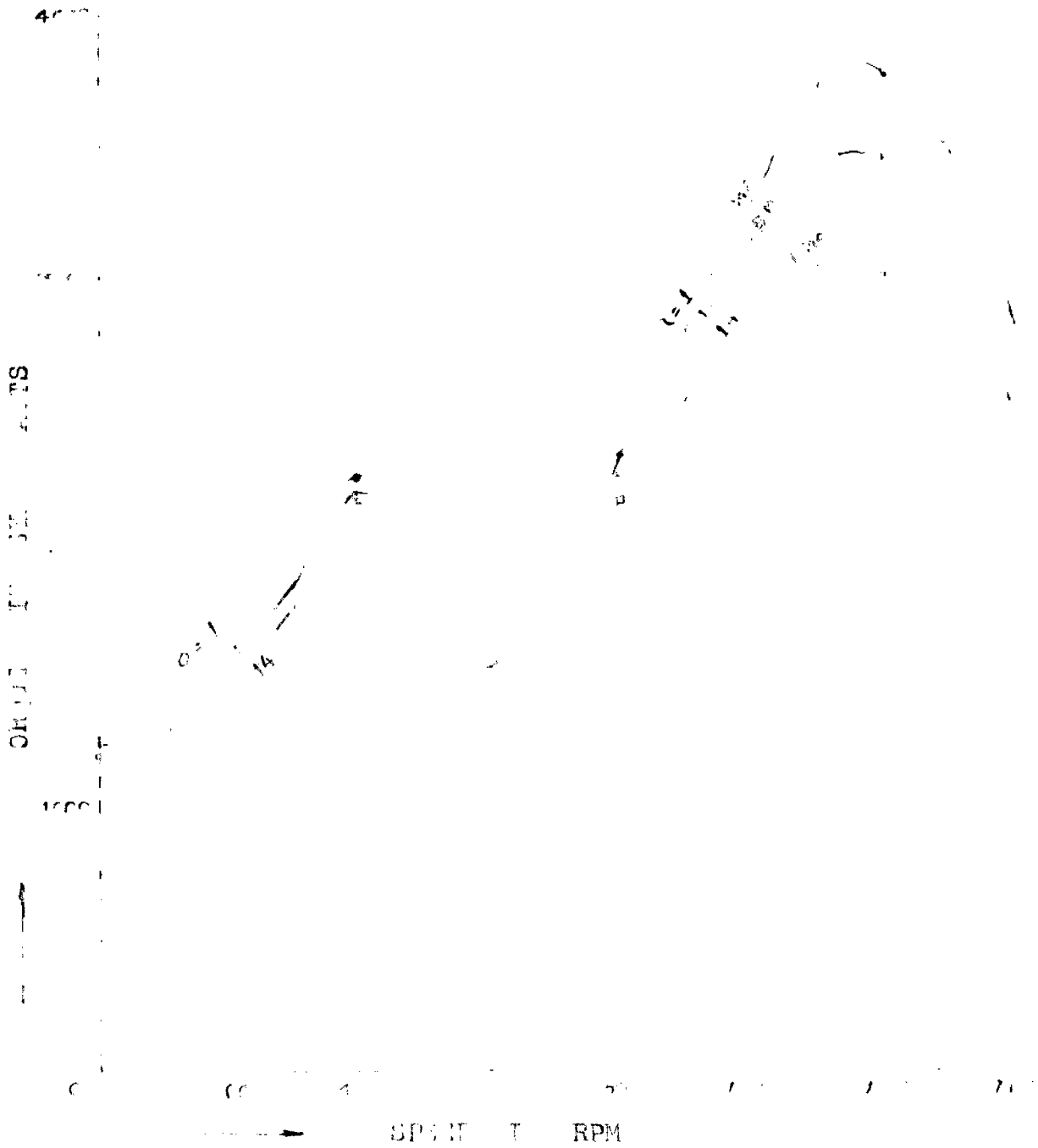
Fig. 3.12

1000

1000

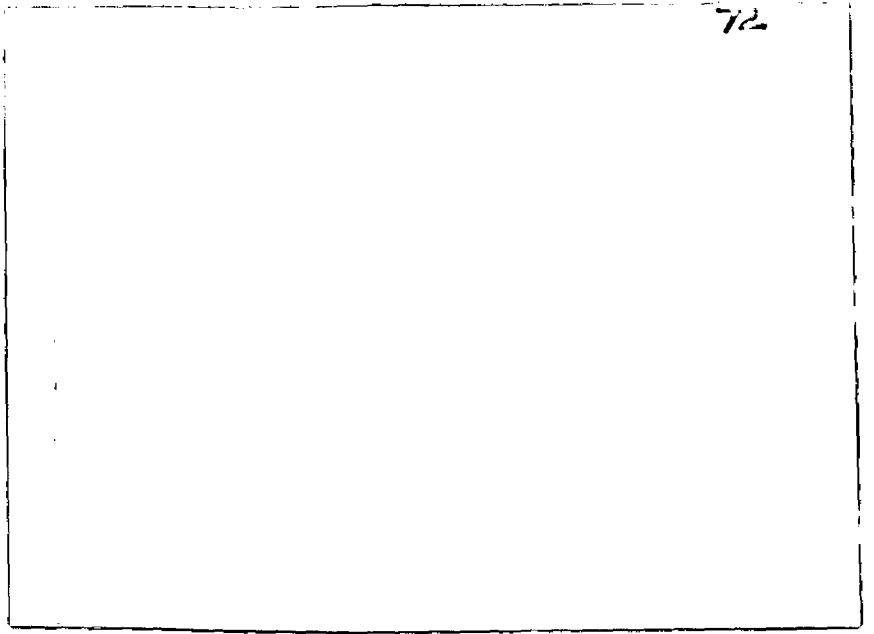


MI-1173 57 104
120° SPREAD-ANGLE



72

(a)



(a)

FIG 3.13(a)
DIP-SUPPRESSION
 $\delta = 100^\circ, 32 \text{ MF}$

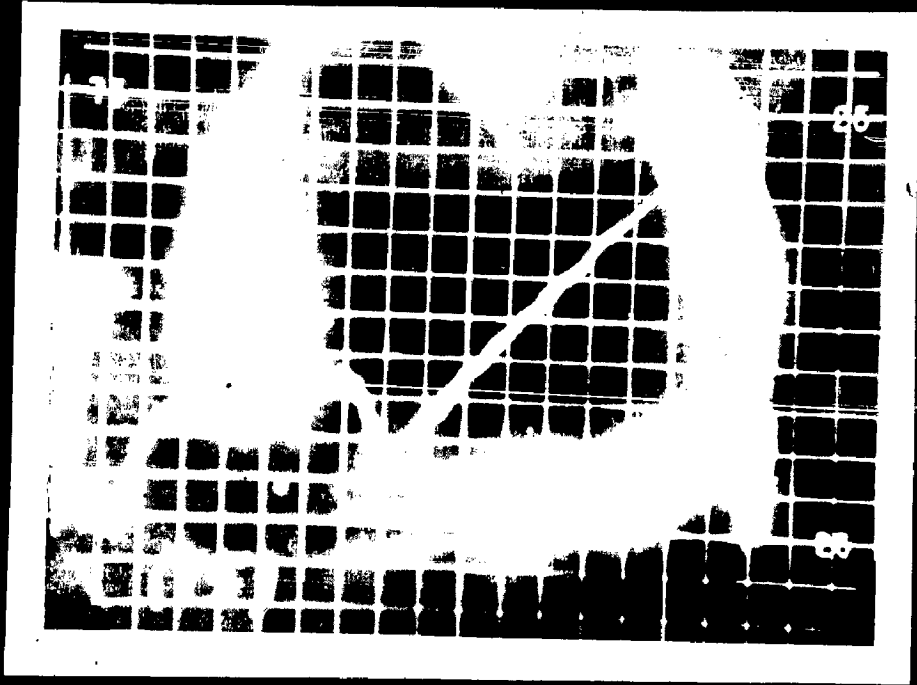
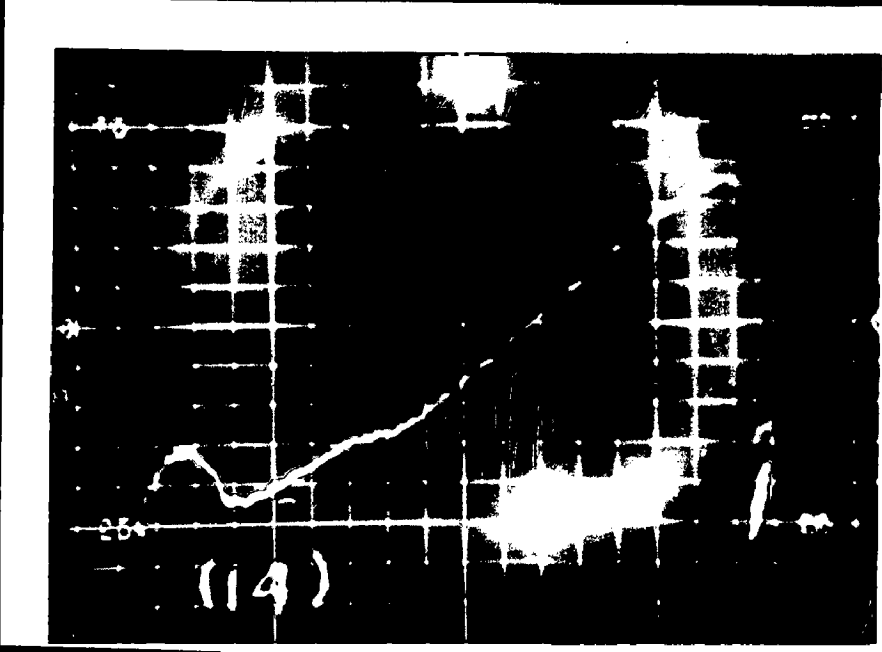


FIG 3.13(a)
DIP-SUPPRESSION
 $\delta = 120^\circ, 36 \text{ MF}$

The critical capacitor for 80° space-angle is very nearly equal to the optimum capacitor from starting-torque consideration. It may be remembered that 30° case has shown no third harmonic dip with the optimum starting capacitor.

The 100° space angle with 82 microfarad shows absolutely no third harmonic dip. Figures 3.12 and 3.12(a). In Figure 3.12(a) the fifth harmonic dip is still more clearly visible.

The worst affected case of 120° space angle shows much improvement with 86 MF capacitor. Machine no longer crawls. Fig. 3.13 and 3.13(a)

It may be noted that with a capacitor suitable for torque dip suppression the starting torque is very much impaired. For lower turns-ratio it reduces to about 50% of the value obtained with the optimum capacitor from starting-torque consideration. For higher turns ratio ($\alpha = 1.4$) the starting torque is decreased to about 65% of the optimum value.

Hence it is in no way advantageous to try to eliminate the complete dip in torque-speed curve, though it shows up a sufficiently low starting-capacitor

**TABLE 3.2: Performance with Capacitor to Suppress
Third Harmonic Dip, Unity Turns- Ratio**

Space angle	Capacitor MF	Starting Torque			Starting Current Amperes			%3rd T Harmo nic. Dip	T IL	T $I_m^2 + a^2 I_s^2$
		T ₁	T ₃	T	I ^m	I ^s	I _L			
100°	82	1275	-300	975	14.9	11.3	15.3	-	63.7	2.79
120°	86	1260	0	1260	14.2	13.5	16.7	33	75.4	3.32

Table 3.3 Same as Table 3.2 except 1.2 Turns Ratio

100°	62.6	1242	-290	952	14.9	9.3	15.1	-	63.1	2.74
120°	65	1252	0	1252	14.4	10.9	16.1	35	77.6	3.33

Table 3.4 With 1.4 Turns Ratio

100°	49	1182	-277	905	15	7.5	15	-	60.4	2.71
120°	51	1220	0	1220	14.5	8.9	15.8	43.5	77.2	3.35

3.3 Reduction of Third Harmonic Dip

An attempt can be made to determine such a starting-capacitor and space-angle which will not affect the starting torque seriously, say 10% reduction, but which will reduce the dip by a large percentage, say of the order of 50%

The 80° and 90° space-angles were left in calculations because they already show very small third harmonic effect in torque-speed curves with the optimum starting capacitor. Only three cases of 60°, 100° and 120° space-angles were tried.

In the tables 3.5 to 3.7, 80° and 90° cases were included just for the sake of comparison. In these cases the starting capacitor is that for optimum starting torque.

(A) 60° Space Angle:

We have to increase the capacitor above the optimum value for starting torque to reduce the dip. At about 10% loss in starting torque the capacitor has to be increased by about 20% of the optimum value. Thus it was possible to reduce the dip by about 50% or even more in higher turns-ratio case Table 3.5 to 3.7 and Fig 3.14. But both Torque per ampere line current and Torque per watt copper loss values have decreased below the optimum capacitor value case - Table 2.3 to 2.5

Thus there is no advantage in reducing the dip.

(B) 100° Space Angle

In this case with a loss of 10% starting torque the capacitor is reduced by about 20 - 25% Table 3.5 to 3.7 and this gives no dip in the torque speed curve - Fig 3.15. There is about 15% increase in the T/I^L value as compared to the optimum capacitor case, the torque per watt stator copper loss value has improved too.

FIG. 3.14 DIRECTIONAL
60° SPREAD ANGLE

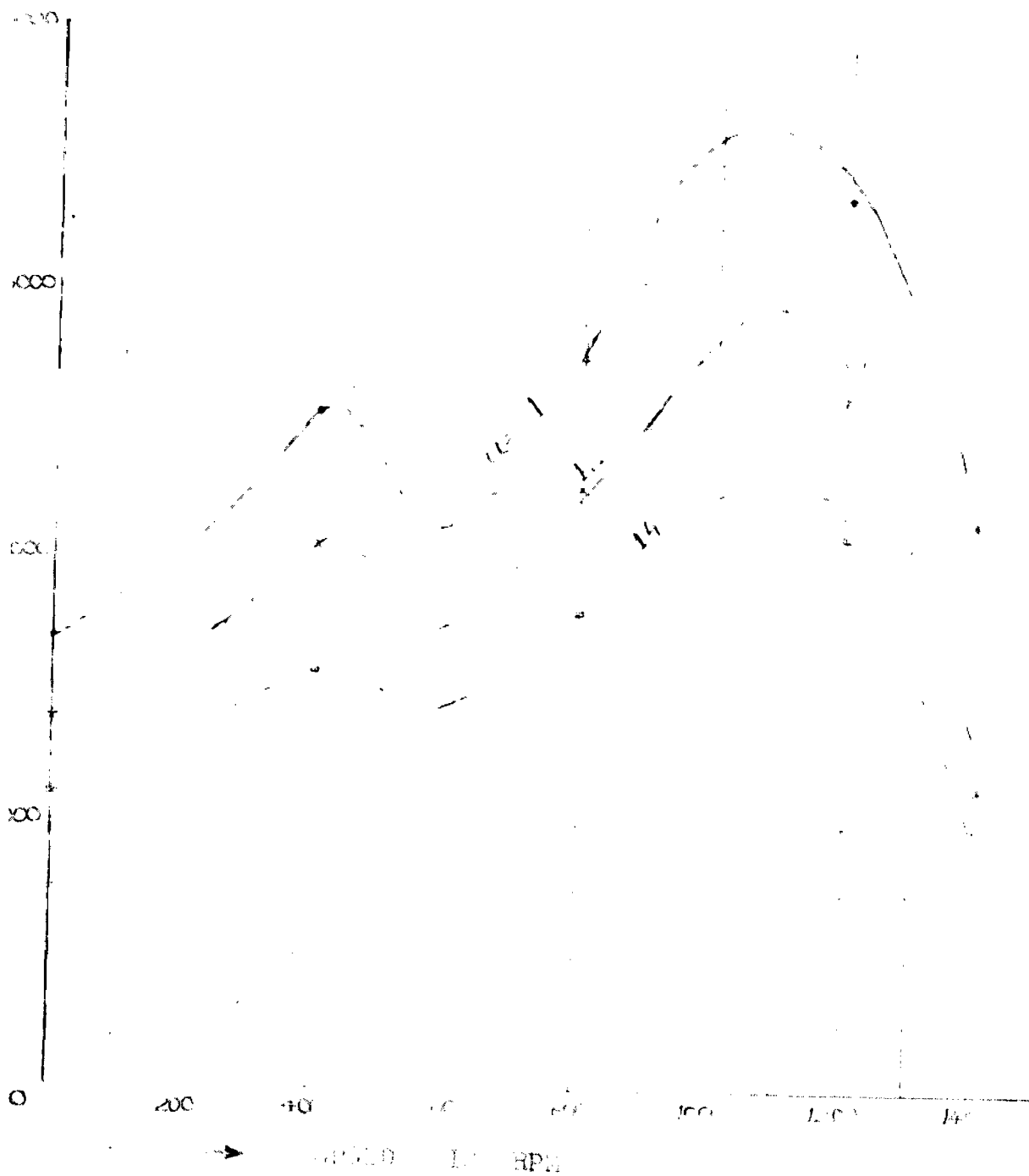


FIG. 9.15

DEFLECTION

100° 1950-1958

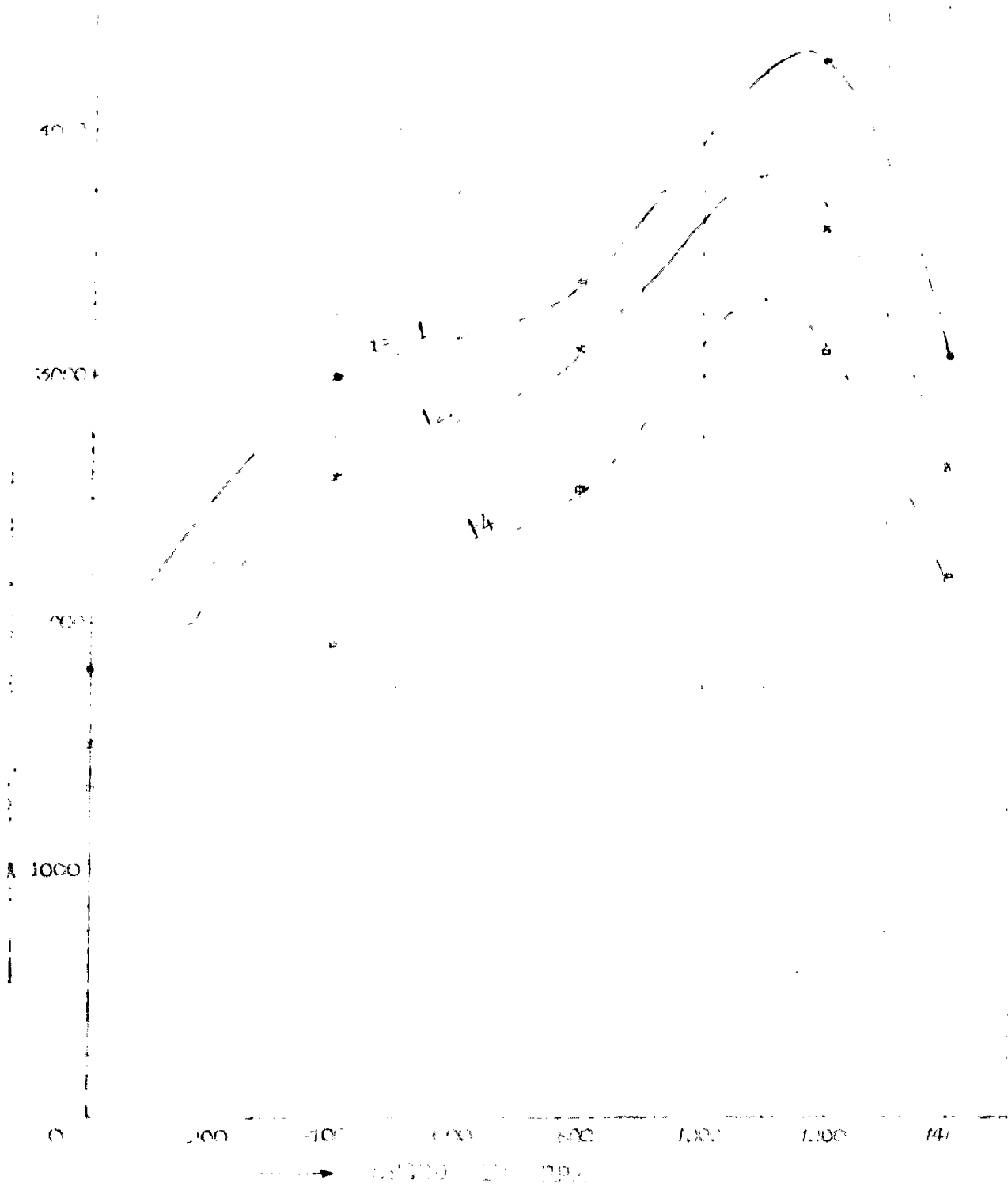


FIG. 3. ...

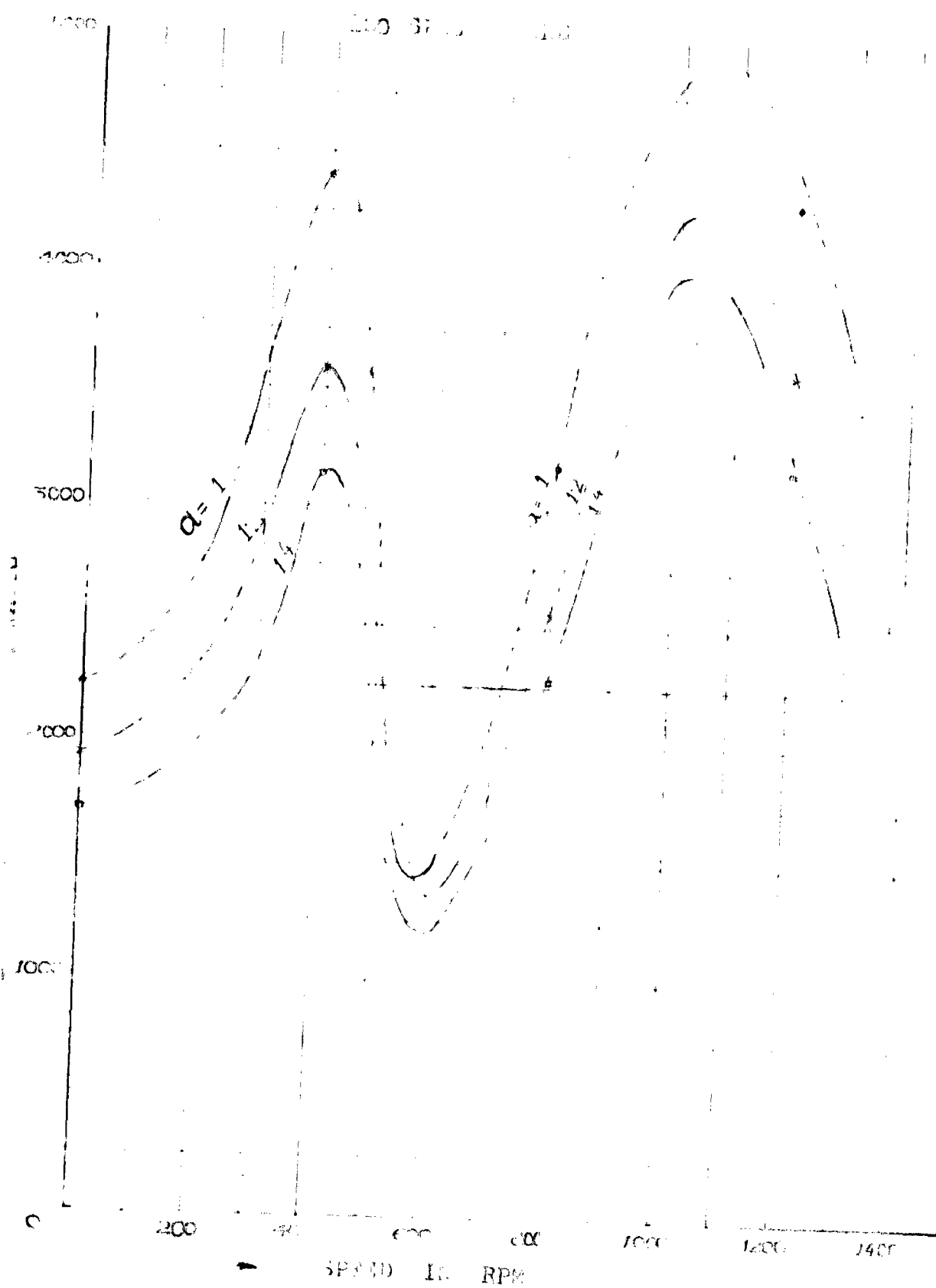


TABLE 3.5 STARTING PERFORMANCE WITH CAPACITORS TO REDUCE THE
DIP ($a = 1$) Unity-Turns Ratio

Speed ANGLE	Starting Capacitor (μF)	Starting Torque Lbs. Feet		Starting Torque (Angulo)	Starting Currents			β 3rd Harmonic DIP	$\frac{I}{I_L}$	$\frac{1}{I^{1.4} \cos^2 \alpha}$
		I_{11}	I_{12}		I^L	I^D	I^L			
60°	330	1620	0	1620	13.7	29.4	29.4	13.0	63.4	2.70
80°	175	2300	-400	1900	14.9	22	30.0	-	59	2.57
90°	175	2500	-570	1930	15.3	23.3	33	-	56	2.30
100°	120	2300	500	1955	15.1	20.2	26.7	-	67.7	2.84
120°	120	2220	0	2220	15.1	22	29.4	93	76	3.08

TABLE 3.6 STARTING PERFORMANCE WITH CAPACITORS TO REDUCE THE
DIP ($a = 1.2$) - Turns Ratio

60°	140	1300	0	1300	14.1	13.6	24	15.6	57.5	2.94
80°	120	1900	-450	1450	14.0	15.1	25	-	59.4	2.7
90°	120	2100	-500	1540	15.3	16.2	23.7	-	57.7	2.63
100°	80	1970	-400	1510	15.1	14	21.6	-	70	3.05
120°	80	1925	0	1925	15.2	15.3	23.0	83	60.4	3.27

TABLE 3.7 STARTING PERFORMANCE WITH CAPACITORS TO REDUCE THE DIP
Turns-Ratio = ($a = 1.4$)

60°	107.5	1100	0	1100	16.2	9.6	20.9	0.3	52.6	2.89
80°	80	1650	-300	1300	16	11	21.7	-	53	2.75
90°	80	1300	-450	1320	16.5	11.7	23	-	57.3	2.6
100°	65	1750	-205	1325	16.2	11.5	19.3	-	70.4	2.83
120°	67	1700	0	1700	16.1	12	22	83	61.1	3.24

It may be noted from the above tables that even with the 10% decrease in starting torque the not starting torque is still almost equal to the optimum starting-torque for 120° space angle.

(6) 120° in 120°

In this case too about 20 - 25% decrease in the starting cap after yielding 10% of the maximum starting torque, there is about 20% reduction in third harmonic dip, still the dip is about 100% error. Fig 3.10 and some tables as above.

There is improvement in T/Y^2 and Torque per unit stator Cu loss values.

Since in 120° space-angle case maximum advantage can be obtained by thus reducing the dip. Whereas with the optimum starting capacitor the T/Y^2 values for both 120° and 180° space-angle are very nearly equal, a sacrifice of 10% in starting torque in case of 120° space angle yields about 15% increase in T/Y^2 value with large (20 - 25%) associated decrease in starting capacitor. Torque per unit stator copper loss value also improves and in 120° dip is almost eliminated.

Handwritten: $A = 0.16$
CENTRAL LIBRARY UNIVERSITY OF ROO...

3.4 A Study of Third Harmonic Torque Over Whole Speed Range

In this section the nature of third harmonic torque variation with space angles for unity turns-ratio case is studied. The curves are calculated from performance equations.

(A) 60° space Angle

Fig. 3.17 shows the third harmonic torque over whole speed range, from negative syn. speed to positive syn. speed, with the three starting capacitors of values 150, 175, and 200 microfarads.

The Figure shows dips at speeds just above + 500 rpm and -500 rpm, 500 rpm is the syn. speed for the third space harmonic. The curves of forward and plugging regions are identical.

(B) 80° Space Angle

Fig 3.18 shows there is a large dip at speed just above - 500 rpm but the values of the third harmonic torque during forward running is always negative, decreasing with increase in speed.

(C) 90° Space Angle

Fig. 3.19 shows large dip at speed just above - 500 rpm. The curves show slight undulations near + 500 rpm.

(D) 100° Space-Angle

Fig. 3.20 indicates that for 100° space-angle there is large dip near -500 rpm and some dip at speed just above + 500 rpm. This angle is like 90° space angle except that the dips are more pronounced.

FIG. 3.17 THIRD SPACE HARMONIC TORQUE-SPEED CURVE

30° SPACE ANGLE (a = 1)

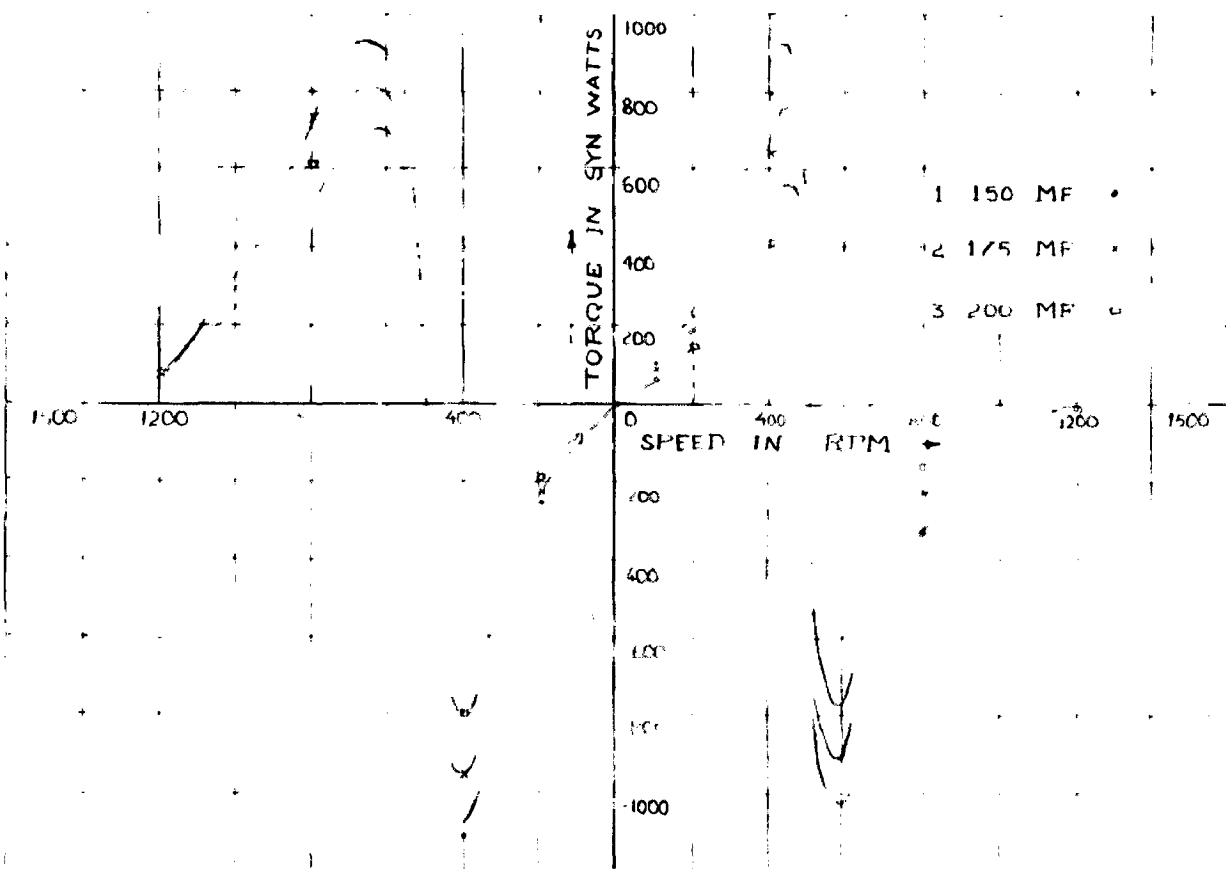


FIG. 3-18 THIRD SPACE HARMONIC TORQUE SPEED CURVE
 3rd SPACE HARMONIC (c = 1)

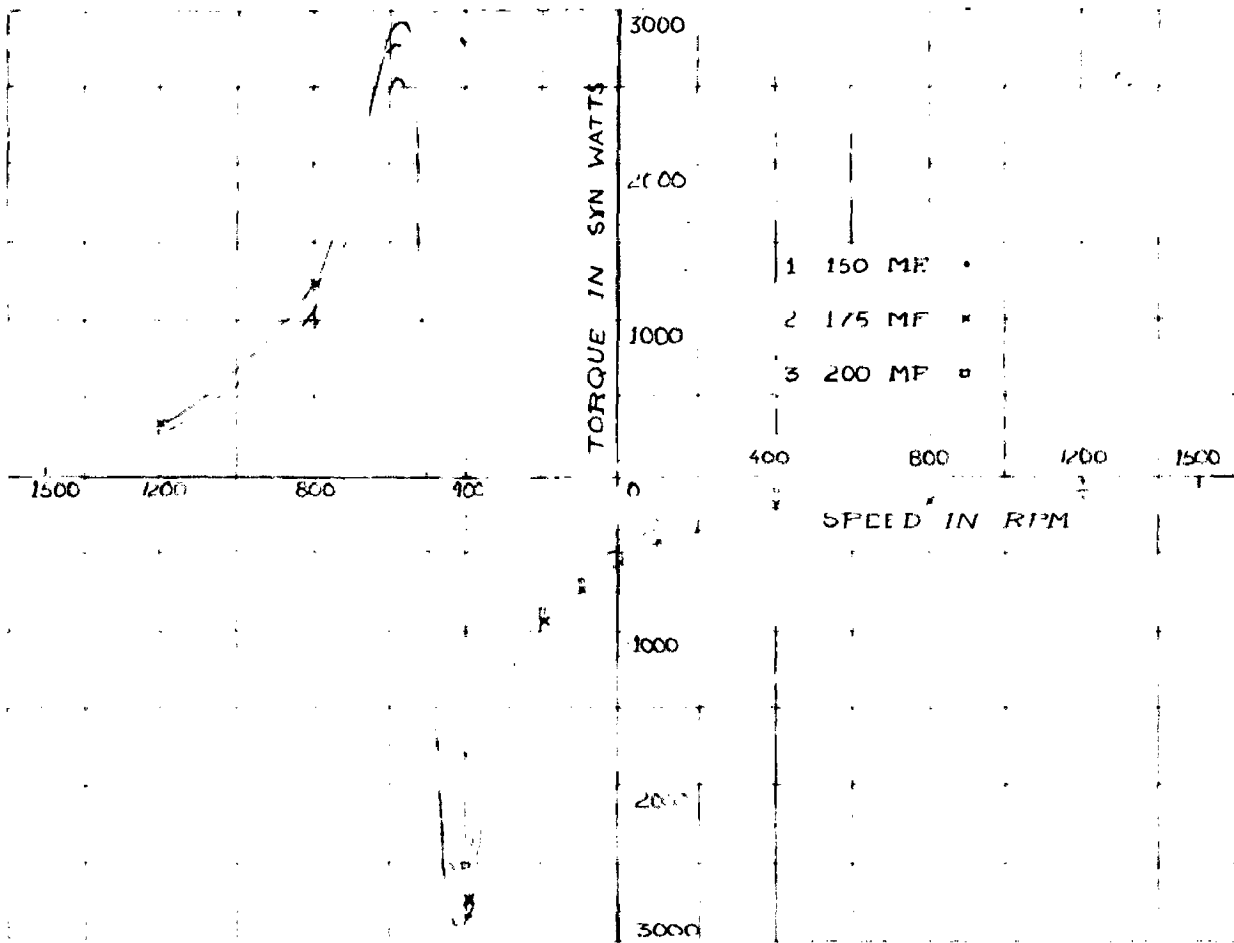


FIG. 3.19 THIRD SPAC HARMONIC TORQUE SPEED CURVES
90° SPAC INTR (a = 1)

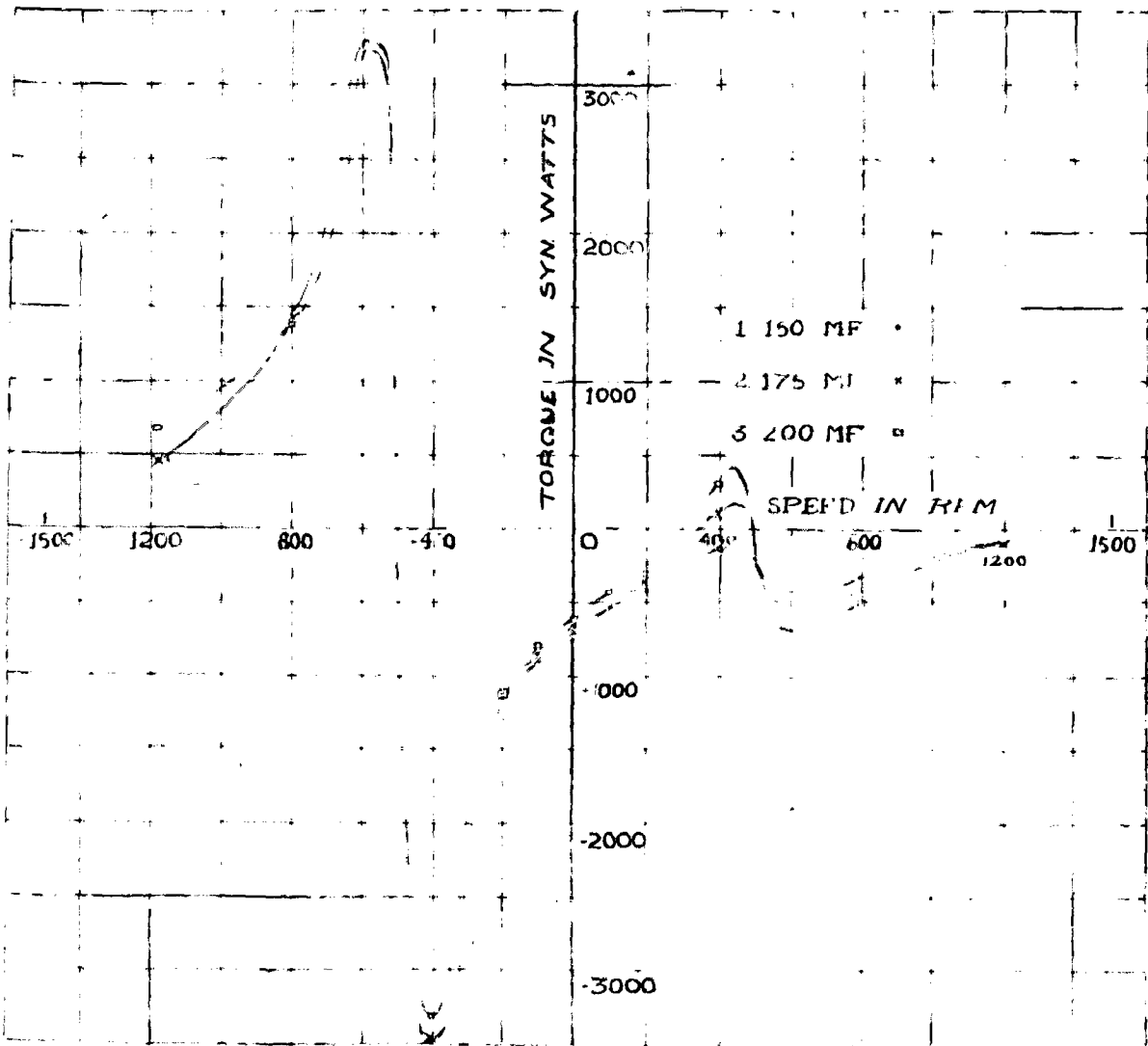


FIG. 3.20 THIRD SPACE HARMONIC TORQUE-SPEED CURVES

100° SPACE ANGLE (L = 1)

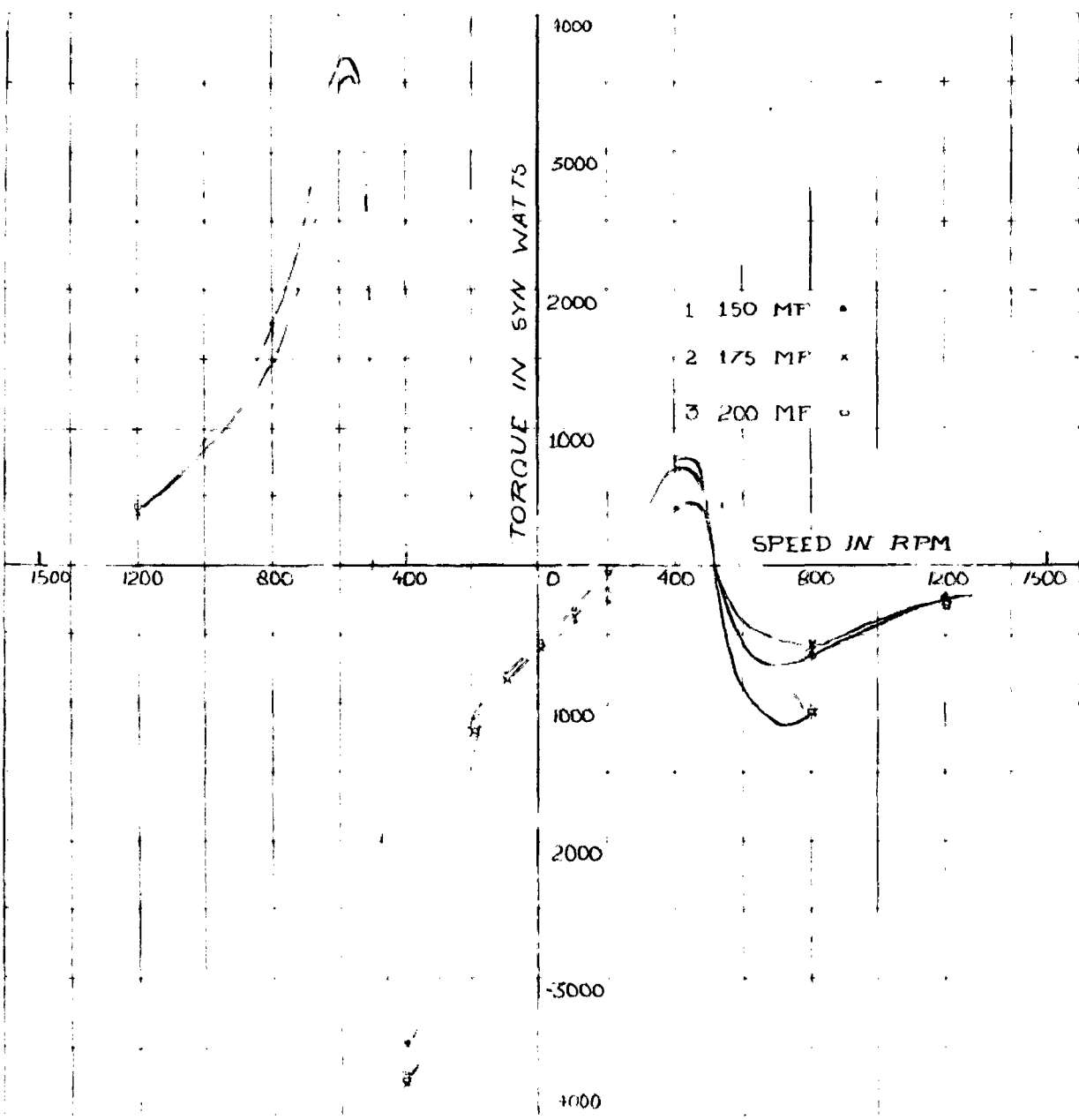
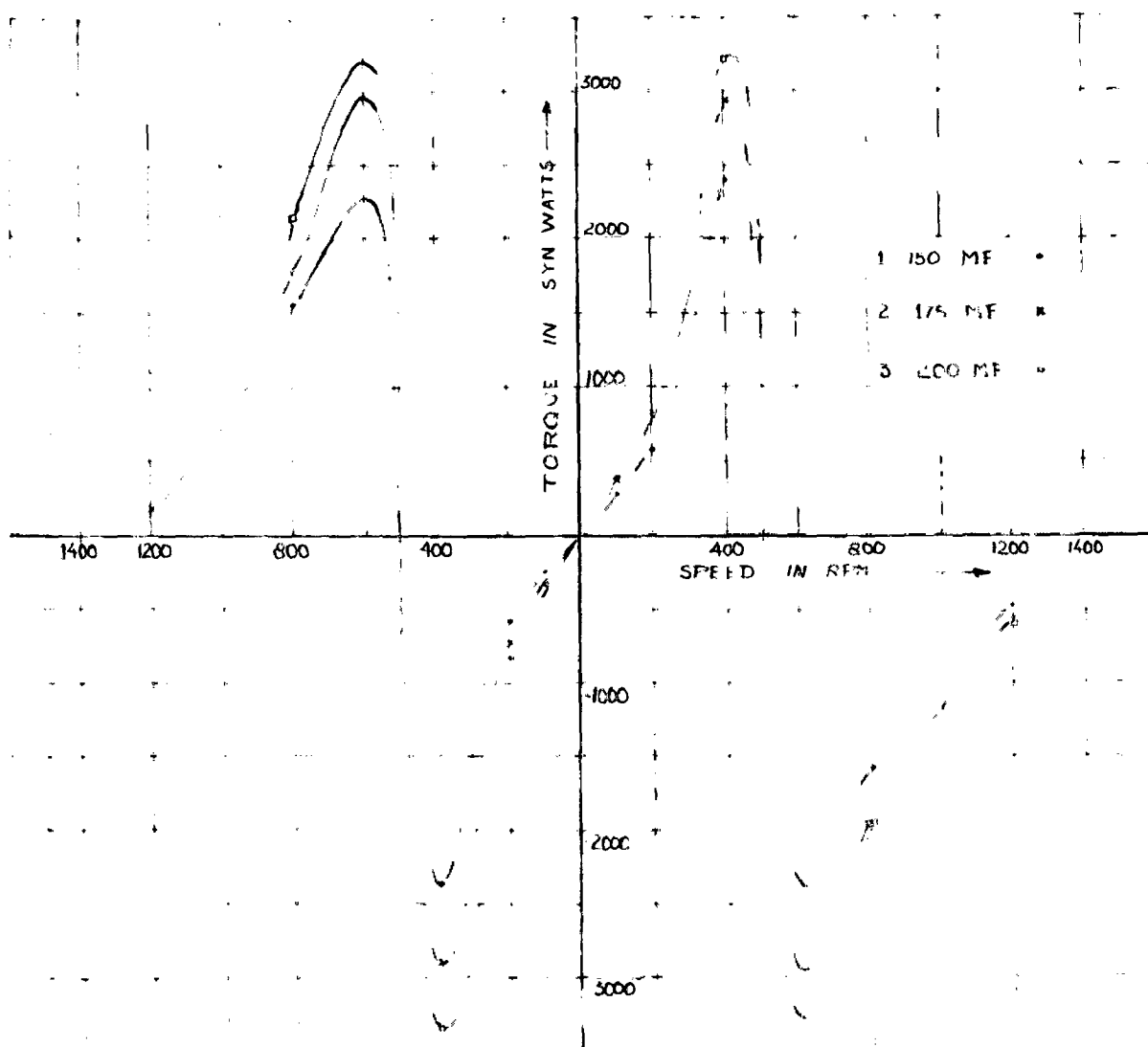


FIG. 8.21 THIRD HARMONIC TORQUE SPEED CURVES
 120° SPACE ANGLE ($a = 1$)



(E) 120° Space Angle

Fig. 3.21 shows that the curves are like that for 60° space-angle case but the dips are much more pronounced.

The following explanation looks some what satisfactory for such behaviour of the third harmonic torque:-

For 120° space angle case the third space harmonic mmfs due to the two stator windings will be in space-phase and the two space mmfs will have a time phase difference of near about 90°. The resultant is as if there is a single field pulsating along a particular axis. Hence the torque nature due to it will be like that of a single phase induction motor with single winding without starting torque. At 500 rpm in either direction the torque should reach a zero value and then afterwards above its syn. speed (i.e. + 500 rpm) or below its negative syn. speed (i.e. - 500 rpm) it should show the same nature of torque variation as during subsynchronous operation.

Taking the case of 90° space angle the two third harmonic mmfs should now be in space quadrature. As the starting winding current is leading, the third space harmonic machine must produce a third harmonic torque in opposite direction to the fundamental torque. During forward running of the machine the third space harmonic is as if producing braking of machine. and hence its torque must show decreasing negative values. During negative running of the machine the third space harmonic will then produce torque speed curve like an ordinary induction

motor. The general nature of curves in Fig 3.19 confirms the above statement.

For some variation in space angle about 90° the same explanation approximately holds. For 80° case the curves are perfectly as predicted above.

For 60° space angle case the third space-harmonic mmfs due to the two stator-windings will be in space-opposition and with a time-phase difference of near about 90° . The resultant will be a single field pulsating along a particular axis. Hence the third harmonic torque due to it will be like that of a single-phase induction motor. Thus the curves will have a general nature like that for 120° space-angle case. Though calculations show a large difference in magnitude of 3rd harmonic torque in these two cases yet a satisfactory explanation could not be found.

Chapter - 4Running - Performance

In this chapter the two extreme cases of 60° and 120° space angle between the two stator windings have been neglected. With these angles the machine shows a very poor starting performance and hence these space angles between the stator windings will not be suitable for a pure capacitor start single phase motor or a capacitor start and capacitor run motor using two capacitors. Performance has been determined for 90° and 100° and 120° space angles with 1, 1.2 and 1.4 turn-ratios.

A running capacitor in each case is calculated by equations (23) which will give near balanced operation at an assumed slip of 4 per cent.

Table 4.1 shows the running capacitor thus selected.

Table 4.1 Running Capacitors

Space Angle	Turns Ratio	Running Capacitor (μF)
90°	1	84
	1.2	10
	1.4	16.4
100°	1	82
	1.2	17
	1.4	22.7
120°	1	81.3
	1.2	16.7
	1.4	22.9

It may be noted here that the running capacitor required for space angle greater than 60° is smaller than that for 60° space angle, it being larger for space angle less than 60° .

It may be pointed out here that the running capacitor reduces if the machine is balanced at lower slip.

Hence, say, if the angle between the stator windings is 120° and the machine is balanced at 4 percent slip then with 60° space angle, obtained by reversal of either of stator windings, the machine will balance at still smaller slip with same running capacitor.

The performance is calculated neglecting the space-harmonic which is reasonably justified at such low slip.

The following curves (Fig 4.1 to 4.3) show the torque, torque per ampere line current, power-factor and efficiency curves.

In the efficiency calculations frictional and winding losses were neglected which will be nearly constant in all the cases dealt. Only copper loss is taken into account. Hence it seems because of this omission the efficiency curves do not show a conventional maximum, but rather show a continuously decreasing efficiency with load.

The performance curves for all these space angles are found to be very much alike.

(A) Remarks

Usually always 120° space angle curves show slightly more torque than others at any slip.

... (a = 3)

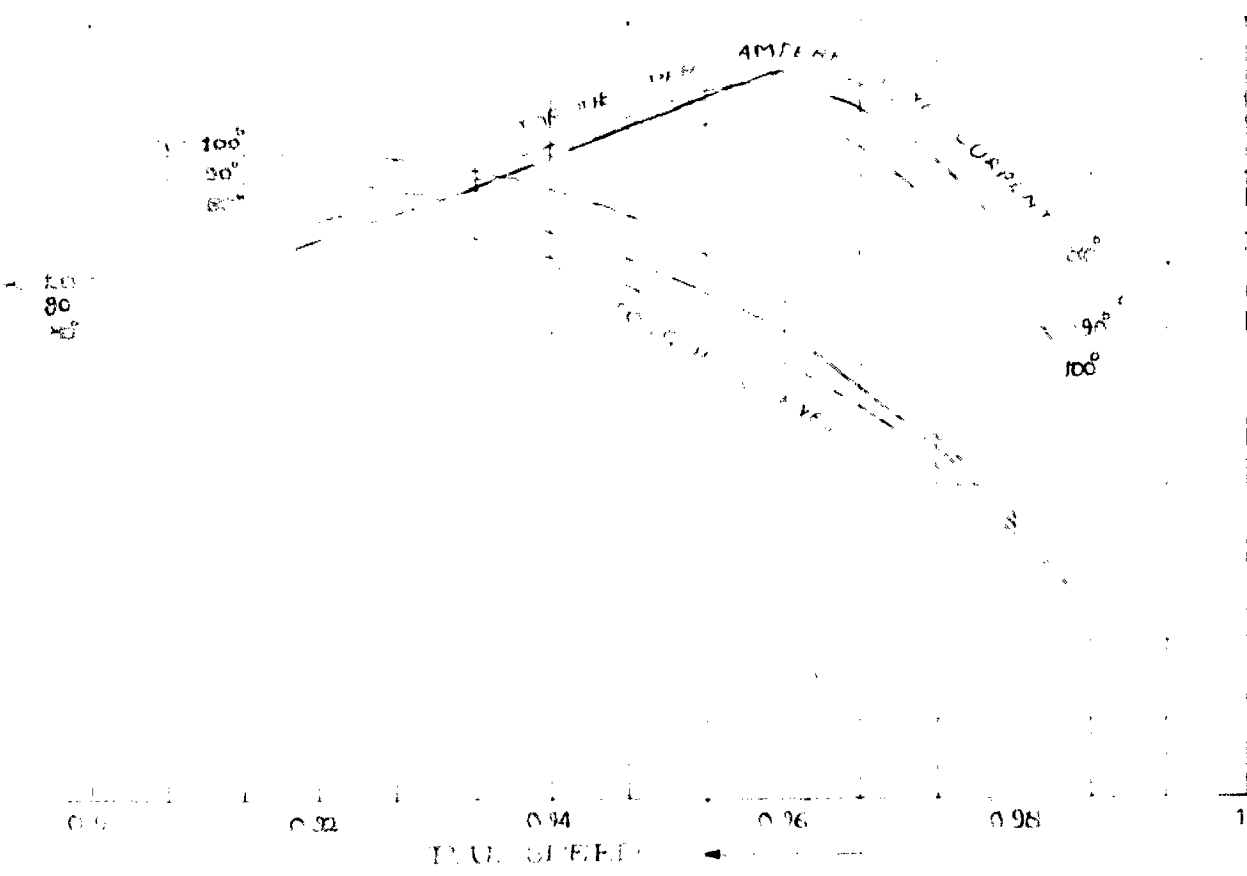
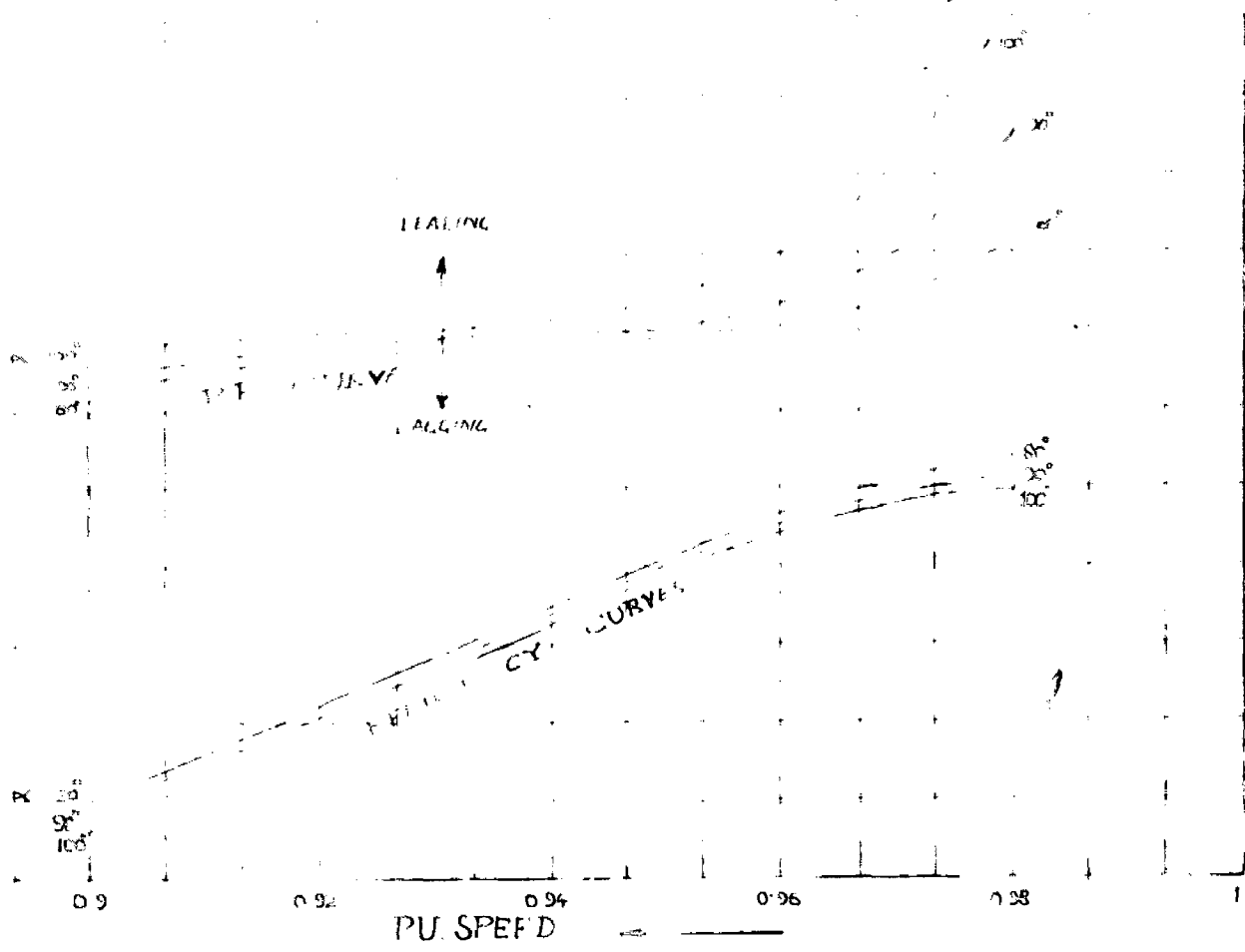
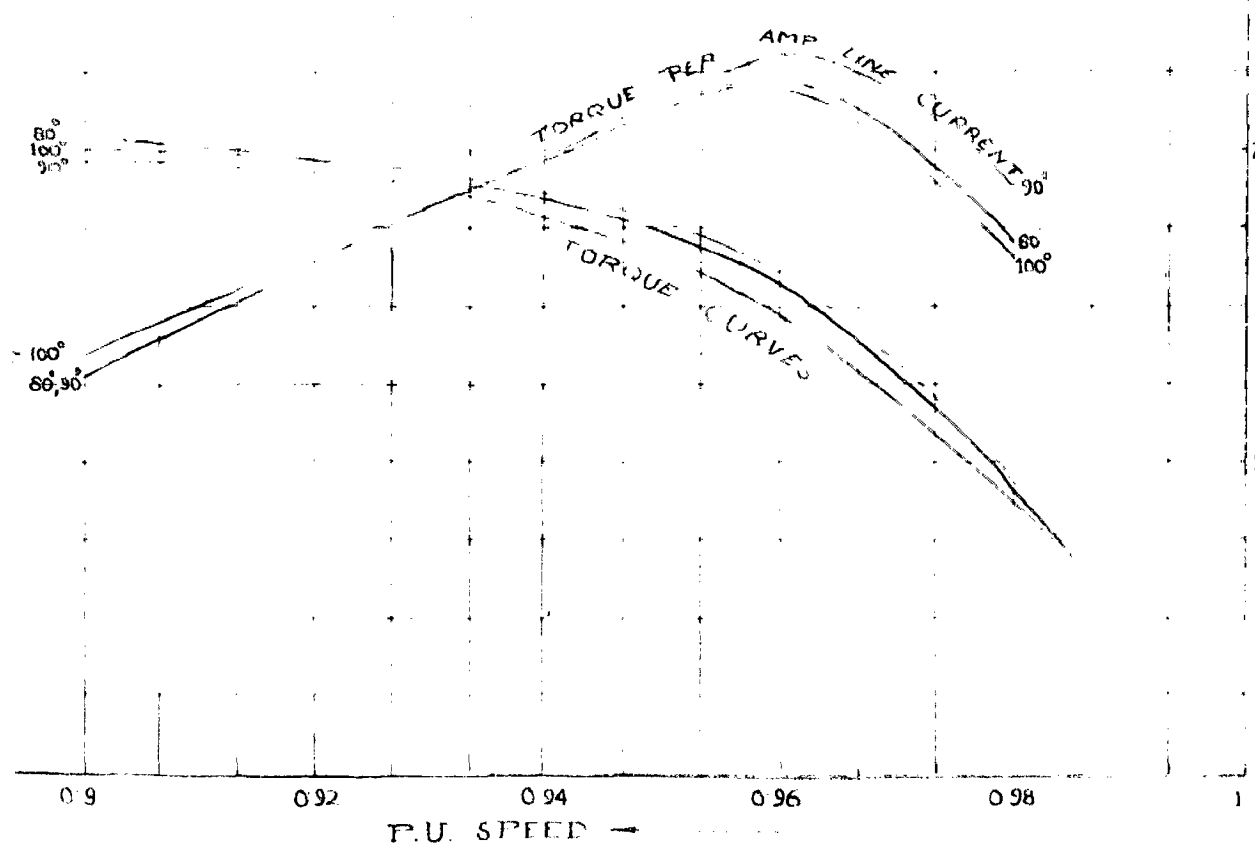
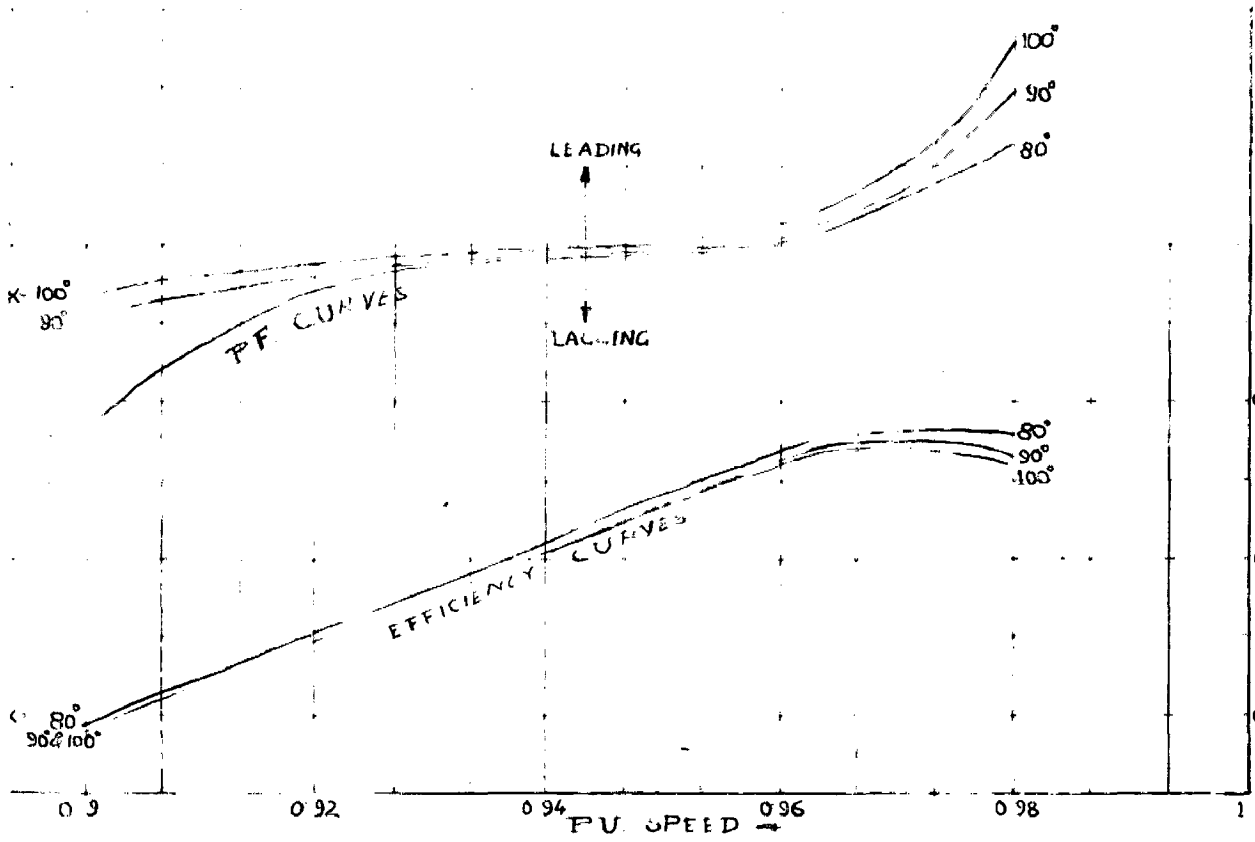


FIG. 10. Efficiency and Power Factor vs. P.U. Speed (Z = 1.4)



(B) Space per ampere Line Current

Example per ampere line current curves show a maximum at the designed balanced operation point. For lower slips 100° case shows slightly lower values than others, 90° space angle being the best. Towards higher slips 100° case improves slightly over the other cases. With change in turns ratio the curves are almost unchanged.

(C) Power-Factor

On lighter loads 100° case show slightly poor power factor than other cases. 90° being the best but on higher loads i.e. greater slips, 100° case improves over the other two.

(D) Efficiency

These curves are very much coinciding with each other. The change in turns-ratio does not produce any noticeable change.

It may be concluded that slight variation in the space angle between the stator windings does not much change the full-load running power factor.

Chapter - 5

Plugging

For sudden and quick reversal of induction motors perhaps plugging is the simplest method which requires no accessories then already available.

In single phase machines plugging is possible by the reversal of either the main or the auxiliary winding connections and using the same starting capacitor in the starting-winding phase. Hence while plugging the nonquadrature stator-windings motor the space-angle between the two stator windings will change from α electrical degrees to $(180 - \alpha)$ electrical degrees.

The machine with unity turns ratio only has been studied both analytically and experimentally for this purpose. In analysis - only the third harmonic is considered, the rotor is thought to have perfectly insulated bars, and the high frequency tooth losses are neglected. Because of these limitations the theoretical curves do not compare well with the experimental curves, except for some salient features.

Effect of Tooth Frequency Loss⁸

The effect of tooth frequency loss is to produce a drag on the rotor which in this respect is similar to friction and windage effect. Thus the torque resulting from it has a negative value over the complete range of positive directional speed, reducing the available torque of the motor. However, during the reverse rotation the torque from this loss tends to stop the motor, thus operating in the same direction as the torque from the machine magnetic field. Consequently both quantities are considered as positive over this range of speed. Even though

the tooth frequency loss does not appear large compared to the rotor copper loss, yet it produces a relatively large torque at high slips. At the point of negative synchronous speed, the tooth frequency loss may be less than one-half the value of rotor copper loss. While the tooth frequency loss results from forces occurring at the rotor speed, the rotor resistance loss is produced by reaction with the stator field which is moving at double synchronous speed with respect to the rotor. Since the torque from any rotor loss varies inversely as the speed of the force reaction producing it, the difference in speed results in torque from the tooth frequency loss which is nearly equal to that from the rotor resistance loss at this point.

This also by the way, gives a reason why analytically calculated curves for forward running were comparing well with the experimental curves.

It is also evident that the experimental results should show great departure from the curves obtained by pure performance calculations.

For all space angles the calculated curves (Figures 5.1 to 5.5) show a predominant third π space harmonic dip at about -400 rpm. In case of lower space angles between the stator windings such as 60° curves show lesser dip and peaky nature. For 100° and 120° space separation the curves show very peaky nature with large dip.

In the experimental curves Fig 5.1(a) to 5.5 (e) 60° space angle curves are found to show more nearly flat braking torque characteristic, with minimum peaky nature. The curves does not vary noticeably with the three capacitors used.

FIG. 3.1 TORQUE SPEED CURVES FOR PLUGGING
 30° SPAC. ANGLE ($\alpha = 1$)

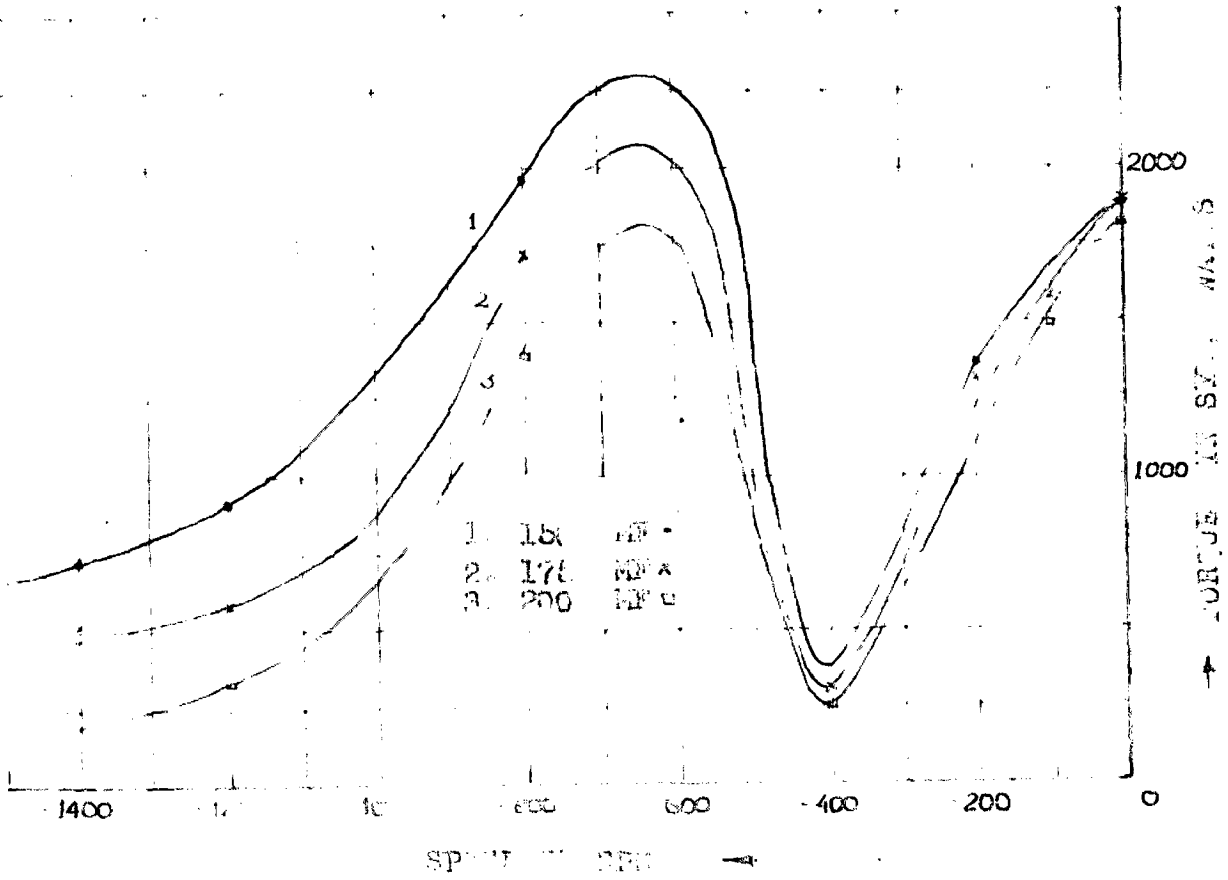


FIG 5.1 (a)
T.S. CURVE
 $\alpha = 60^\circ, 150 \text{ MP}$

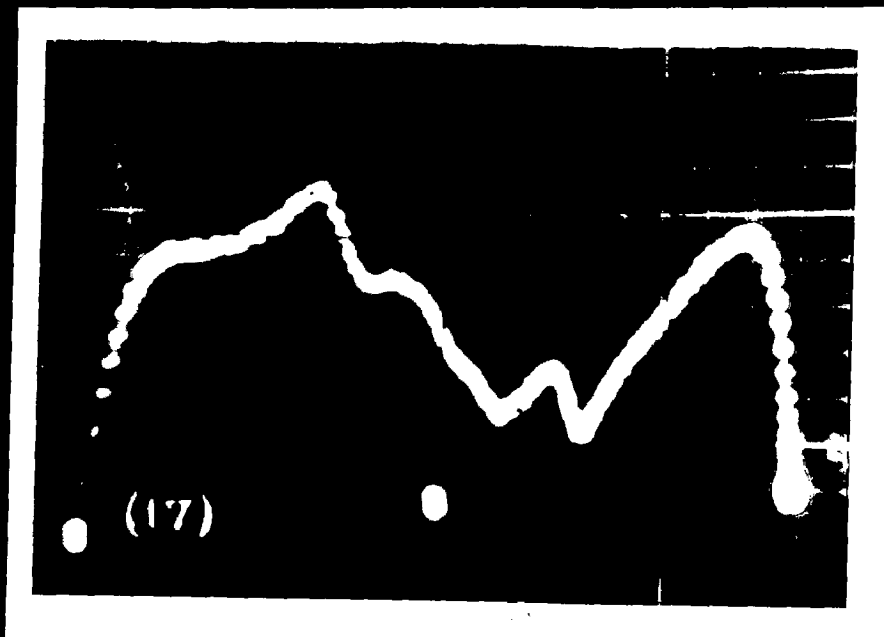
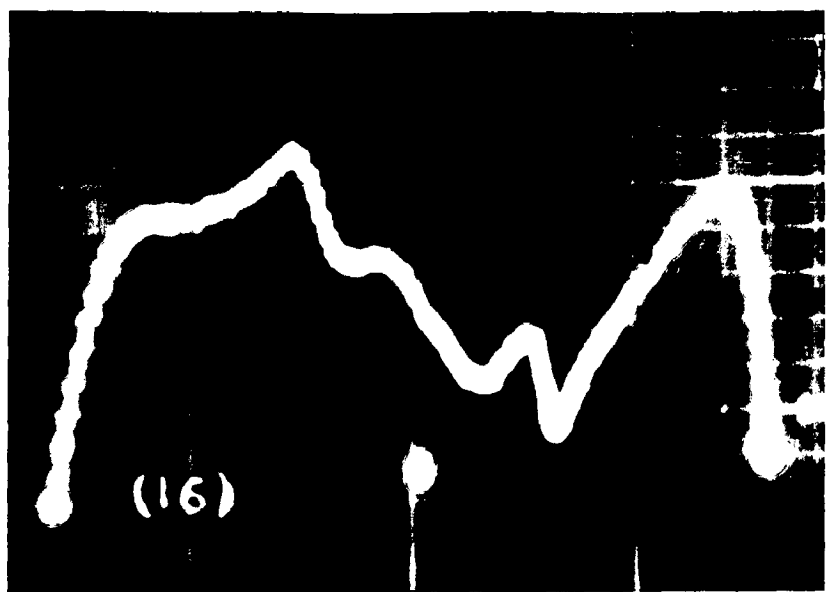


FIG 5.1 (b)
T.S. CURVE
 $\alpha = 60^\circ, 175 \text{ MP}$

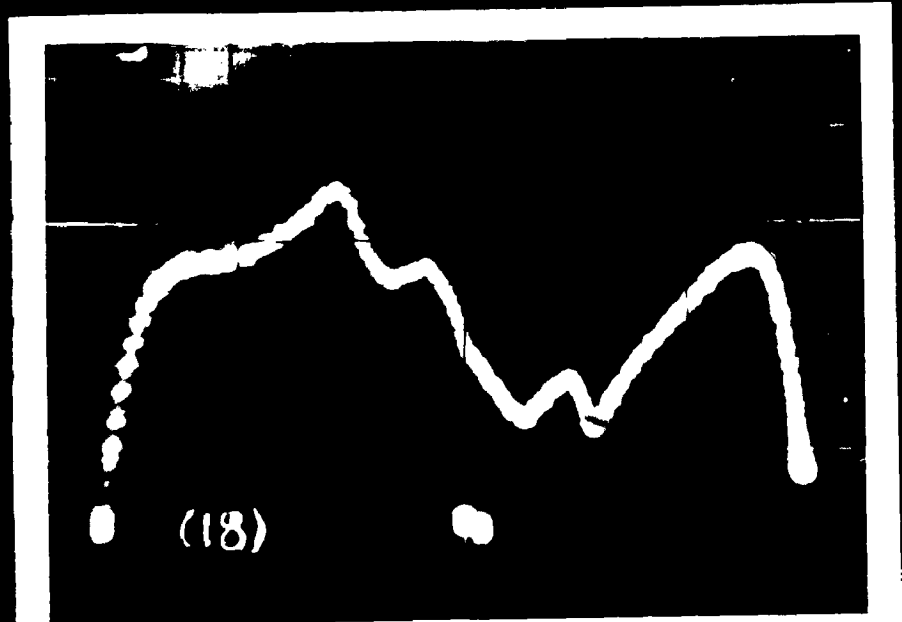


FIG 5.1 (c)
T.S. CURVE
 $\alpha = 60^\circ, 200 \text{ MP}$

(a)

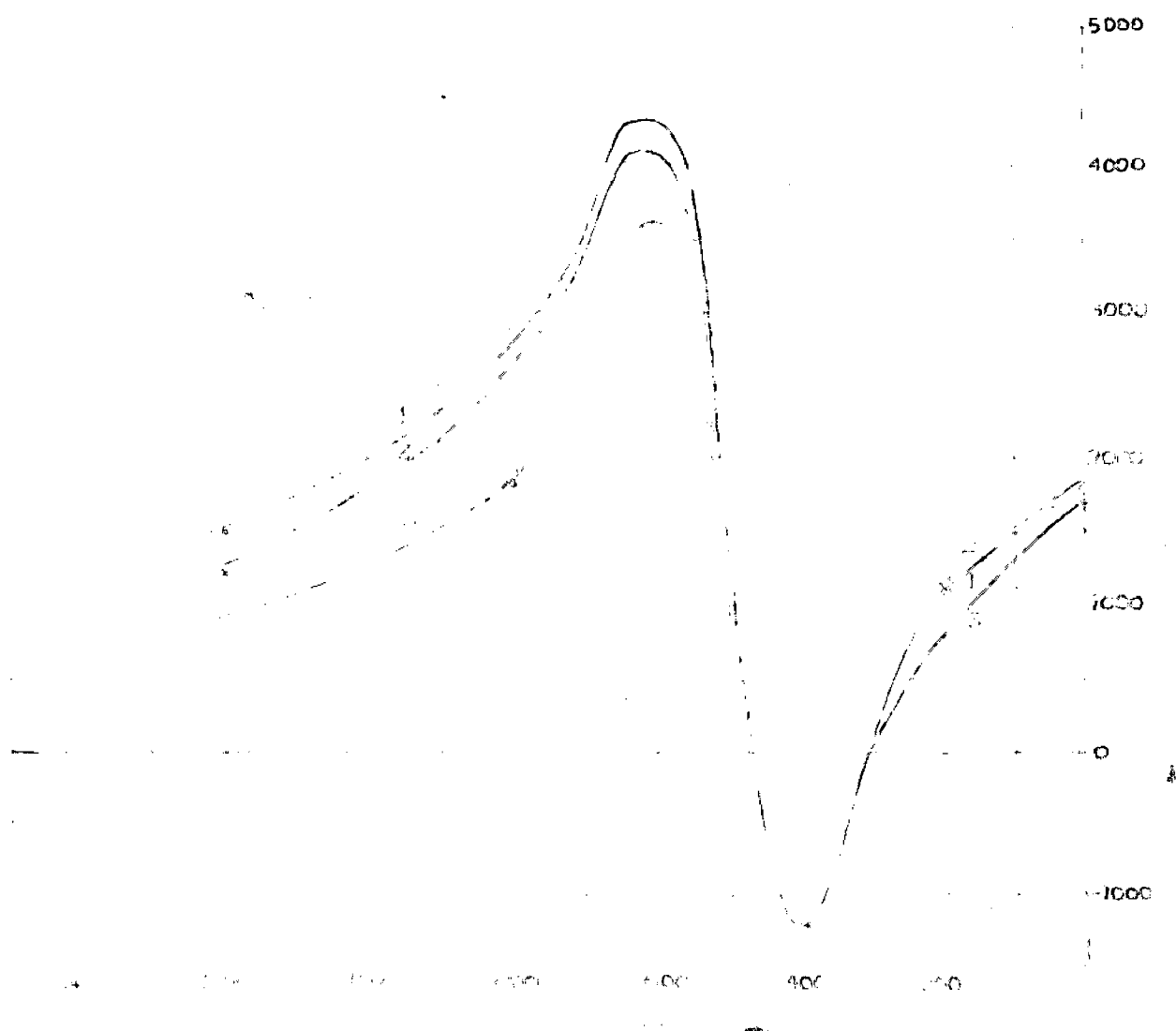


FIG 5.2 (a)
T.-S. CURVE
 $\alpha = 80^\circ$, 150 MF

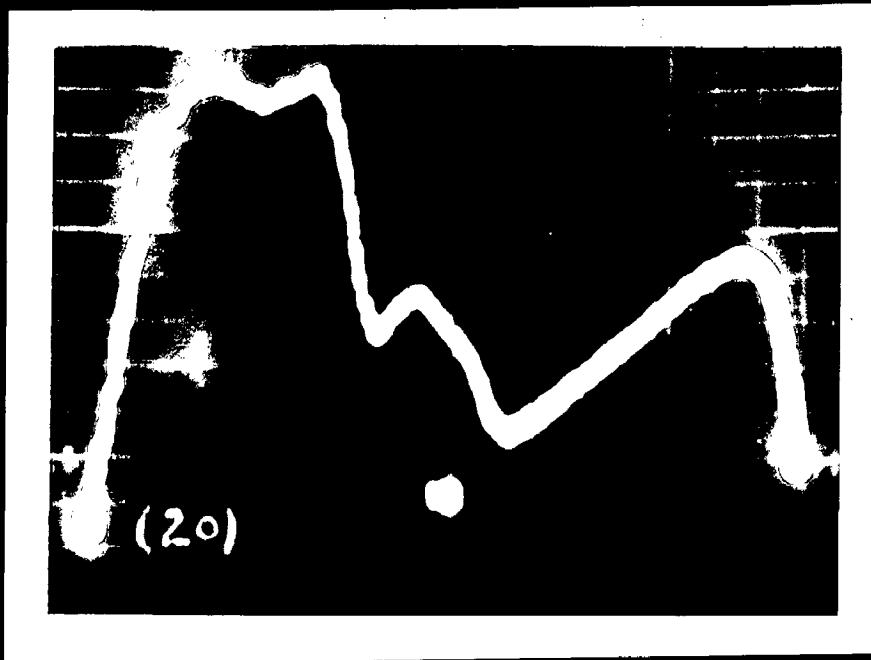
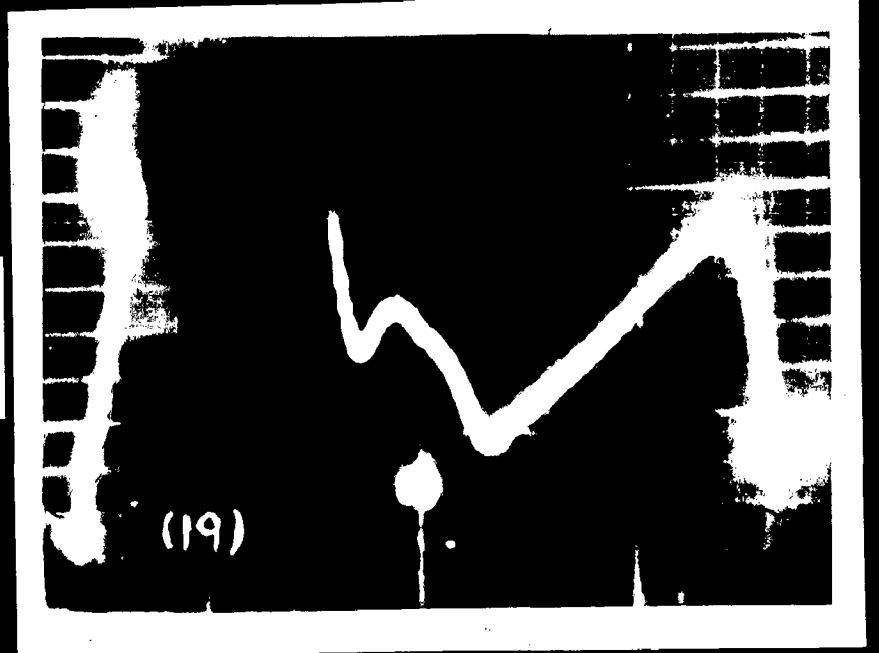
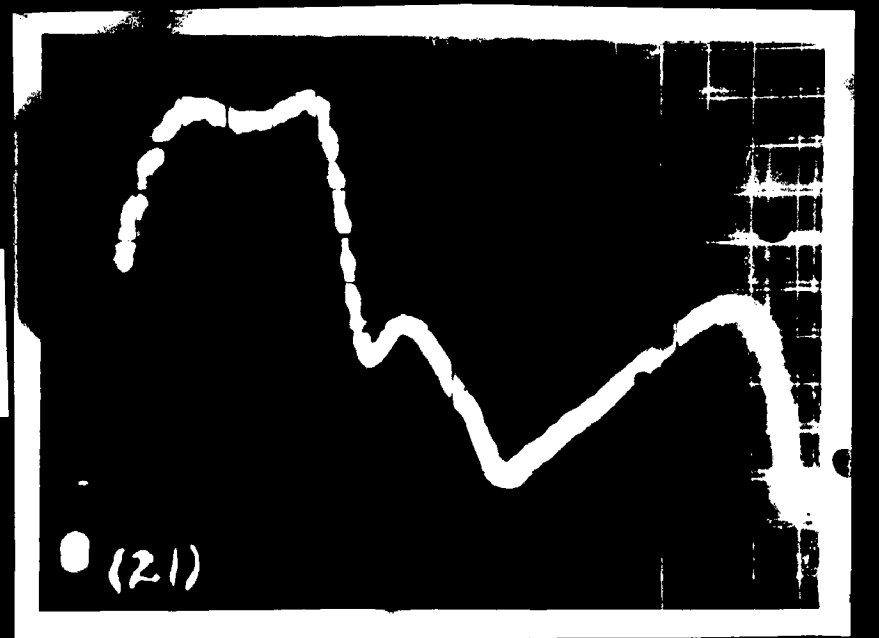


FIG. 5.2 (b)
T.-S CURVE
 $\alpha = 80^\circ$, 175 MF

FIG. 5.2 (c)
T.-S CURVE
 $\alpha = 80^\circ$, 200 MF



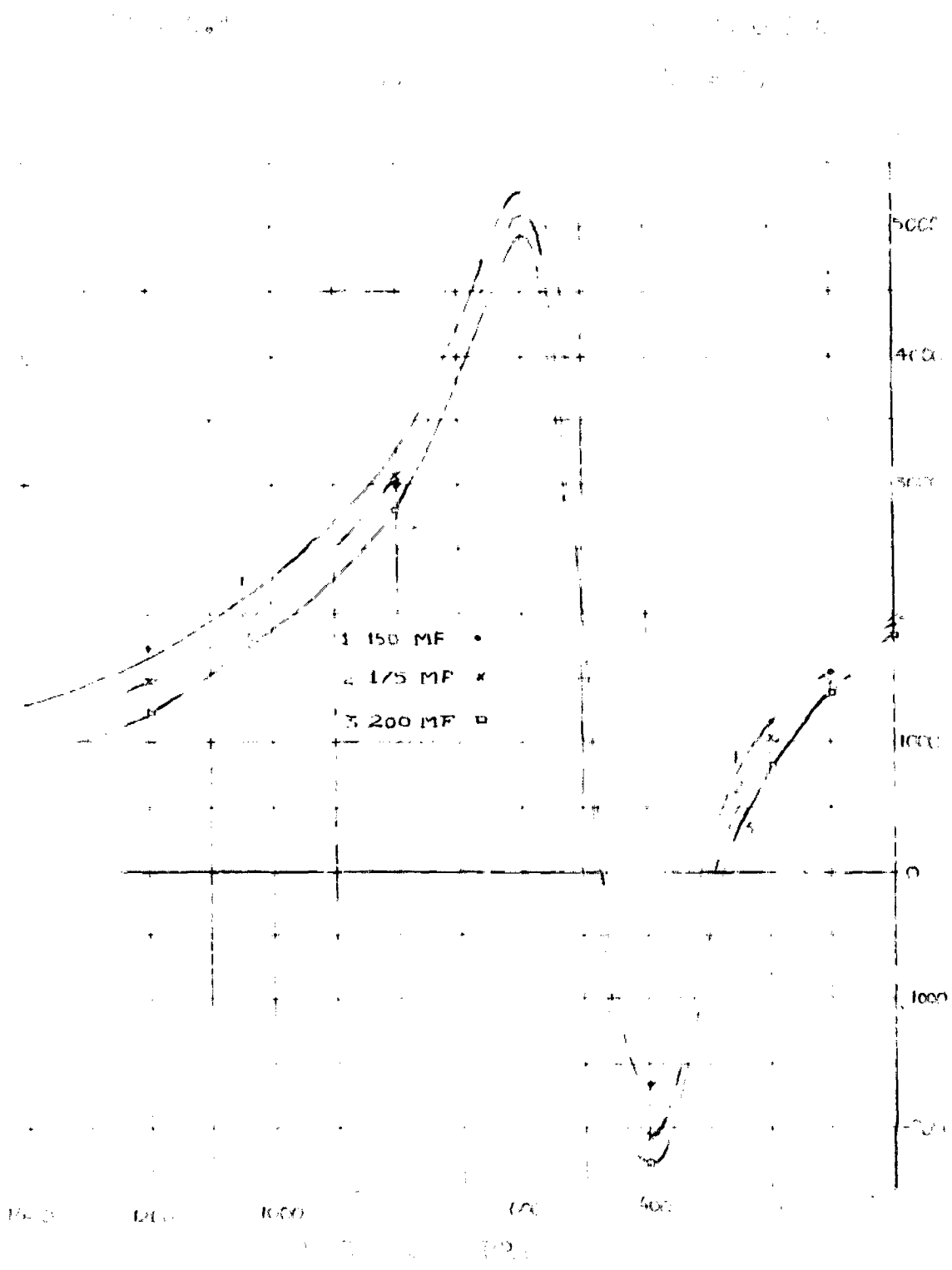


FIG 5.4 (a)
T.-S. CURVE
 $\alpha = 100^\circ, 180 \text{ MP}$

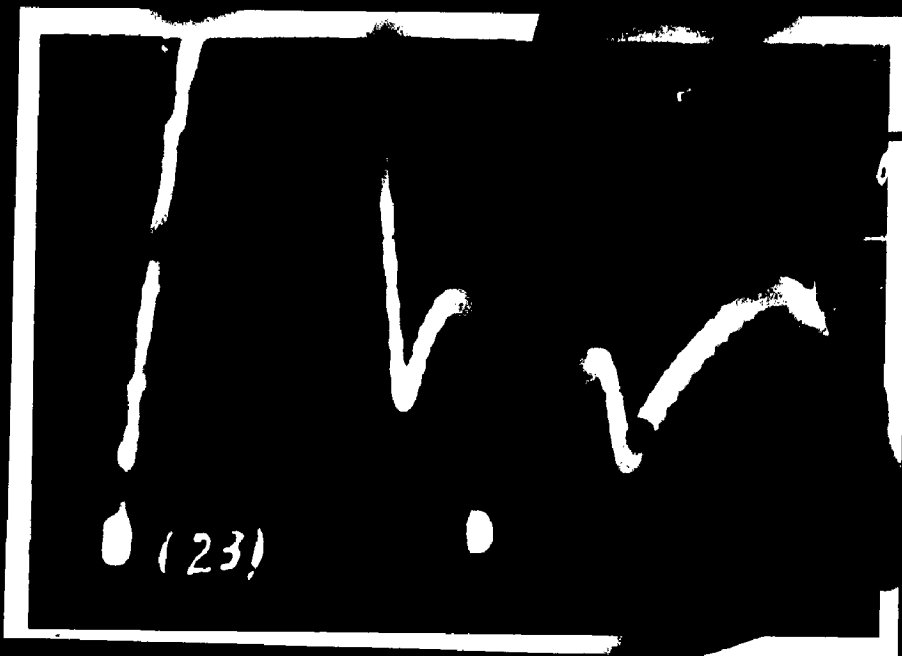
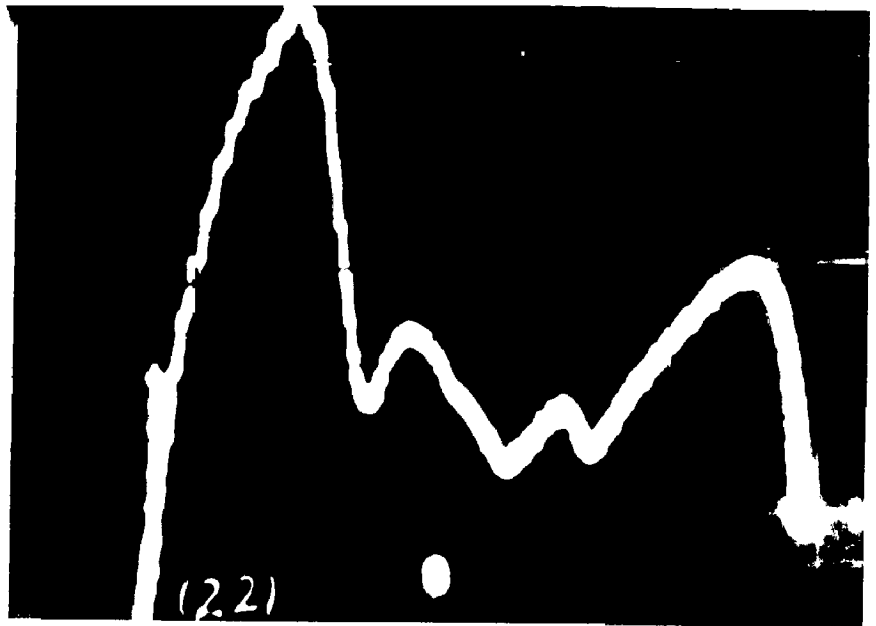
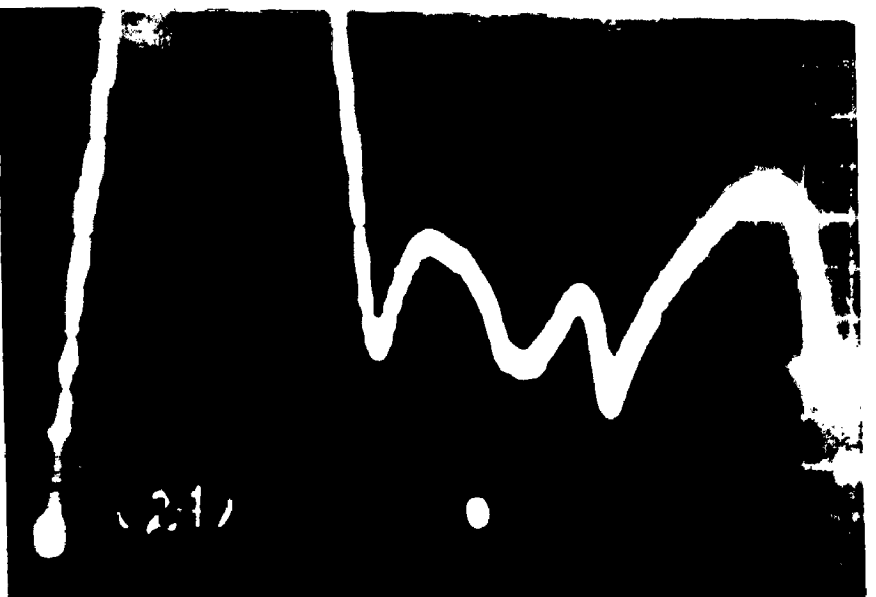


FIG. 5.4 (b)
T.-S. CURVE
 $\alpha = 100^\circ, 175 \text{ MP}$

FIG 5.4 (c)
T.-S. CURVE
 $\alpha = 100^\circ, 200 \text{ MP}$



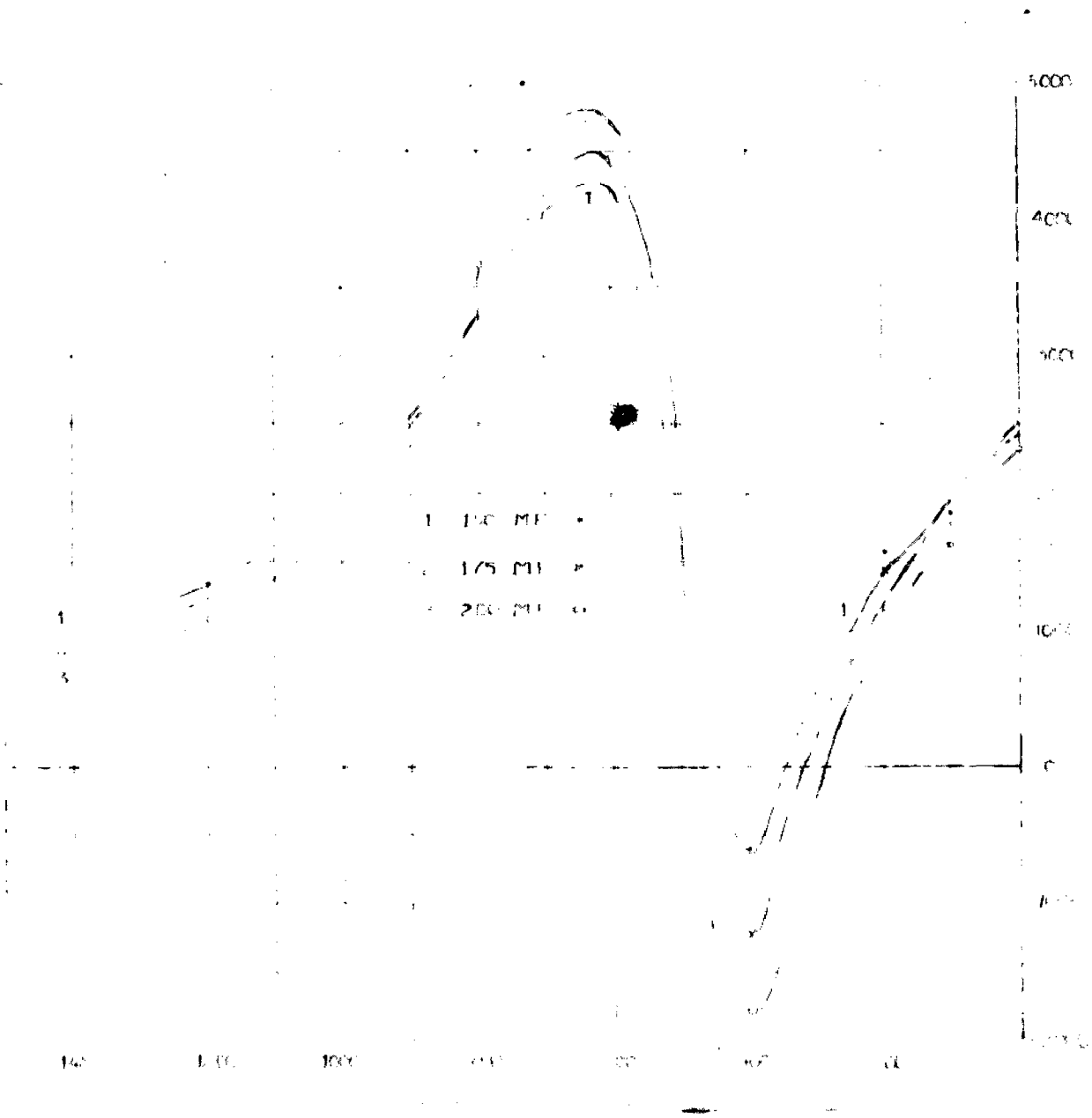


FIG 5.5 (a)
T.-S. CURVE
 $\alpha = 120^\circ, 150 \text{ MF}$

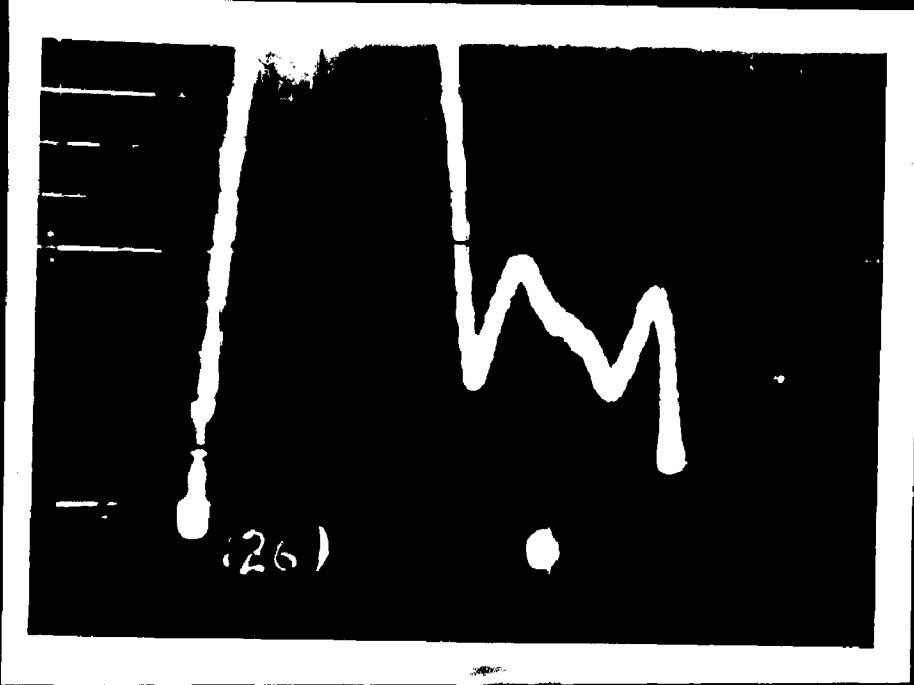
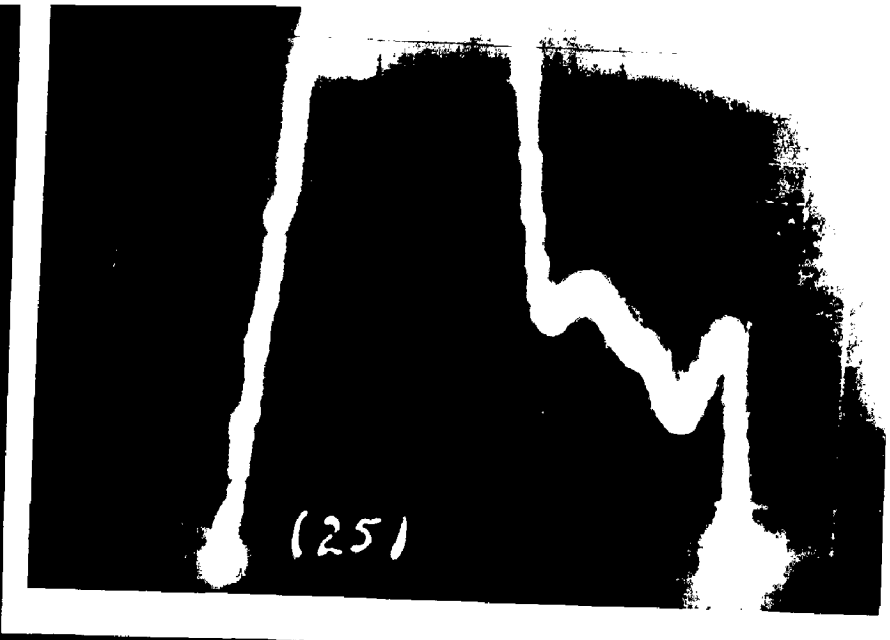


FIG 5.5 (b)
T.-S. CURVE
 $\alpha = 120^\circ, 175 \text{ M}$

FIG 5.5 (c)
T.-S. CURVE
 $\alpha = 120^\circ, 200 \text{ MF}$



For 80° space angle the curves show some more third harmonic dip, but they are not much changed from a flat nature. The average braking torque is more than 60° case. The braking curves again are quite identical for the three capacitors used.

Both 100° and 120° space angles between stator windings show very peaky braking torque characteristics with high third harmonic dip.

Hence from plugging point of view 90° space angle gives sufficiently high and nearly flat nature braking torque characteristic. It may be noted that 80° is the supplementary angle of 100° which was giving best starting performance.

Chapter - 6

Some Applications of Non-Quadrature, 1 Phase Induction Motor (Capacitor-Run)^{10,11}

Because of its various unique characteristics an induction motor with asymmetrically spaced stator-windings is some times preferred to a conventional machine with quadrature stator windings. Following are the few important applications of such a machine:-

6.1 Single Phase Hoist Motor

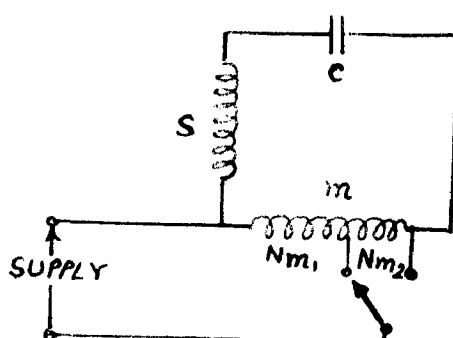
The load of this type of motor is heavy in the event of hauling up operation and it operates with light load when the hoist is going down. To obtain low motor temperature over a period of continuous operation, it is essential to keep the overall efficiency high. This can be accomplished by making the angle between main and start windings larger than 90 degrees. The motor is balanced at heavy loads in this direction. In the reverse run the starting winding is reversed and then space angle between the stator windings becomes less than 90 degrees, and hence with the same running capacitor the motor will now balance at light loads or no-load, of course at lower slip as pointed out in the "Running Performance" Chapter .

6.2 Two Speed Fan Motor (Capacitor run)

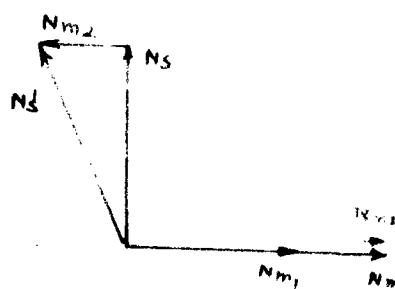
In fan motors to reduce the capacitor requirement two windings are perfectly balanced at a space angle between them

greater than 90° . An ingenious arrangement is shown in Fig. (A). The operating position as shown is for high speed corresponding to the winding vector diagram of (B). This arrangement not only gives 2-speed operation but also balances the motor at higher speed with a relatively small capacitor.

FIG. 6.1.



(A) Circuit



B Winding Vector Diagram.

5.3 Subfractional H.P. Motor

Many subfractional horse power motors require very quiet operation. To achieve balance with ordinary two-winding arrangement, the designer usually chooses a very small running capacitor + but with a start winding of many turns of fine wire. Windings spaced at less than 90° are used to reduce the winding cost as well as balance the motor.

6.4 A High P.F. One-Running-Capacitor 2-Motor System

A fan motor having non-quadrature concentrated windings spaced at 120° may be used with its starting winding in series with the running capacitor of the compressor motor

in an air-conditioning plant. The following points have been established.

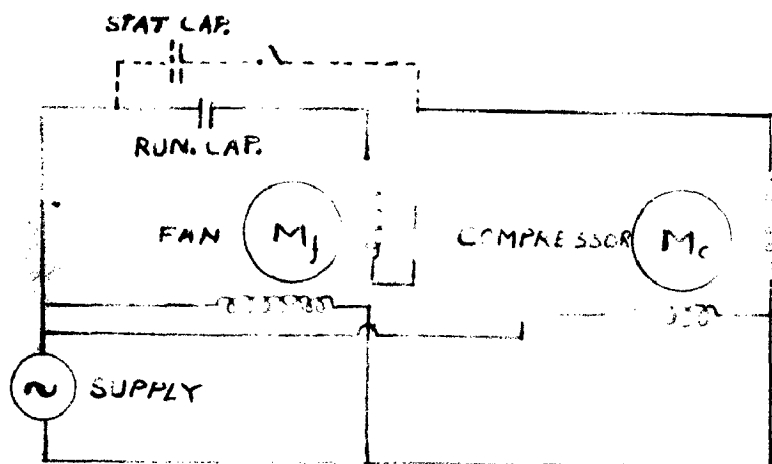


FIG. 6-2

(i) The overall efficiency, power factor and starting torque compare favourably with a system employing a separate permanent capacitor fan motor.

(ii) There is a good possibility that the motor cost is comparable with that of a shaded pole motor. While the winding cost is higher than that of a shaded pole motor, the motor size is considerably reduced. This is possible, as the efficiency of the new motor is comparatively high. It is expected that the reduction in material cost might be sufficient to effect the higher winding cost.

(iii) There is no detrimental effect on the compressor motor whatever.

Chapter - 7

CONCLUSIONS

1. It is possible to develop a satisfactory cross-field approach for the analysis of single-phase motors having two stator-windings, not in strict space quadrature. In this approach by cross-field theory space-harmonics have been considered. The performance equations so developed are of course the same as obtained by the revolving field theory³

2. It is shown that higher starting torque can be obtained through the use of non-quadrature stator-windings.

Due to extremely high stator resistance the value of σ ($= \frac{R_r}{R_r + R_m}$) is only 0.34 in our experimental machine,

and hence only about 4% to 8% more starting torque was possible. For normal squirrel-cage motors a maximum of about 20% more fundamental starting torque is possible by making the space separation between the stator windings greater than 90°

Though the increase in torque is relatively small, the difference in torque in the two alternative directions of rotation can be considerable - a characteristic which could possibly be useful in certain types of reversible drives.

3. The optimum capacitor to give maximum fundamental starting torque is independent of the space angle between the stator-windings. For unity turns-ratio its reactance is numerically equal to standstill impedance of the main-winding.

With increase in turns-ratio the optimum starting capacitor

goes on decreasing, being inversely proportional to the square of turns ratio.

4. The total starting torque depends on the harmonic contents of the air-gap field. Harmonics always produce detrimental effect. A proper stator winding, such as 90° phase spread and $2/3$ rd pitch, is necessary to reduce the harmonic contents.

The points deserved in preceding section are also noted by other authors *.

5. For space angles other than 90° , starting torque per ampere line current and per watt stator copper loss are found to be better than with 90° space angle.

6. The run-up performance of the machine may be very much impaired due to the asynchronous torques produced by space-harmonics, mainly the third space harmonic

For 30° and 90° space angles the predominant third harmonic do not produce any dip in the torque-speed characteristic, though it diminishes the available torque considerably.

For all other space angles 60° , 100° and 120° the third harmonic produces dip. The extreme cases of 60° and 120° space angles are the most severe in respect of run-up performance as the harmonic dip assumes dangerous proportions, 120° case being the worst.

7. A proper selection of the starting capacitor for any space angle can help in suppressing the third or seventh harmonic dip from the torque-speed curve.

For a space angle greater than 90° to suppress the ^{3rd} harmonic dip completely in the torque-speed curve, capacitor of much lower value (50% of critical starting capacitor) is needed.

Opposite is the case for space angle less than 90° . But of course in these cases of ~~high~~ dip suppression there is reduction in starting torque. Therefore attempt for complete suppression of dip is not advisable.

However an attempt can be made to reduce the dip by so changing the starting capacitor that the loss in starting torque is not more than 10% (say) but the reduction in dip is 50% or more.

It has been shown that for 100° space angle the third harmonic dip can be almost suppressed by using a 20% to 25% smaller capacitor than the optimum starting capacitor, still the starting torque is very nearly equal to the maximum available for 90° space case.

For still higher angle (120°) inspite of dip reduction by about 50%, the dip is still sufficient to produce crawling.

Torque per ampere line current and per watt stator copper loss have much improved and are much better than that for 90° space angle with optimum starting capacitor.

For angles lesser than 90° dip reduction is possible only through use of still higher capacitors, for 60° space angle the value of such capacitor increases very much.

8. In certain reversible drives by making the space angle greater than 90° , the motor may be made to balance at high slip (i.e. greater load) with a proper running capacitor whereas during the reverse drive when the load is small, the starting windings may be reversed which in effect makes the space angle less than 90° and now the machine will balance at smaller slip (i.e. light load or no-load). Thus the use of ^{non} quadrature

windings leads to higher overall efficiency for such types of drives.

D. It is found that for plugging a space angle slightly less than 90° , 80° in our case, gives sufficiently high and flat top braking torque characteristic. It may be noted that this space angle is the supplementary angle of the space angle for best run-up performance.

In comparison with other space angles, a space angle of nearly 100° is found to be more suitable from starting performance view. It gives higher starting torque than 90° case, maximum increase about 20% for capacitance-start motors, and 10% for capacitance start and run motors (considering turns-ratio limitations in these cases).

Hence for capacitance-start single phase induction motors a 100° space angle slightly greater than 90° is certainly preferable.

In capacitor start and run motors the ratio of starting to running capacitor can be reduced through the use of a space angle slightly greater than 90° . The running performance is quite comparable with that obtained by 90° space angle between windings.

APPENDIX - AFundamental Torque - Expression

Fundamental torque

$$T_e = \text{Real} \left[i^{dr} B_d^* + i^{qr} B_q^* \right] \quad \dots (23)$$

From Fig. 9

$$B_d^* = \frac{E_{r1}}{1-v^2} (v i^{dr} + j i^{qr})$$

$$j B_q^* = \frac{E_{r1}}{1-v^2} (i^{dr} + j v i^{qr})$$

$$\text{Hence } B_d^{1*} = \frac{E_{r1}}{1-v^2} (v i^{dr,*} - j i^{qr,*})$$

$$\text{and } B_q^{1*} = \frac{E_{r1}}{1-v^2} (j i^{dr,*} + v i^{qr,*})$$

$$\therefore T_e = \text{Real} \left[\frac{E_{r1}}{1-v^2} \left\{ v i^{dr} i^{dr,*} - j i^{dr} i^{qr,*} + j i^{dr} i^{qr,*} + v i^{qr} i^{qr,*} \right\} \right] \quad \dots (A1)$$

From equations (15) and (16)

$$i^{dr} = \frac{j X_{M,2} Z_{r1} i^m + \{ j X_{M,2} a \cos \alpha (Z_{r1} + v R_{r1} X_{M,2} \sin \alpha) \} i^s}{Z_{r1}^2 - v^2 R_{r1}^2} \quad \dots (15)$$

$$j i^{qr} = \frac{j X_{M,2} v R_{r1} i^m + \{ X_{M,2} \sin \alpha (Z_{r1} + j X_{M,2} \cos \alpha v R_{r1}) \} i^s}{Z_{r1}^2 - v^2 R_{r1}^2} \quad \dots (16)$$

$$\text{Where } Z_{r1} = R_{r1} + j X_{r1}$$

$$= \left(\frac{E_{r1}}{1-v^2} + j X_{r1} \right)$$

Hence

$$i_{dr}^* = \frac{-jX_M Z_r^* i^m + \left\{ -jX_M Z_r^* a \cos \alpha + vR_r X_M a \sin \alpha \right\} i^s}{(Z_r^2 - v^2 R_r^2)^*} \dots (A2)$$

$$-j i_{qr}^* = \frac{-j X_M vR_r i^m + \left\{ X_M a \sin \alpha Z_r^* - jX_M a vR_r \cos \alpha \right\} i^s}{(Z_r^2 - v^2 R_r^2)^*} \dots (A3)$$

$$i_{dr}^* \cdot i_{dr}^* = \frac{1}{(Z_r^2 - v^2 R_r^2)(Z_r^2 - v^2 R_r^2)^*} \left[\begin{aligned} & X_M^2 Z_r Z_r^* i^m \cdot i^m \\ & + (X_M^2 Z_r Z_r^* a \cos \alpha - jX_M^2 vR_r Z_r^* a \sin \alpha) i^m \cdot i^s \\ & + (X_M^2 Z_r Z_r^* a \cos \alpha + jX_M^2 vR_r Z_r^* a \sin \alpha) i^m \cdot i^s \\ & + \left[\begin{aligned} & X_M^2 Z_r Z_r^* a^2 \cos^2 \alpha - jX_M^2 vR_r Z_r^* a^2 \sin \alpha \cos \alpha \\ & + jX_M^2 vR_r Z_r^* a^2 \sin \alpha \cos \alpha \\ & + X_M^2 v^2 R_r^2 a^2 \sin^2 \alpha \end{aligned} \right] i^s \cdot i^s \end{aligned} \right] \dots (A4)$$

$$j i_{dr}^* \cdot i_{qr}^* = \frac{-1}{(Z_r^2 - v^2 R_r^2)(Z_r^2 - v^2 R_r^2)^*} \left[\begin{aligned} & X_M^2 vR_r Z_r^* i^m \cdot i^m \\ & + (-jX_M^2 Z_r Z_r^* a \sin \alpha + X_M^2 vR_r Z_r^* a \cos \alpha) i^m \cdot i^s \\ & + (X_M^2 vR_r Z_r^* a \cos \alpha + jX_M^2 v^2 R_r^2 a \sin \alpha -) i^m \cdot i^s \\ & + \left[\begin{aligned} & -jX_M^2 Z_r Z_r^* a^2 \sin \alpha \cos \alpha \\ & + X_M^2 Z_r^* vR_r a^2 \cos^2 \alpha \\ & + jX_M^2 v^2 R_r^2 a^2 \sin \alpha \cos \alpha \\ & + X_M^2 vR_r Z_r^* a^2 \sin^2 \alpha \end{aligned} \right] i^s \cdot i^s \end{aligned} \right] \dots (A5)$$

$$-j1dr, .iqr, = \frac{-1}{(Z_T^2 - v^2 R_T^2)(Z_{Tf} - v^2 R_{Tf})^*}$$

$$\left[\begin{aligned} & X_M^2 v R_T Z_T i^m i^m^* \\ & + (X_M^2 Z_T v R_T a \cos d - j X_M^2 v^2 R_T a \sin d) i^m . i^s^* \\ & + (X_M^2 v R_T Z_T a \cos d + j X_M^2 Z_T Z_T^* a \sin d) i^m . i^s^* \\ & + \left[\begin{aligned} & j X_M^2 Z_T Z_T^* a^2 \sin d \cos d \\ & + X_M^2 Z_T v R_T a^2 \cos^2 d \\ & - j X_M^2 v^2 R_T a^2 \sin d \cos d \\ & + X_M^2 Z_T v R_T a^2 \sin^2 d \end{aligned} \right] i^s . i^s^* \end{aligned} \right]$$

$$iqr, iqr, = \frac{1}{(Z_T^2 - v^2 R_T^2)(Z_{Tf} - v^2 R_{Tf})^*}$$

$$\left[\begin{aligned} & X_M^2 v^2 R_T^2 i^m . i^m^* \\ & + (X_M^2 v^2 R_T^2 a \cos d - j X_M^2 v R_T Z_T a \sin d) i^m . i^s^* \\ & + (X_M^2 v^2 R_T^2 a \cos d + j X_M^2 v R_T Z_T a \sin d) i^m . i^s^* \\ & + \left[\begin{aligned} & j X_M^2 v R_T Z_T a^2 \sin d \cos d \\ & + X_M^2 v^2 R_T a^2 \cos^2 d \\ & - j X_M^2 v R_T Z_T a^2 \sin d \cos d \\ & + X_M^2 Z_T Z_T^* a^2 \sin^2 d \end{aligned} \right] i^s . i^s^* \end{aligned} \right]$$

...(A7)

By substituting equation (A-4) to (A-7) in equation

(A-1)

$$T_1 = \text{Real} \left[\frac{R_{r1} / (1-v^2) \cdot X_{M1}^2}{(Z_{r1}^2 - v^2 R_{r1}^2)(Z_{r1}^2 - v^2 R_{r1}^2)^*} \left\{ \begin{aligned} &v(X_{r1}^2 - R_{r1}^2 + v^2 R_{r1}^2) (i^m \cdot i^{m*}) \\ &+ 2a \cos \phi (i^m i^s + i^m i^{s*}) \\ &+ a^2 (i^s \cdot i^{s*}) \\ &- j a \sin \phi (X_{r1}^2 + R_{r1}^2 - v^2 R_{r1}^2) \cdot \\ &\quad \cdot (i^m i^{s*} - i^{m*} i^s) \end{aligned} \right\} \right]$$

$$= \frac{R_{r1}}{(1-v^2)} \frac{1}{\left(\frac{R_{r1}^2}{(1-v^2)^2} + X_{r1}^2 + \frac{2R_{r1}^2 X_{r1}^2}{1-v^2} \right)} \left[\begin{aligned} &v X_{M1}^2 (X_{r1}^2 - \frac{R_{r1}^2}{1-v^2}) (I^m + 2a \cos \phi \\ &\quad \cos \phi I^m I^s + a^2 I^s) \\ &+ 2 X_{M1}^2 a \sin \phi \sin \phi (X_{r1}^2 + \frac{R_{r1}^2}{1-v^2}) \\ &\quad \dots (A-8) \end{aligned} \right]$$

Where $i^m = I^m \mid \underline{d}_1$

$i^s = I^s \mid \underline{d}_2$

$\phi = (d_1 - d_2)$

Equation (A-8) gives the fundamental torque in dyn.watts acting in the direction d to q -axis, v being positive in this direction of rotation of machine.

APPENDIX - BDevelopments of Standstill-equations

From equation (32)

$$I^M = \frac{V_s}{aZ_0} \left[\frac{a(y|\phi_0 - \beta + \alpha) - x|-\phi_x + \phi_0}{1+y|\phi_0 - \beta - x^2|-2\phi_x + 2\phi_0} \right] \dots (B-1)$$

Where $Z_0 = (Z_0) |-\phi_0$

$$z = |z| |-\beta$$

$$y|-\delta = \left| \frac{z}{Z_0} \right| |-\beta + \phi_0$$

$$\text{and } x|-\gamma = \left| \frac{\sum Z_n \cos n \alpha}{Z_0} \right| |-\phi_x + \phi_0$$

Hence

$$I^M = \frac{V_s}{aZ_0} \left[\frac{a^2 + a^2 y^2 + x^2 + 2a^2 y \cos \delta - 2ax \cos \gamma - 2ayx \cos(\gamma - \delta)}{1 + y^2 + x^2 + 2y \cos \delta - 2yx^2 \cos(\delta - 2\gamma) - 2x^2 \cos 2\gamma} \right]^{1/2} \dots (B-2)$$

From Equation (33),

$$I^S = \frac{V_s}{aZ_0} \left[\frac{1 - ax|\phi_0 - \phi_x}{1 + y|\phi_0 - \beta - x^2|2\phi_0 - 2\phi_x} \right] \dots (B-3)$$

$$\therefore I^S = \frac{V_s}{a^2 Z_0} \left[\frac{1 + a^2 x^2 - 2ax \cos \gamma}{1 + y^2 + x^2 + 2y \cos \delta - 2yx^2 \cos(\delta - 2\gamma) - 2x^2 \cos 2\gamma} \right]^{1/2} \dots (B-4)$$

$\phi = \phi_1 - \phi_2$, ϕ_1 and ϕ_2 being phase-angles of I^M and I^S

$$\sin \phi = \frac{(1 - ax \cos \gamma)(x \sin \gamma - a y \sin \delta) - ax \sin \gamma (a + ay \cos \delta - x \cos \gamma)}{(1 + a^2 x^2 - 2ax \cos \gamma)^{1/2} [a^2 + a^2 y^2 + x^2 + 2a^2 y \cos \delta - 2ax \cos \gamma - 2axy \cos(\gamma - \delta)]^{1/2}} \dots (B-5)$$

$$\therefore I^M \cdot I^S \cdot \sin \phi = \frac{-v_s^2}{a^2 z_0^2} \left[\frac{a^2 x \sin \gamma + a y \sin \delta - x \sin \gamma + a^2 y x \sin(\gamma - \delta)}{1 + y^2 + x^2 + 2y \cos \delta - 2yx^2 \cos(\delta - 2\gamma) - 2x^2 \cos 2\gamma} \right] \dots (B-6)$$

DERIVATION OF RESISTANCE START EQUATION

$$\left[\frac{T_\alpha}{T_{90^\circ}} \right]_n = \frac{\sin n \alpha}{\sin \frac{n\pi}{2}} \left[1 + ax \sin(\gamma - \delta) \operatorname{cosec} \delta \right] \dots (39)$$

For resistance start

$$Z \approx R, \beta \approx 0^\circ$$

$$\text{Hence } \delta = -\phi_0$$

$$\text{and } \gamma - \delta = \phi_x$$

$$\therefore \left[\frac{T_\alpha}{T_{90^\circ}} \right]_n = \frac{\sin n \alpha}{\sin \frac{n\pi}{2}} \left[1 - ax \sin \phi_x \operatorname{cosec} \phi_0 \right]$$

$$\text{As } x \frac{|\phi_0 - \phi_x|}{|\phi_0|} = \frac{(\sum Z_n \cos n \alpha) \frac{|\phi_x|}{|\phi_0|}}{(Z_0) \frac{|\phi_0|}{|\phi_0|}} = \frac{\sum (R_n + jX_n) \cos n \alpha}{Z_0 \frac{|\phi_0|}{|\phi_0|}}$$

$$\therefore Z_0 \times \cos \phi_x = \sum R_n \cos n \alpha$$

$$Z_0 \times \sin \phi_x = -\sum X_n \cos n \alpha$$

$$\text{Hence } \left[\frac{T_\alpha}{T_{90^\circ}} \right]_n = \frac{\sin n \alpha}{\sin \frac{n\pi}{2}} \left[1 - a \frac{\sum X_n \cos n \alpha}{Z_0} \right] \dots (40)$$

DERIVATION OF 'CAPACITANCE -START' EQUATION

$$Z \approx X_C, \beta \approx 90^\circ$$

$$\begin{aligned} (\gamma - \delta) &= (\phi_x - 90^\circ) \\ &= 90^\circ - \phi_0 \end{aligned}$$

$$\therefore \left[\frac{T_\alpha}{T_{90^\circ}} \right] = \frac{\sin n \alpha}{\sin n \frac{\pi}{2}} \left[1 - a x \cos \phi_x \sec \phi_0 \right]$$

$$\text{But } x \cos \phi_x = \frac{\sum R_n \cos n \alpha}{Z_0}$$

Hence

$$\left[\frac{T_\alpha}{T_{90^\circ}} \right] = \frac{\sin n \alpha}{\sin n \frac{\pi}{2}} \left[1 - a \frac{\sum R_n \cos n \alpha}{R_0} \right] \dots (41)$$

REFERENCES

1. Kron, G. "Equivalent Circuit of Electric Machinery"
Book, General Electric Series.
2. Kron, G. "Equivalent Circuits of the Shaded Pole
Motor with space Harmonics "
AIEE, Vol 69, 1950, pp 735-41
3. Jha, C.S "Starting of 1-phase Induction Machines
Having Asymmetrical Stator Windings not
in Quadrature "
Proc. IEE, 1962, Vol 109, pt A, pp 47
4. Jha, C.S. and
Daniels " Starting of 1-phase Induction Machines
having Asymmetrical stator Winding in
Quadrature "
Proc. IEE, 1959 Aug., pp 326- 34
5. Adkins, B "The General Theory of Electrical Machinery"
Book, Chapman and Hall Ltd, London
6. Lyon and
Kingsley "Analysis of Asymmetrical Machines "
AIEE, 1936, Vol 55, pp 471
7. Handerson, E.W "Electrical Motor Torque And Its
Measurement "
Publication 13-112, English Electric Canada.
8. Morgon, Brown
and
Schumer " Induction Motor Characteristics at High
Slip."
AIEE, 1940, Vol 59, pp 464-8
9. Odok, A.M. "Starting Load Losses and ^{Stray} Torques
in Induction Motors "
AIEE, 1958, pt III, pp 43-53

10. Chang, S.S.L. "Equivalent Circuit, Analysis and Synthesis of - 1-phase Induction Machines With Multiple Non-Quadrature Windings " AIEE, 1956, pt III, pp 913-16
11. Chang, S.S.L. " A High P.F. One Running, Two-Capacitor Motor System" AIEE, 1957, pt III, pp 720-4
12. Puchstein, A.F., and Lloyd, T.C. "Capacitor Motors With Windings Not In Quadrature " AIEE, 1935, pp 1235- 39